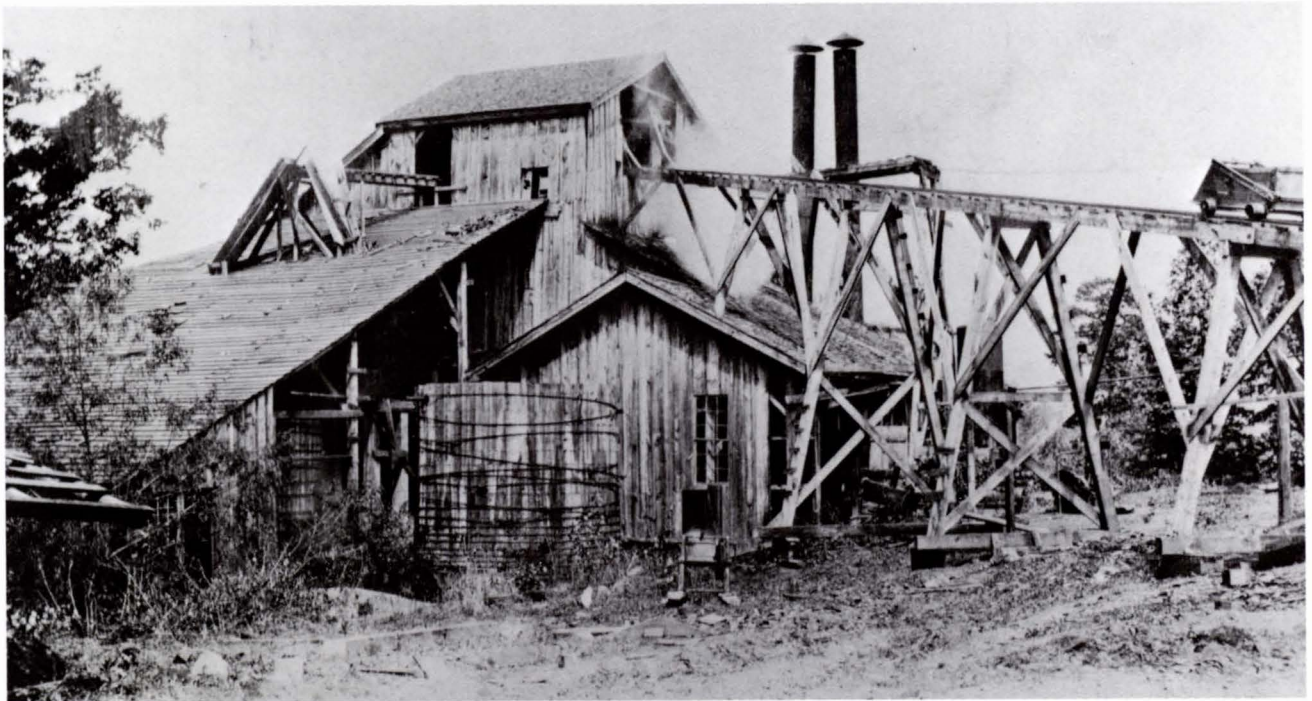


GOLD IN EAST-CENTRAL GEORGIA

by

**Vernon J. Hurst
University of Georgia**

with contributions by
Kenneth D. Plemons



**Georgia Department of Natural Resources
Environmental Protection Division
Georgia Geologic Survey**

BULLETIN 112

Cover photo: Milling Plant, Parks Gold Mine, McDuffie County, Georgia.

Photo courtesy Georgia Department of Archives and History.

GOLD IN EAST-CENTRAL GEORGIA

by

**Vernon J. Hurst
University of Georgia**

**with contributions by
Kenneth D. Plemons**

Prepared as part of the Accelerated Economic Minerals Program

**GEORGIA DEPARTMENT OF NATURAL RESOURCES
J. Leonard Ledbetter, Commissioner**

**ENVIRONMENTAL PROTECTION DIVISION
Harold F. Reheis, Assistant Director**

**GEORGIA GEOLOGIC SURVEY
William H. McLemore, State Geologist**

Atlanta

1990

BULLETIN 112

TABLE OF CONTENTS

	Page
INTRODUCTION	1
Historical Sketch of Gold Mining in Georgia	1
Purpose of this Investigation	1
Synopsis of Gold Mining in the East-Central Georgia District.....	2
Greene County	2
Lincoln County	2
McDuffie County	2
Oglethorpe County	2
Warren County	4
Wilkes County	4
TYPES OF INFORMATION DEVELOPED FOR THIS STUDY.....	4
GEOLOGY OF EAST-CENTRAL GEORGIA.....	4
General Setting	4
Lithology	5
Metamorphic Rocks	5
Plutonic Rocks	7
Danburg Granite	7
Appling Granite	7
Siloam Granite	8
Sparta Granite	8
Elberton Granite	8
Delhi Syenite	8
Other Intrusives	8
Structure	8
Metamorphism.....	9
Deposits of Coarser Aluminosilicates and their Significance.....	12
Graves Mountain Kyanite Deposit.....	15
Hillsborough Andalusite Deposit.....	16
Conclusions	16
KNOWN GOLD OCCURRENCES	16
Mines and Prospects	16
Auriferous Veins	17
PHYSICAL STATE OF THE GOLD IN EAST-CENTRAL GEORGIA	17
General Remarks	17
Gold at the Landers Prospect, McDuffie County	19
Gold at the Parks Mine, McDuffie County	22
Gold at the Latimer Mine, Wilkes County	30
Summary and Interpretation of Information Derived from the SEM Study	42
ORIGIN OF THE GOLD IN EAST-CENTRAL GEORGIA	44
Perspectives	44
Distribution of Background Gold	45
Occurrence of Coarser Gold	46

TABLE OF CONTENTS (CONT.)

	Page
Origin of Quartz Veins and Siliceous Zones	46
Metamorphic Generation of Hydrothermal Fluids	46
Nature of Hydrothermal Fluids	47
Geochemical Behavior of Gold	48
Colloidal Gold	53
The Quartz-Gold Association	53
Geochemical Behavior of Silica	53
Synopsis of Origin	55
 REFERENCES CITED	 55

LIST OF ILLUSTRATIONS

Figure	1. A plot of known gold occurrences in Georgia and the location of the East-Central Georgia Gold District.	3
	2. Representative stratigraphic section of the Little River series at the headwaters of Wells Creek near Lincolnton, Georgia.	6
	3. Chronologic chart of principal events in southeastern United States, Precambrian to Cretaceous.	10
	4. Stability field of kyanite-sillimanite-andalusite and associated minerals in relation to metamorphic grade.	13
	5. Location of principal aluminosilicate deposits in southeastern United States.	14
	6. Frequency versus thickness of quartz veins in east-central Georgia.	18
	7. SEM photomicrograph showing gold enclosing the end of a euhedral quartz crystal, Landers Prospect.	20
	8. SEM photomicrograph showing auriferous silica in contact with gold and with quartz, Landers Prospect.	20
	9. SEM photomicrograph showing enlargement of a portion of Figure 8.	21
	10. SEM photomicrograph showing large gold surface in contact with porous limonite (pseudomorphous after pyrite), Landers Prospect.	21
	11. SEM photomicrograph showing gold particle against pyrite replicating its striated and perhaps slightly altered surface, Landers Prospect.	22
	12. SEM photomicrograph showing gold surface which is a cast of the mica books against which it was deposited, Landers Prospect.	23
	13. SEM photomicrograph showing a replicating gold particle in which the ends of some mica books still are embedded, Landers Prospect.	23

LIST OF ILLUSTRATIONS (CONT.)

	Page
Figure 14. SEM photomicrograph showing small euhedral quartz crystals that have grown into micro-openings in vein quartz, Parks Mine.	25
15. SEM photomicrograph showing etched quartz crystals along a micro-fracture in vein quartz, Parks Mine.	25
16. SEM photomicrograph showing gold-quartz contact in vein quartz, Parks Mine.	26
17. SEM photomicrograph showing surface of a gold particle that was deposited on, and now is a replica of, an etched quartz surface, Parks Mine.	26
18. SEM photomicrograph showing etched quartz surface over which gold was deposited, Parks Mine.	27
19. SEM photomicrograph showing gold-quartz contact in vein quartz, Parks Mine.	27
20. SEM photomicrograph showing typical distribution of gold along an etched micro-fracture in vein quartz, Parks Mine.	28
21. SEM photomicrograph showing euhedral, striated pyrite crystal surrounded by etched K-feldspar and quartz in a micro-fracture of vein quartz, Parks Mine. ...	29
22. SEM photomicrograph showing gold in contact with highly corroded K-feldspar and quartz along a continuation of the micro-fracture shown in Figure 21. ...	29
23. SEM photomicrograph showing auriferous micro-fracture in vein quartz, Parks Mine.	30
24. SEM photomicrograph showing magnified view of a portion of Figure 23.	31
25. SEM photomicrograph showing irregularly shaped gold in strongly etched quartz and near slightly altered pyrite, Parks Mine.	31
26. SEM photomicrograph showing gold in contact with striated and slightly altered pyrite and with strongly altered pyrite, Parks Mine.	32
27. SEM photomicrograph showing covellite etched along basal cleavage, Parks Mine.	32
28. SEM photomicrograph showing euhedral gold in quartz and near covellite, Parks Mine.	33
29. SEM photomicrograph showing gold adjacent to covellite and quartz, Parks Mine.	33
30. SEM photomicrograph showing subhedral gold associated with covellite, Parks Mine.	34
31. SEM photomicrograph showing spheroidal gold as commonly seen in the vicinity of covellite, Parks Mine.	34
32. SEM photomicrograph showing gold in contact with partially altered galena, Parks Mine.	35

LIST OF ILLUSTRATIONS (CONT.)

		Page	
Figure	33. SEM photomicrograph showing a portion of the gold surface in Figure 32. ...	35	
	34. SEM photomicrograph showing gold in planar contact with apparently unaltered galena and in contact with altered galena, Parks Mine.	36	
	35. SEM photomicrograph showing the planar gold-galena contact in Figure 34.	36	
	36. SEM photomicrograph showing gold in highly altered galena in vein quartz, Parks Mine.	37	
	37. SEM photomicrograph showing gold-silver telluride associated with altered galena, Parks Mine.	37	
	38. SEM photomicrograph showing some of the better-formed gold-silver telluride associated with altered galena, Parks Mine.	38	
	39. SEM photomicrograph showing gold with altered mica, Parks Mine.	38	
	40. SEM photomicrograph showing gold deposited along sprung cleavages of amphibole and replicating both its surface texture and cleavage angles, Latimer Mine.	39	
	41. SEM photomicrograph showing X-ray map showing the distribution of gold in Figure 40.	39	
	42. SEM photomicrograph showing gold in amphibole partly altered to limonite, Latimer Mine.	40	
	43. SEM photomicrograph showing close-up of goethitic septa, formed by alteration of amphibole, in contact with gold, Latimer Mine.	41	
	44. SEM photomicrograph showing uneven surface of gold which appears to have formed on partly altered amphibole, Latimer Mine.	41	
	45. SEM photomicrograph showing alternating tabular masses of gold and amphibole, Latimer Mine.	42	
	46. Schematic frequency distribution curves for the gold in the East-Central Georgia Gold District.	43	
	47. Alteration model of a typical hot spring system.	45	
	48. Electron affinity versus first ionization potential.	49	
	49. Temperature-pressure field within which the solubility of silica decreases with increasing temperature.	54	
	Table	1. Standard electrode potentials for selected half-cells	50
		2. Comparison of reported values that relate to the ionization of selected elements.	51
		3. Relative abundance of elements having an electroaffinity higher than that of gold.	51

Plate	A. Geologic map of East-Central Georgia, a partially synthesized compilation of geologic mapping up to 1986.	separate envelope
	B. Distribution of metamorphic index minerals in alluvium in East-Central Georgia.	separate envelope
	C. Strike and dip of quartz veins and silicified zones in East-Central Georgia ..	separate envelope

GOLD IN EAST-CENTRAL GEORGIA

by

Vernon J. Hurst
University of Georgia

INTRODUCTION*

HISTORICAL SKETCH OF GOLD MINING IN GEORGIA

Gold was first discovered in Georgia in 1823 in McDuffie County, 11 miles northwest of Thomason. Other discoveries soon followed near Dahlonega and other parts of the State. Some of the new finds were rich and easily worked. By 1830, when 6,000-10,000 persons were engaged in gold mining, Georgia had become the foremost gold-producing State, a position it maintained until the late 1840's, when major strikes were made in the western States.

Georgia's gold production, derived mainly from small placer and saprolite deposits, peaked in 1833-34, when the reported annual yield was 20,077 fine ounces. In 1838 a U.S. Branch Mint opened in Dahlonega, but production already had begun to decline. As the better placer and saprolite deposits were worked out, some miners moved to the west in search of new fields. Those who remained gave increasing attention to the development of lode deposits, but total production continued to decline. The Dahlonega Mint closed in 1861 after having coined about 12.3 tons of gold, then equivalent to \$6,115,569. A short time later, during the Civil War, virtually all gold mining ceased. There was a resurgence of mining after the war, particularly hydraulic mining of low-grade saprolite deposits, but gold mining's earlier importance to the economy of Georgia was not regained.

From 1823 to 1907, the value of total reported gold production from Georgia was \$17,519,390. In 1908 reported production was a little more than \$56,000. From 1908 to the beginning of World War I, annual output ranged from \$14,000 to \$35,000. Even less mining was carried on from the end of World War I to the 1930's, when gold mining ceased for a few years. Since 1940 output has been negligible (Hurst, et al., 1966a and 1966b).

A reading of Georgia Geologic Survey Information Circular 83 entitled "Geochemical Reconnaissance for Gold in East-Central Georgia" is essential for proper understanding of this Bulletin.

The Coinage Act of 1792 defined the dollar as equivalent to 24.75 grains of fine gold, making an ounce of gold worth about \$19.39. The Coinage Act of 1834 adjusted the definition of the gold dollar from 24.75 to 23.2 grains, which made an ounce of gold worth \$20.67. During the Civil War inconvertible currency was introduced. In 1920 a fixed U.S. price of \$20.67 per ounce was reestablished and was maintained until 1933, when it was changed to \$35.00 per ounce. The fixed price was abandoned in 1968. The current price (April 1988) is about \$445.00 per ounce.

Total production of Georgia gold from 1823 to 1944 was worth about \$17,945,000 (Furcron, 1948). This indicates a production of about 868,000 troy ounces, or about 36 tons, the current value of which is more than a quarter-billion dollars.

PURPOSE OF THIS INVESTIGATION

The higher value of gold since 1968 has triggered intense interest in the development of new gold deposits, worldwide, and has focused attention on all areas with a history of significant production.

Past production in Georgia came mainly from small placer and saprolite deposits in which gold was relatively coarse. Recent developments, however, have involved a different type of deposit, a large-scale, low-grade deposit in which the gold may be megascopically invisible. This type of deposit was uneconomic in the early days, and hardly any prospecting was undertaken for it in Georgia.

Any major new mineral development, ordinarily, is preceded by costly, high-risk exploration. The commitment of venture capital to exploration usually depends upon the availability of any geological or geochemical information that might reduce the cost or risk of exploration.

In 1981 the Georgia Geologic Survey initiated a full-scale investigation of the gold resources of the State. The aims of this investigation are to delineate the more favorable areas for exploration and to gather background information that might attract venture capital and facilitate modern prospecting. Detailed information is being gathered on the distribution of gold in the State's auriferous rocks,

on geologic and geochemical parameters that influenced the distribution of gold, on the physical state of the gold, and on visible or measurable features that might be used as guides in the search for new deposits.

A plot of known gold occurrences reveals many shows scattered over much of the central Piedmont Upland and Highland, areas underlain by metamorphic and igneous rocks. The plot also delineates four main auriferous areas or districts within which old gold mines and prospects are clustered (Figure 1). One of the principal districts is in east-central Georgia, where gold was first discovered in Georgia, and where several placer and lode deposits have been mined. Part of this district once was called the McDuffie County Gold Belt (Jones, 1909), but recent work has shown the same pattern of mineralization over a much larger area. Further work might show that gold occurrences in Madison, Elbert, and Hart Counties also belong to this district. A second major district is a poorly defined belt extending southwestward from Clarkesville in Habersham County through Hall Counties and northern Gwinnett County to Fulton County. Jones (1909) called this the Hall County Belt. A third major district, the Dahlonega Belt of Jones, is a narrow belt extending from northern Rabun County southwestward through Lumpkin County to Canton in Cherokee County. According to Jones, the Dahlonega Belt bifurcates in Cherokee County, with one branch extending through Paulding and Haralson Counties, and the other branch through Carroll County. No major production has come from shows southwest of Cherokee County. The Dahlonega District and the East-Central Georgia District have been the two major gold-producing areas of the State. This report deals only with the East-Central Georgia District.

SYNOPSIS OF GOLD MINING IN THE EAST-CENTRAL GEORGIA DISTRICT

Six of the eight counties in this district have a history of past gold mining: Greene, Lincoln, McDuffie, Oglethorpe, Warren, and Wilkes. The only gold mining, at present, is in Lincoln County at the old Magruder Mine, where intermittent placer mining has been carried on during the last five years. During the same period, a little placer gold has been recovered from prospecting with a small dredge in the vicinity of the old Warren Mine on the east side of Warren County.

Greene County

Both before and after the Civil War, gold was mined along a low ridge of sheared quartzose rock 6

miles northeast of Union Point, close to the Greene-Taliaferro county line. A Chile mill, an early type used for fine grinding, was operated during the 1850's. No reliable record has been found of how much was produced. Around 1900, a mining company drove an adit into the ridge for several hundred feet, ran several cross drifts from the adit, and erected a cyanide plant. Work was suspended about 1908 (Jones, 1909). Three samples of the quartzose rock that was mined, collected in 1963, assayed an average 0.03 ounces of gold per ton (Hurst, et al., 1966a and 1966b).

Lincoln County

Several gold mines operated before the Civil War and near the turn of the century. The first mines were placers. Later, lodes were developed and stamp mills built. Rich returns were reported. The most important mine was the Magruder Mine on the western edge of the county (Hurst, et al., 1966a and 1966b). Intermittent, small-scale placer mining has recovered coarse gold from the old tailings area of the Magruder Mine during the last five years.

McDuffie County

Both placer and lode deposits were worked, beginning in 1823. Principal mines were the Columbia Mine, Hamilton Mine, Parks Mine, Porter Mine, Tatham Mine, Woodall Mine, and Griffin Mine. The Columbia Mine was one of the more extensive lode mines in the State (Hurst, et al., 1966a and 1966b). A stamp mill, perhaps the first in the United States, was built at this mine in 1833. After 1846, Cornish pumps were used as the shafts were deepened. Total production prior to the Civil War was about two million dollars (4 tons). Mining after the Civil War was intermittent. In 1925 considerable bullion was recovered at a 50-ton cyanide plant, but production records were not published. The deepest shaft was about 400 feet.

Oglethorpe County

Within a belt up to 2 miles wide, extending northeastward across the southeast part of the county, were many small lode prospects and mines, about which little detailed information is available. The belt extends from a point 3 miles northeast of Bairdstown, in the southwestern part of the county, into the vicinity of Goose Pond near the Oglethorpe-Elbert county line, a distance of about 25 miles (Hurst, 1966). Five small lode mines once operated along the southwestern half of this belt: Briscoe Mine, Drake Mine, Buffalo or Howard Mine,

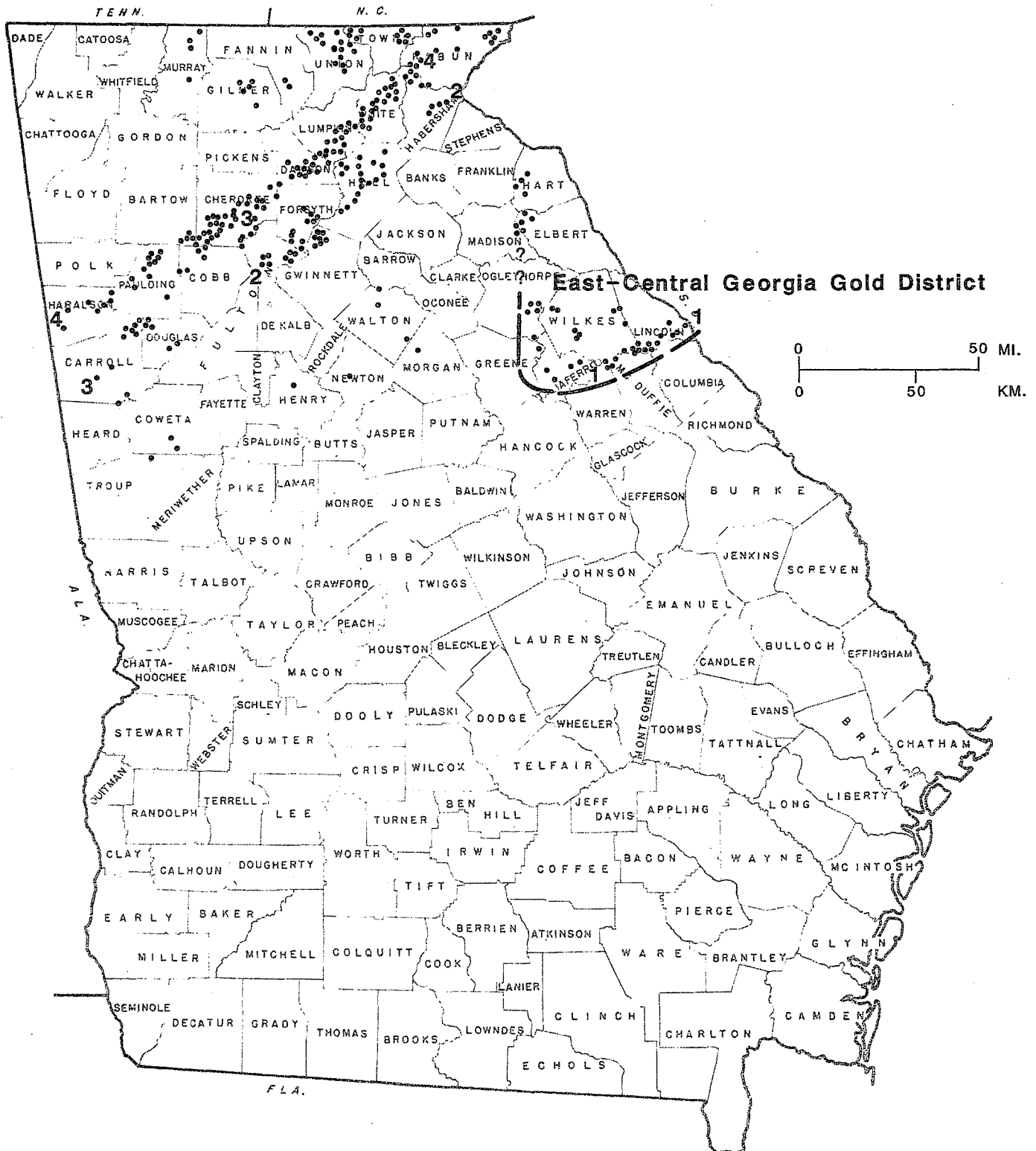


Figure 1. A plot of known gold occurrences in Georgia, and the location of the East-Central Georgia Gold District. The principal gold belts of Jones (1909) are identified by two numbers, one at each end of the belt: 1-McDuffie County Belt; 2-Hall County Belt; 3-Carroll County Belt; and 4-Dahlonega Belt.

Guarantee Mine, and Morgan Mine, which appears to have been the largest. The only producing mine in 1932 was the Arnold Mine. Since about 1933 no gold mining has been carried on in Oglethorpe county.

Warren County

Immediately west of the Warren-McDuffie county line, in the vicinity of Cadley, are several gold prospects, but gold has been mined at only one of them, the Warren Mine (Jones, 1909; Hurst, et al., 1966a and 1966b). A stamp mill was erected there in the 1880's. Work was carried on intermittently for about 20 years. Production appears to have been small. During the last 5 years a little gold has been recovered during prospecting with a portable dredge in the vicinity of the old Warren Mine.

Wilkes County

Both placer and lode deposits have been worked on a small scale. The Stony Ridge Mine was 6 miles southwest of Washington; the Kendall Mine 11 miles northeast of Washington.

Relatively recent mining has been carried on at the Latimer Mine in northwestern Wilkes County, along the Danielsville road, a mile from the Wilkes-Oglethorpe county line. Some sluicing was reported on this property before the Civil War. A small rich vein was discovered in 1901. A thousand pounds of ore from this vein was milled at the Columbia Mining Company's mill and yielded about 7 pounds of gold. Other rich but small veins have been discovered since then. In 1964-66 soil and residual vein material was mined on a small-scale (Hurst, et al., 1966a and 1966b) and another thin, but very rich, vein discovered.

TYPES OF INFORMATION DEVELOPED FOR THIS STUDY

The East-Central Georgia District encompasses eastern Greene and Oglethorpe Counties, and all of Wilkes, Lincoln, Taliaferro, Warren, McDuffie, and Columbia Counties. All available information, unpublished as well as published, has been assembled on the 1) geology of the district; 2) location of known gold occurrences; and 3) the location, attitude, and gold content of outcropping veins.

New data have been generated on the 1) geochemical distribution of gold within the district; 2) electrophoretic mobility of colloidal gold (Scarborough, 1983); 3) physical state of the gold and associated minerals as revealed by scanning

electron micrography (Hurst, et al., 1982; Plemons and Hurst, 1983); and 4) the origin of the gold.

The plan of this study is to present three major classes of information (e.g., the geology of the gold, the reconnaissance geochemical survey of background gold values, and the scanning, electron microscope study) bearing directly on the distribution and origin of the gold; and, then, to deduce from this information the temporal relations and physical conditions that controlled localization of the gold. The section of this Bulletin dealing with the geology of East-Central Georgia is a synthesis of the geology of the district, incorporating the extensive reconnaissance geologic mapping done in the 1960's and subsequent geologic studies up to 1986. This synthesis provides an essential frame-work of lithology and geologic history for ordering and relating the results of the other studies. A discussion on deposits of coarse aluminosilicates is included because of the concept that these deposits and the gold deposits might have had a common origin. The collection and gold assays of 1,968 saprolite and rock samples from throughout the district are described in a separate document, Information Circular 83. Correlations of background gold values with lithology and structure are examined. This reconnaissance geochemical survey delineates nine areas that appear to warrant more detailed exploration. The section dealing with the physical state of the gold in East-Central Georgia describes a scanning electron microscopic (SEM) study of auriferous specimens from three representative occurrences. The high resolution imaging and analytical capabilities of the SEM yield more definitive information about ore mineral genesis than earlier types of microscopes, as this study demonstrates. The final section of this Bulletin considers all of the data in relation to the geochemical behavior of gold and silica and the metamorphic generation of hydrothermal fluids. These considerations reveal new details about the origin of the gold: its metamorphic rather than volcanogenic origin, how it was transported, the principal mechanism responsible for its precipitation, and the close association of gold concentrations with faults and fractures produced during Alleghenian tectonism. These details should guide future exploration in the East-Central Georgia District.

GEOLOGY OF EAST-CENTRAL GEORGIA

GENERAL SETTING

The rocks of East-Central Georgia were grouped by Crickmay (1952) into five belts,

following earlier workers: the Belair, Kiokee, Uchee, Little River, and Dadeville Belts. He described the Little River and Belair belts as low-grade metavolcanics and intercalated metasediments and named them the Little River Series, a part of the Carolina Slate Belt. He described the Kiokee, Uchee, and Dadeville belts as higher grade gneisses and schists of the Carolina Series. Subsequently, his Dadeville Belt was subdivided into an Inner Piedmont Belt and a Charlotte Belt (Hatcher, 1972; Williams, 1978; Snoke, 1978).

The 'belt' subdivisions were based more on general appearance and interpretative license than on lithology. For example, the Kings Mountain Belt, Pine Mountain Belt, Carolina Slate Belt, and much of the Charlotte Belt consist of lithologically similar metasedimentary and metavolcanic rocks. The differences between belts appear to relate more often to changes in structure and metamorphic grade than to changes in lithology. Despite wide usage of the belt terminology in recent years, most of the belts remain poorly defined and their mutual relations largely conjectural. The following geologic synthesis continues, necessarily, the use of belt terminology in referring to previous work, but it emphasizes lithology and metamorphic history. References to poorly defined belts, like the Charlotte Belt, should diminish in the future as reconnaissance regional syntheses give way to syntheses based on detailed lithology and structure.

The first systematic lithologic mapping in East-Central Georgia began in 1964 during a mineral resource survey of 13 Central Savannah River Area (CSRA) counties, six of which are in the East-Central Georgia District. Results of the CSRA study were incorporated in a two-volume report (Hurst, et al., 1966a and 1966b), and a series of county geologic maps (Hurst and Crawford, 1968a-1968f). Since then, reconnaissance mapping has been reported for Greene and Hancock Counties (Humphrey, 1970; Geologic Map of Georgia, 1976). More detailed mapping has been done in several small areas (Hurst, 1959; Medlin, 1964; McLemore, 1965; Fouts, 1966; Cook, 1967; Medlin and Hurst, 1967; Humphrey, 1970; Paris, 1975; Rosen, 1978; Reusing, 1979; Goldstein, 1980; Davis, 1980; Fay, 1980; Potter, 1981; Davidson, 1981; Roberts-Henry, 1982; Delia, 1982; Lovingood, 1983; Murphy, 1984; Vincent, 1984; Young, 1985). The small areas of detailed mapping, mainly by graduate students at the University of Georgia, total about five percent of the District.

All available geologic maps have been reduced to a common scale and synthesized to form a composite map of the district. Some geologic units

of the original maps have been combined on the composite map. Initial units consisting of a single rock type or a well-characterized group of related rocks, however, have been retained. The resulting geologic map (Plate A) is a partial lithologic synthesis of work available through early 1985.

LITHOLOGY

Metamorphic Rocks

Metavolcanics and associated metasediments of the Little River Series crop out over most of the district, their metamorphic grade varying from greenschist to amphibolite facies. Where the rocks have undergone little pervasive deformation and where recrystallization has caused only minor coarsening, original structures and textures are well preserved. In central and southern Lincoln County, shards, amygdules, corroded phenocrysts, pumiceous and tuffaceous textures, and other features characteristic of volcanic rocks are readily apparent, as well as bedding, graded bedding, scour-and-fill, and other structures. Similar features are preserved at other places in the district, though generally not as strikingly.

A stratigraphic section, more than 4,000 meters thick, has been described in Lincoln County (Whitney, et al., 1978). The oldest unit, the Lincolnton Metadacite, originally consisted of rhyodacitic to dacitic flows, with lesser mafic flows, mafic and felsic tuffs, and sediments. The principal rock type is porphyritic metadacite. This unit is more than 1500 meters thick. It is cut by numerous metamorphosed mafic and felsic dikes, and by unmetamorphosed lamprophyre, basalt, rhyolite, and diabase dikes. Rb-Sr whole rock isochrons and U-Pb analysis of zircons indicate a 560-570 m.y. or Early Cambrian age for the metadacite (Carpenter, et al., 1978).

Overlying the Lincolnton Metadacite is a pyroclastic sequence about 1000 meters thick (Figure 2), dominated by metamorphosed crystal tuffs, lapilli tuffs, and dacitic tuffs. Interbedded rocks include metamorphosed tuffaceous graywackes, argillites, and cherts. Above the pyroclastic sequence, and gradational to it, is a thickness of more than 1500 meters of mainly banded argillites with interbedded mafic metavolcanics and meta-graywackes. From similar rocks near Batesburg, South Carolina, 30 miles to the northeast, an assemblage of Middle Cambrian trilobites has been described (Secor, et al., 1983).

Lithologically-similar metamorphic rocks are found throughout most of the district, though they differ a little, areally, in metamorphic grade, type or

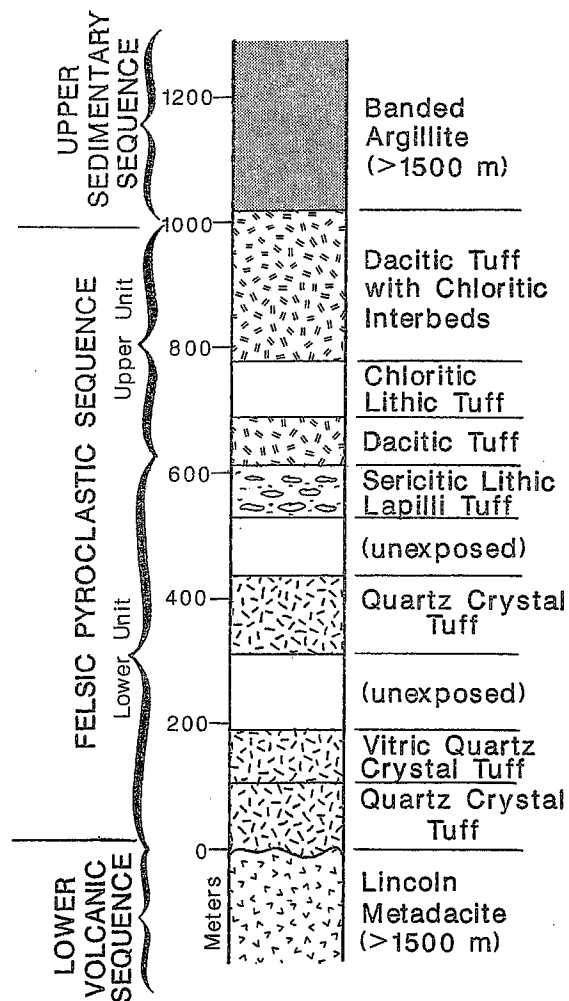


Figure 2. Representative stratigraphic section of the Little River series at the headwaters of Wells Creek near Lincolnton, Georgia (from Whitney, et al., 1978).

degree of deformation, and stratigraphic detail. Where protolithic textures are clearly preserved, the rocks are recognized as mainly phyllites, felsic metavolcanics, mafic metavolcanics, metagraywackes, and metacherts. Where original textures have been largely obliterated, the rocks are mica schists, quartz-sericite schists, amphibolites, various quartzo-feldspathic gneisses, and quartzites.

Previous subdivisions of these rocks into the Charlotte, Little River, Uchee, Kiokee, and Belair 'Belts' have proven to be largely artificial. Crickmay (1952) described the Belair Belt as "an exact replica of the Little River Belt." The equivalence, or near-equivalence, of these two belts and the Carolina Slate Belt has been generally accepted (King, 1955; Hurst, et al., 1966a and 1966b, Chowns, 1976; Howell and Pirkle, 1976; Carpenter, 1976; Maher,

1979). Lithologic similarity of the Carolina Slate and Charlotte Belts has been well noted (Secor and Wagener, 1968; Overstreet, 1970; Lawrence and Chalcraft, 1980), and their stratigraphic and structural continuity recognized (Hurst, et al., 1966a and 1966b; Secor, et al., 1983). Similarities in the lithologic, metamorphic, and structural features of the Charlotte, Uchee, and Kiokee Belts have been noted repeatedly (Crickmay, 1952; Hatcher, 1972; Chowns, 1976).

Rocks that have come to be regarded as characteristic of the Carolina Slate Belt terrane underlie all of the central part of the district in Lincoln, Wilkes, Taliaferro, Warren, and Hancock Counties. The Carolina Slate Belt does not terminate in this area, as several have suggested, but continues southwestward past Macon almost to Talbotton (Higgins, et al., 1984).

Metamorphic rocks, once thought to be distinctly different from those in the Carolina Slate Belt (Crickmay, 1952) but sometimes regarded as stratigraphic equivalents (Tewhey, 1977; Snoke, et al., 1980), are in the Kiokee belt. The accompanying geologic map (Plate A) shows the northern boundary of what has been called the Kiokee Series (McLemore, 1965) along the lower course of Keg Creek in northern Columbia County. Westward, the boundary runs parallel to and about 2.5 miles south of the Lincoln-Columbia County line, then arcs southwestward across central McDuffie County and the upper panhandle of Warren County. This is several miles south of where Williams (1978), Snoke (1978), and others have drawn it. Rocks that might be correlative extend from northern Putnam County northeastward across central Greene County to northern Taliaferro County, reappear farther northeast in southeast Elbert County, and extend on toward the southeast in South Carolina. Their possible equivalence has long since been recognized (Crickmay, 1952; Overstreet and Bell, 1965). The stratigraphic relationship between Kiokee rocks and those in the Carolina Slate Belt is obscured in this district by faulting and cataclasis, but northeastward in South Carolina they are gradational (Secor and Snoke, 1978). Overstreet and Bell (1965) and Howell and Pirkle (1976) also have suggested that Kiokee rocks grade upward into Carolina Slate Belt rocks.

The most prevalent Kiokee lithology is fine- to medium- grained biotite gneiss, most of which probably originated as sediments and felsic volcanics. Other principal rock types are orthogneiss, adamellite, hornblende gneiss, amphibolite, chloritic amphibolite, garnetiferous quartz-muscovite schist (in the northern part of the belt), quartzite, and serpentinite. Sillimanitic schist and gneiss are sparingly associated with some of the larger adamellite plutons, where the sillimanite commonly formed at the expense of biotite (McLemore, 1965). The serpentine bodies are structurally segmented and highly altered. They are associated with garnetiferous magnetite quartzites (metacherts?) and gneisses whose protoliths might have been spilites. Such an association is characteristic of ophiolites.

If generally accepted structural interpretations are correct, the Kiokee rocks stratigraphically underlie the Carolina Slate Belt rocks, and the metaserpentinites may be the oldest rocks exposed in the district. These general stratigraphic relationships are consistent also with the new tectonostratigraphic interpretations of Higgins and others (1984).

PLUTONIC ROCKS

At least 50 relatively large plutons of Alleghenian age (330-260 m.y.) are scattered from Maryland to Georgia (Sinha and Zeitz, 1982) within and around the Charlotte-Carolina Slate-Kiokee Belt terrane. Geophysical data indicate that more are to the south, beneath overlapping Coastal Plain sediments. As shown by the regional compilation of Williams (1978), most Alleghenian intrusives are peripheral to the Carolina Slate Belt, so they are mostly peripheral to the East-Central Georgia District, which is near the southwestern end of the Charlotte-Carolina Slate-Kiokee terrane.

Within the East-Central Georgia District, Alleghenian plutons were intruded into rocks that already had been deformed and metamorphosed to greenschist or amphibolite grade. Contact metamorphic effects are common but generally not striking. Below is a brief description of the larger Alleghenian granitic intrusives. Notably, all of the coarsely porphyritic plutons are oval-shaped, and their long axes trend northeast at a high angle to the regional trend (Plate A).

Danburg Granite

The oval-shaped Danburg granite occupies about 125 square km in northeastern Wilkes County. It is a coarse-grained, porphyritic quartz monzonite (Whitney and Stormer, 1977). Euhedral alkali feldspar phenocrysts up to 2 cm across, commonly showing overgrown plagioclase in a rapakivi texture, are enclosed by medium- to coarse-grained, euhedral plagioclase, anhedral quartz, and euhedral biotite, with minor sphene and rare hornblende (Whitney and Stormer, 1977). Feldspar crystallization temperatures range from 780° to 690° C. The temperature calculated from the exsolved phases of the perthites is around 400° C. A Rb-Sr whole rock age of 295 \pm 2 m.y. has been reported (Fullagar and Butler, 1974). Joints are poorly developed in this massive pluton. Pegmatites are small and scarce. Cross-cutting quartz veins are notably scarce.

Appling Granite

About 5 km southeast of Appling, in Columbia County, a porphyritic granite like that at Danburg has intruded, and contains large inclusions of older, non-porphyritic granites and granitic gneisses. Its outcrop area is about 30 square km. Associated pegmatites are sparse and generally less than 12 cm thick. Quartz veins are scarce. Some sillimanite is associated with the vein quartz and pegmatites.

Siloam Granite

The Siloam granite is exposed over most of the southern half of Greene County (Vincent, 1984). It is a heterogeneous body of granite somewhat similar to the Danburg granite. In the porphyritic coarse-grained part, the alkali feldspar phenocrysts are larger than in the Danburg granite, up to 5 cm across, and show a strong flow foliation (Whitney and Stormer, 1977). The matrix is non-foliated. A medium-grained phase, gradational to the porphyritic phase, makes up nearly a fourth of the pluton. Additional phases are (1) fine-grained, (2) coarse-grained but not porphyritic, and (3) garnet-bearing. There is no indication of pervasive post-intrusion metamorphism. Feldspar crystallization temperatures range from 730° to 660° C. Temperatures calculated from the exsolved phases of perthite are around 400° C. Recrystallization, accompanying slow cooling, apparently destroyed the original alkali feldspar composition. Jones and Walker (1973) defined a whole rock Rb-Sr isochron of 269 ±3 m.y. The age is nearly concordant, suggesting rapid cooling after emplacement.

Sparta Granite

The Sparta granite intrudes metavolcanic rocks and granitic gneisses in southern Hancock County. It is a heterogeneous intrusive, chiefly a medium- to coarse-grained, equigranular rock composed of quartz, oligoclase, microcline, and biotite, with minor hornblende in the southern part of the mass (Roberts-Henry, 1982). Accessory minerals are sphene, iron-titanium oxides, apatite, and zircon. The Sparta granite is an igneous complex formed by multiple magma injections. An age of 295 ±2 m.y. was reported by Fullagar and Butler (1979).

Elberton Granite

Along the northern edge of the district, in Oglethorpe and Elbert Counties, is the Elberton granite, a fine-grained, equigranular rock composed of about equal proportions of quartz, microcline, and plagioclase. Minor components are biotite, muscovite, allanite, and occasionally sphene. The minor opaque minerals, in order of decreasing abundance, are hematite-ilmenite, ilmenite-hematite, and magnetite (Whitney and Wenner, 1980). A very fine opaque phase (magnetite?) is scattered throughout the feldspar and is responsible for the gray color. Where the granite is pink, this phase is replaced by hematite. The reported radiometric ages are 450-490 m.y., based on ²³⁵U/²⁰⁷Pb, and ²⁰⁷U/²⁰⁶Pb of separated zircons

(Gruenenfelder and Silver, 1958). K/Ar data from micas indicate about 250 m.y. (Fairbairn, et al., 1960). Whitney and Wenner (1980) reported a 350 ±11 m.y. age based on a well defined Rb-Sr whole rock isochron and a 320 ±20 m.y. age based on U/Pb of zircon. Most studied samples have come from the northern part of the pluton, where all quarries are located, from stone carefully chosen by quarrymen for homogeneity and freshness. Prominent evidence in other areas of stoping and assimilation, xenoliths of what might be related, earlier intrusives, and significant post-crystallizational alteration suggest a somewhat more complex history than has been presented so far in the literature.

Delhi Syenite

Along the contact between the Danburg granite and the Little River Series are three small syenite plutons. The largest is about 1.5 miles north of Delhi. It is circular in plan and a little more than a kilometer in diameter. The other two syenite plutons, too small to be shown on Plate A, are southwestward from the Delhi pluton and are along the margin of the Danburg granite.

Other Intrusives

Small intrusives, mainly dikes and sills, of metarhyolite or metadacite, metaandesite, metabasalt, and metagabbro, are found throughout the area. They are particularly abundant in central Lincoln County.

Unmetamorphosed dikes include Triassic or Jurassic diabases and lamprophyres.

STRUCTURE

The structural trend is northeast in the northern part of the district and east-northeast in the southern part (Plate A), with variations due to folding and faulting. The prevailing dip of foliation is steep northwest to southeast in the northern part of the district, and southeast in the southern part. Folding generally is tight and isoclinal. In central Lincoln County tight vertical folds plunge north-eastward (Whitney, et al., 1978).

According to several interpretations, the Carolina Slate Belt is essentially synclinal (McCauley, 1961; Overstreet and Bell, 1965; Sundelius, 1970), the Kiokee belt is anticlinal (Howell and Pirkle, 1976), and possible Kiokee equivalents along the northern part of the district also are anticlinal (McCauley, 1961; Overstreet

and Bell, 1965). These major folds plunge north-eastward and become somewhat more open in South Carolina than they are in Georgia. South-westward, they narrow and appear to close in a series of smaller, tight, interfingering folds. Most of the main pattern of folding developed before Ordovician metamorphism, 495-470 m.y. ago (Kish, et al., 1979), and since 525 m.y., an age of the older metamorphosed rocks (Butler, 1979). The fold pattern has been modified by extensive post-Taconic faulting. Figure 3 outlines the temporal relations of volcanism, metamorphism, intrusion, and tectonism in this area.

Strong post-Taconic cataclasis is apparent in a wide zone across northern Columbia County, in Kiokee rocks as well as in the Little River Series along the Lincoln-Columbia county line (McLe-more, 1965). The north edge of this zone appears to be continuous with the Modoc Fault in South Carolina (Daniels, 1974; Howell and Pirkle, 1976). The Modoc Fault fades out northeast of Batesburg, South Carolina, where the contact between Carolina Slate Belt and Kiokee rocks becomes gradational through a wide almandine garnet zone (Secor and Snoke, 1978).

Other northeast-trending cataclastic zones are shown in the western part of the district by the Geologic Map of Georgia (1976). The prominent Middleton-Lowndesville Fault (Rosen, 1978) crosses the northern part of the district, and the Augusta Fault crosses the southeast edge. These and many smaller faults, mostly unmapped, attest to major tectonism postdating Ordovician deformation and regional metamorphism. The larger post-Taconic faults appear to relate to Late Paleozoic Alleghenian tectonism (Prowell, 1980; Snoke, et al. 1980).

According to a new structural interpretation (Higgins, et al., 1984, 1986) the metamorphic rocks exposed in the East-Central Georgia Gold District are parts of an allochthonous thrust stack (autochthonous to Africa). The uppermost thrust sheet in this stack is the Little River Allochthon, to which the Little River Series belongs. Beneath the Little River Allochthon is an enormous melange, the Macon Melange, consisting of three principal "slices," the Potatoe Creek slice, Juliette slice, and Po Bidy slice. The Potatoe Creek slice includes what has been called the Belair Belt, Uchee Belt, and part of the Kiokee Belt. Another part of the Kiokee Belt and parts of the Inner Piedmont and Charlotte Belts are included in the Juliette slice. The Po Bidy slice is interpreted as Iapetus ophiolite. It includes the serpentinites in Lincoln County and other ultramafics scattered through the outcrop belt of the Juliette slice between Forsyth and Middleton. A generalized

geologic map of the Macon Melange and the Little River Allochthon in east-central Georgia is presented as Figure 16 in Higgins and others, (1984).

According to this new interpretation, the assembly of the Little River thrust stack took place from Africa towards the North American craton, from bottom to top, as its sheets were thrust upon the already assembled and moving Georgiabama Stack. Thrusting took place continuously from about Middle Ordovician through Carboniferous time and is thought to account for most of the deformation. Burial caused by the moving thrust sheets and thrust stacks is thought to account for most of the metamorphism.

METAMORPHISM

Pelitic metasediments with Al_2O_3/K_2O+Na_2+CaO high enough to allow crystallization of the principal metamorphic index minerals are well distributed throughout the district. Any major change in metamorphic grade, therefore, should be apparent from changes among the index minerals.

An area subjected to a single period of regional metamorphism might show a clear zonal distribution of index minerals; the pattern modified, perhaps, by postmetamorphic deformation. In this district the pattern has been complicated by polymetamorphism and polydeformation. Isograds generated during the first regional metamorphism, in Early Ordovician time, have been overprinted to some extent by one or more younger metamorphic events, and disrupted by subsequent deformations. The overall pattern of the first event still is clear on a regional scale, but is less distinct on the district scale.

Available information on the distribution of metamorphic index minerals is shown in Plate B. Note that percentages in the Plate refer not to whole alluvium but to the non-magnetic, heavy portion (S.G. V 2.8) of the -32+60 mesh fraction of the alluvium. The alluvial minerals originated locally; except in the colored area of Plate B; where streams might have acquired at least a portion of their alluvium from overlying Coastal Plain sediments.

Sillimanite is found abundantly in: (1) the northern part of the district, and (2) in northeastern Columbia County, where sillimanitic gneisses and schists of sedimentary origin crop out conspicuously. Elsewhere, sillimanite is more scarce, largely peripheral to intrusives, and appears to be a contact metamorphic mineral. In the areas of abundant prograde sillimanite, both andalusite and kyanite are scarce.

Coarse-bladed kyanite crops out conspicuously at four locations, identified on Plate B. At

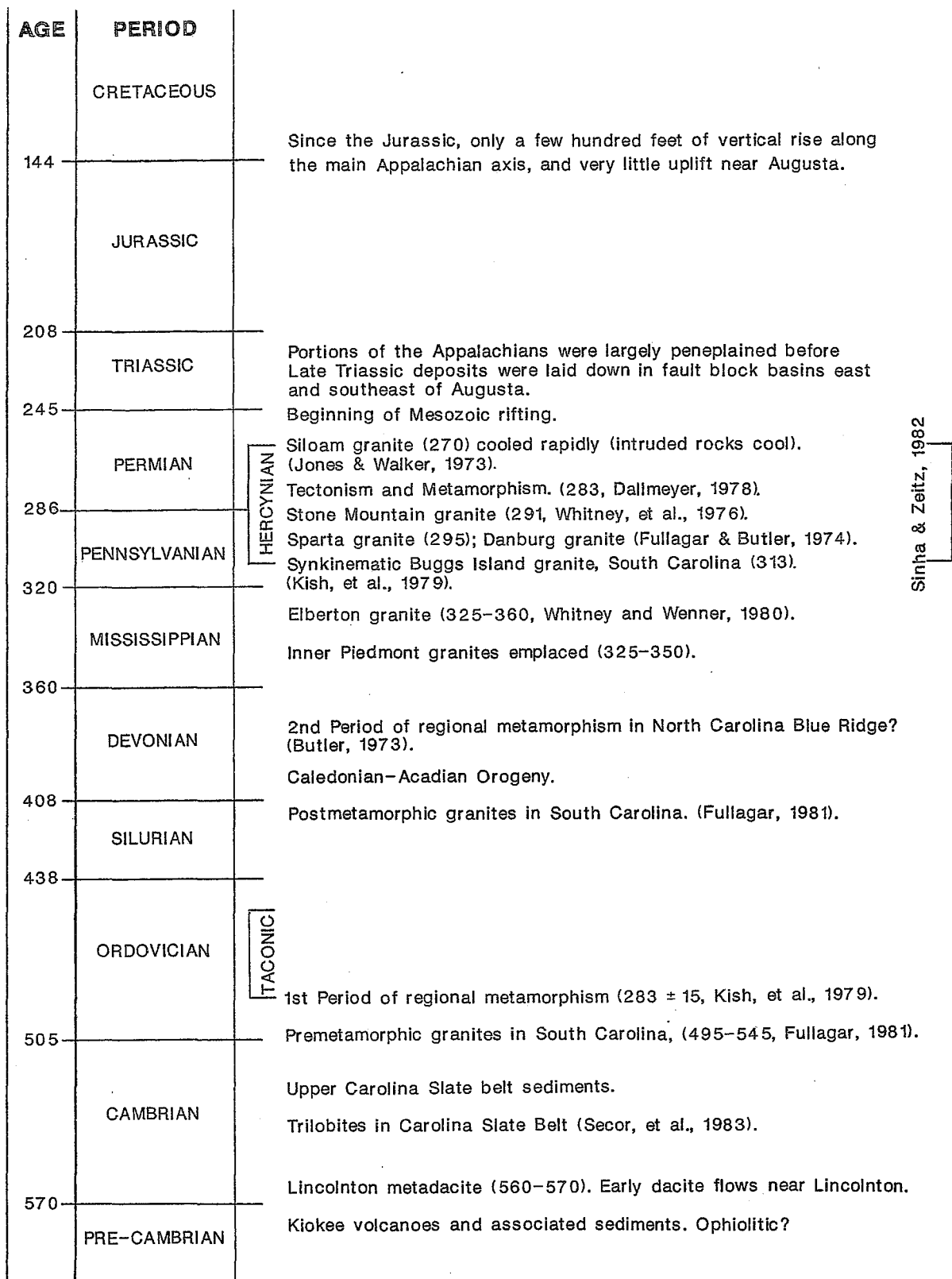


Figure 3. Chronologic chart of principal events in southeastern United States, Precambrian to Cretaceous. Ages from Jones and Walker (1973), Fullagar and Butler (1974), Whitney, et al. (1976), Dallmeyer (1978), Butler (1979), Kish, et al. (1979), Whitney and Wenner (1980), Fullagar (1980), Sinha and Zeitz (1982), and Secor, et al. (1983).

many other places the kyanite is too fine-grained for megascopic identification at the outcrop, but still is detectable in fine alluvium and in thin sections.

Megascopic andalusite has been reported at only two locations, both on Graves Mountain: (1) 30 meters east of the highest summit (now removed by mining) where it was found as small white to gray inclusions in lazulite crystals, associated with mica and kyanite, and (2) 120 meters farther to the northeast where it was found as a minor constituent of thin flesh-colored veinlets transecting the quartz-kyanite rock (Hurst, 1959). Microscopic andalusite is a common, though minor, constituent of alluvium within the kyanite zone. How it formed is still to be established. Possibilities are that it formed (1) as a contact metamorphic mineral along the margins of intrusives, (2) as a prograde mineral where pressure was low enough for rising temperature to move the metamorphic field gradient to the kyanite-andalusite inversion curve, or (3) retrogressively after load pressure had decreased.

Coarse staurolite schists crop out in northeastern Warren County. Metasediments containing sufficient iron and aluminum for staurolite to crystallize are uncommon, so the scarcity of staurolite schists in other parts of the district probably relates not to the absence of staurolite grade metamorphism but to the scarcity of rocks with the requisite composition.

The distribution of metamorphic index minerals reveals a kyanite zone, between the kyanite and sillimanite isograds, across the central part of the district. An adjoining sillimanite zone extends across northern Lincoln, Wilkes, and Taliaferro Counties, and another across northern Columbia County. Lower grade rocks are in central Lincoln County and northern Warren County (see Plate B). Along a NW-SE line on the east side of the district, metamorphic grade drops from sillimanite grade in northern Lincoln County to kyanite grade in the central part of the county and to lower grade for several miles, then rises to kyanite grade in southern Lincoln County, and to sillimanite grade in Columbia County. The grade decreases to the southeast. Along a NW-SE line on the west side of the district, metamorphic grade drops from sillimanite grade in northern Taliaferro County to kyanite grade in the central part of the county and to staurolite grade in northern Warren County, then rises to kyanite grade in McDuffie County, and farther southeast rises to sillimanite grade in Columbia County. This is a remarkably regular series of metamorphic changes, complicated only by faulting along the Modoc Fault and other probable faults south of it (not delineated on Plates A and B).

Short segments of a sillimanite isograd and an oligoclase isograd traced by Paris (1975) are represented by heavy dashed lines in Plate B. Extensions of these isograds, based mainly on the distribution of alluvial minerals, are represented by dotted lines.

The kyanite-sillimanite grade rocks developed during Ordovician regional metamorphism. The time of metamorphism is bracketed by 500 m.y. old pre-metamorphic granites and 415 m.y. old post-metamorphic granites that transect the Carolina Slate Belt rocks in South Carolina (Figure 3). Ordovician metamorphism in this area probably was concurrent with regional metamorphism in the Albemarle area of North Carolina, dated as 483 ± 15 m.y. (Kish, et al., 1979).

After the first period of regional metamorphism and tectonism, the grade and intensity of which increased to the northwest, a suite of 415- to 385-million-year-old late- to postkinematic plutons was emplaced in what has been called the central and northwestern parts of the Charlotte Belt (Secor, et al., 1983). An example of this group in Georgia is the Elberton granite. Most of these plutons are clearly postmetamorphic. Plutons of similar age located along the east side of the Carolina Slate Belt commonly show evidence of Alleghenian metamorphism and deformation.

During the Alleghenian Orogeny, more than 20 granitic plutons were emplaced in the central and eastern Piedmont of the southeastern Appalachians (Fullagar and Butler, 1979). Examples in east-central Georgia are the 300 m.y. old Danburg and Sparta granites and the 270 m.y. Siloam granite. Widespread tectonism accompanied and followed Alleghenian magmatism. Examples of early to synkinematic Alleghenian granites are the Lake Murray gneiss, Batesburg gneiss, and Lexington granite (313 ± 24 , 291 ± 4 , and 292 ± 15 m.y., respectively) of South Carolina (Snoke, et al., 1980). The younger Alleghenian granites appear to be undeformed. An example is the Edgefield granite (S.C.), which gives a Rb/Sr isochron of 254 ± 11 m.y. (Metzgar, 1977). Alleghenian regional deformation and metamorphism are particularly intense in the southeastern Piedmont of South Carolina (Secor and Snoke, 1978; Fullagar and Butler, 1979), where Alleghenian folds, cleavages, and amphibolite-grade metamorphism strongly overprinted the older Ordovician fabric. The grade of Alleghenian metamorphism has been reported as increasing to the southeast (Secor, et al., 1983). In east-central Georgia the extent of the Alleghenian overprint has not been deciphered. The notable discordance between oligoclase isograds in Lincoln County, the sillimanite isograd in northern Columbia and

McDuffie Counties, and the regional structural trend might be a result of Alleghenian metamorphic overprint and tectonism. The zeolitization so prevalent in this district postdates Ordovician metamorphism and probably is Alleghenian, because it is noticeable along young fractures that cross-cut both igneous and metamorphic rocks.

In the Piedmont of southeastern United States, the distribution pattern of high-alumina minerals that formed during Ordovician metamorphism has been complicated by postmetamorphic folding and faulting and younger metamorphism, but enough of the early pattern remains to reveal the regional trends and the physical conditions that prevailed. Within a 50-mile-wide zone, astride the Kings Mountain Belt in Figure 5, sillimanite is the predominant Al_2SiO_5 polymorph. Toward the southeast, sillimanite vanishes and kyanite is the prevalent form. The sillimanite isograd across Lincoln and Wilkes Counties continues northeastward into South Carolina and with some convolution continues across North Carolina. Along this isograd, regional temperatures were along the kyanite-sillimanite inversion curve, and were at least $480^\circ C$ (Figure 4). Along the southeast edge of the Piedmont, kyanite and andalusite commonly are associated, which suggests P-T conditions along the kyanite-andalusite inversion curve, or regional temperatures of $370-480^\circ C$. Between the two kyanite zones is a wide belt of lower grade metamorphic rocks in which pyrophyllite is widely distributed. Andalusite sometimes is associated with the pyrophyllite in this belt. Farther southeast, pyrophyllite is more apt to be associated with kyanite, or with andalusite and kyanite. P-T conditions for the reaction $Pyrophyllite = Andalusite$ (or kyanite) + 3 Quartz + H_2O are shown in Figure 4 by Curve 5. The association at several places of pyrophyllite with andalusite, or pyrophyllite with kyanite, or andalusite with kyanite, suggests that physical conditions were near the intersection of Curve 5 with the kyanite-andalusite inversion curve, and that temperatures were within the range of $350-380^\circ C$.

The regional distribution of Al_2SiO_5 polymorphs and pyrophyllite is compatible with a temperature range within the East-Central Georgia District of as little as $150^\circ C$ during Taconic metamorphism. If, at the onset of early regional metamorphism, the protoliths were essentially horizontal and the thermal gradient was between 25 and $38^\circ C/km$, the observed differences in metamorphic grade could have corresponded to a difference in protolith thickness of 4-6 km, or the difference in load pressure between kyanite-sillimanite and pyrophyllite-kyanite-andalusite assemblages.

In central Lincoln County, Georgia, a 2.5-km-thick metavolcanic sequence is conformably overlain by a 1.5-km-thick sequence of metasediments (Whitney, et al., 1978). In the southeastern part of the South Carolina Piedmont, a 3-km-thick sequence of metavolcanic rocks is conformably overlain by a 5-km-thick sequence of metasediments (Secor, et al., 1983). If the major folding in east-central Georgia followed the peak of Ordovician metamorphism, if the Carolina Slate Belt is essentially synclinal (Overstreet and Bell, 1965; Sundelius, 1970), if the Kiokee belt is anticlinal (Howell and Pirkle, 1976), and if Kiokee equivalents along the northern part of the district are also anticlinal (McCauley, 1961; Overstreet and Bell, 1965), then regional folding and faulting, followed by erosional truncation, could account for the lateral variations now observed in metamorphic grade. Within the area shown on Plate B, major overthrusting would have been required only along the Middleton-Lowndesville Fault, the Modoc Fault, and perhaps lesser faults (not delineated on Plates A and B) south of the Modoc Fault.

If the tectonostratigraphic interpretation of Higgins and others (1984, 1986) is correct; that is, if the rocks in east-central Georgia are a stack of overthrust sheets which accumulated from bottom to top, then the Modoc Fault is at the base of a major thrust sheet, and displacement along the Modoc Fault was greater in South Carolina than in east-central Georgia. These conclusions are apparent from a superposition of the metamorphic isograds of Plate B onto Plate A.

The oligoclase isograd, where albite disappears from epidotic rocks, is widely accepted as the boundary between greenschist and amphibolite facies (Williams, et al., 1982). If this boundary is accepted, most rocks in the East-Central Georgia District belong to the amphibolite facies.

DEPOSITS OF COARSER ALUMINOSILICATES AND THEIR SIGNIFICANCE

In the eastern Piedmont of Georgia, South Carolina, and North Carolina there are scores of aluminosilicate deposits in which the principal mineral is sillimanite, kyanite, andalusite, or pyrophyllite, in addition to quartz. These minerals are widely distributed in gneisses and schists, but at 40 or more sites they are conspicuously coarse or abundant. Locations of the better known sites are shown in Figure 5.

Two origins have been proposed to account for the above-average alumina and silica of these deposits: (1) hydrothermal leaching and (2) weathering (Sykes and Moody, 1978; Zen, 1961;

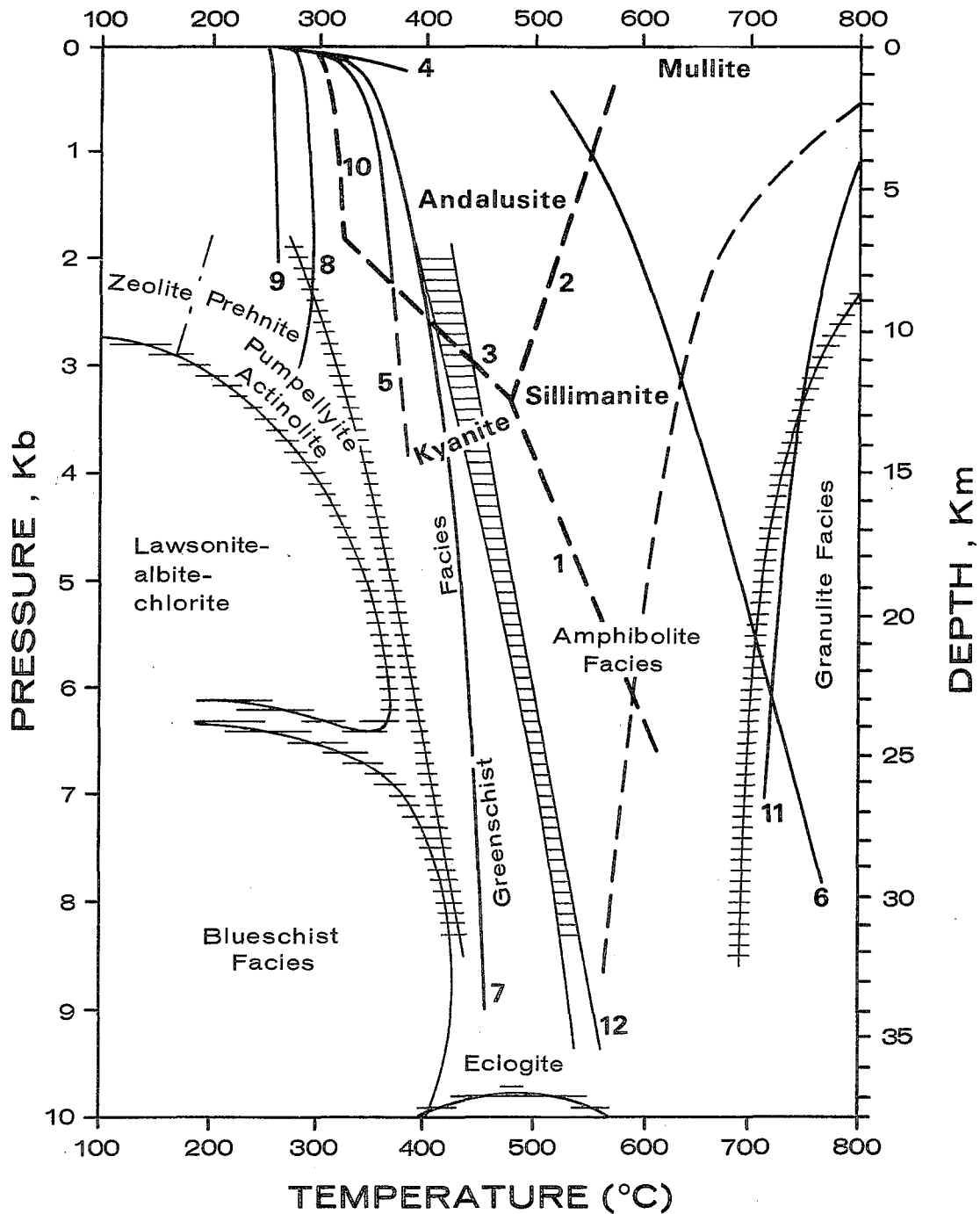


Figure 4. Stability field of kyanite-sillimanite-andalusite and associated minerals in relation to metamorphic grade. Curve 1 is from Day and Kumin (1980). Curves 2 and 3 are from unpublished experimental data of Hurst. Curve 4 is the liquid/vapor curve of water (Handbook of Physics and Chemistry, 1956). Curve 5 is Pyrophyllite = Andalusite + 3 Quartz + H₂O, from Hurst and Kunkle (1985). Curve 6 is Muscovite + Quartz = Sillimanite + K-feldspar + H₂O, from Helgeson, et al. (1978). Curve 7 is Pyrophyllite = Andalusite + 3 Quartz + H₂O, from Hemley, et al. (1980). Curve 8 is 2 Kaolinite = Pyrophyllite + 2 Diaspore + H₂O. Curve 9 is Kaolinite + 2 Quartz = Pyrophyllite + H₂O. Curve 10 is Pyrophyllite + 6 Diaspore = 4 Andalusite + 4 H₂O. Curves 8-10 are from Hurst and Kunkle (1985). Curve 11, the beginning of melting of basaltic rocks, and curve 12, the beginning of melting of granitic rocks, are from Turner (1981). The metamorphic facies boundaries are from Turner (1981).

EXPLANATION

- S - Sillimanite
- K - Kyanite
- A - Andalusite
- p - Pyrophyllite
- d - Diaspore
- t - Topaz

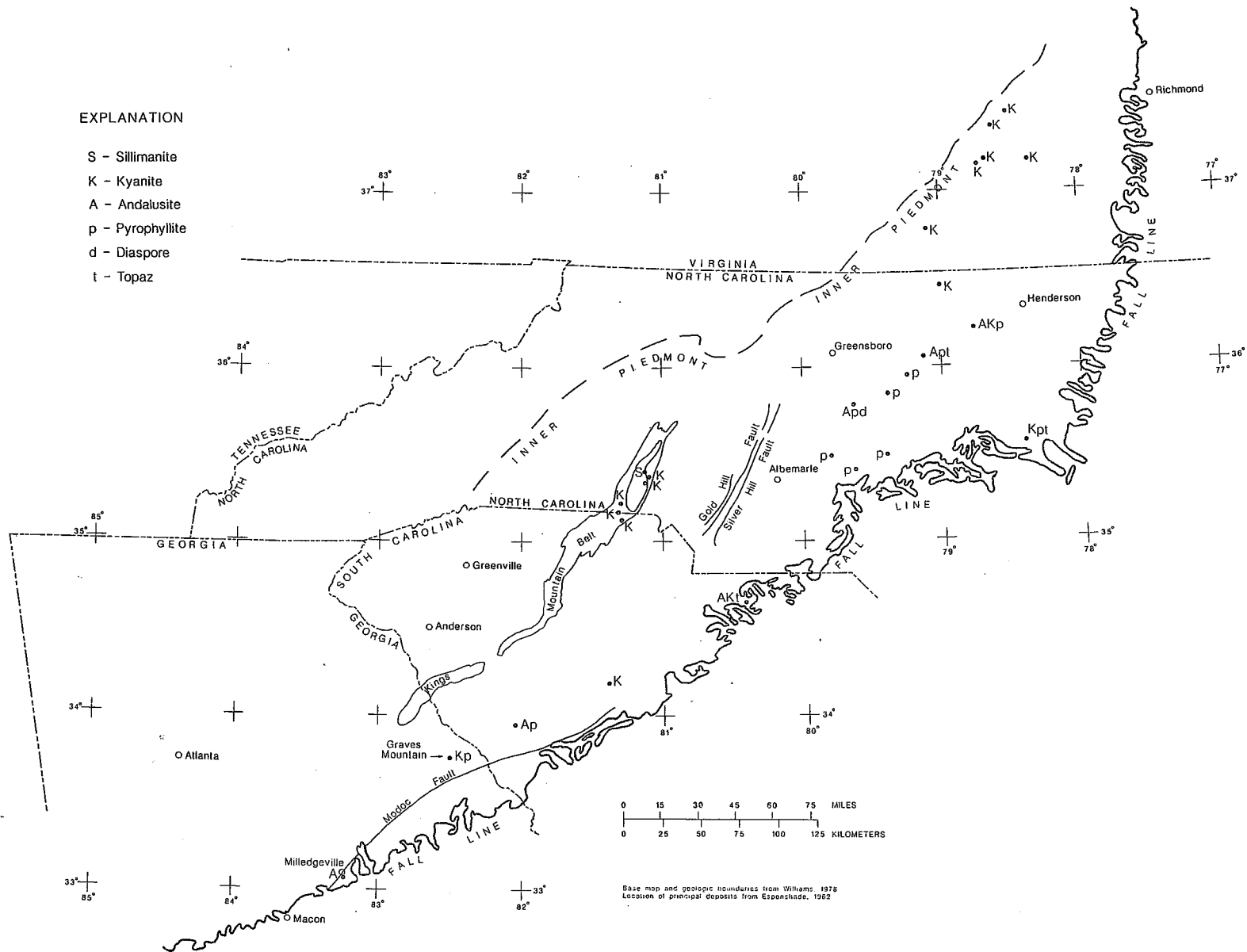


Figure 5. Location of principal aluminosilicate deposits in southeastern United States.

Espenshade and Potter, 1960). According to origin (1), shallow hot spring or fumarolic systems, or possibly geothermal fluids from greater depth, leached volcanic rocks during the waning stage of early Paleozoic volcanism, producing local masses of more aluminous and siliceous alteration products, which were transformed by Taconic metamorphism into the aluminosilicates now observed. According to origin (2), early weathering of volcanic rocks produced saprolite bodies and aluminous sediments which are protoliths of the aluminosilicate assemblages.

Within the last two decades, several geologists have advocated the idea that gold deposits in the Carolina Slate belt originated by the same hot spring or fumarolic activity postulated for the coarse aluminosilicate masses. If these masses do mark sites of early mineralization, then models of modern geothermal systems might be applied as exploration guides (Worthington and Kiff, 1970; Worthington, et al., 1980; Spence, et al., 1980; Carpenter and Allard, 1982; Schmidt, 1985). Both a practical and a scientific interest attaches to the question of whether hydrothermal alteration or weathering generated the protoliths of the coarse aluminosilicate masses.

Field evidence suggests that protoliths of most of the coarse aluminosilicate rocks in the southeastern United States were produced by weathering. The weathering products were eroded and deposited as aluminous sediments. The beds varied in thickness; some were thin and traceable for miles; they were stratigraphically restricted within sequences of sedimentary and volcanic rocks. Their Al_2O_3 contents were above that of average shale (15%) but generally were only moderately high, because the aluminosilicate minerals generally are less than 10% of the rock. In the more conspicuous aluminosilicate masses, Al_2O_3 contents were commonly 30-40% (analyses in Espenshade and Potter, 1960). The coarse aluminosilicate rocks were described by Espenshade and Potter as "metamorphosed high-alumina sedimentary rocks." A few of the thicker and more massive deposits might have been saprolite. Notably, the weathering products were more aluminous than ferruginous, because staurolite is much less common than Al_2SiO_5 minerals.

The less regularly shaped aluminosilicate masses generally are smaller and higher in grade, generally, 10-30% aluminosilicate where they have been mined. Most of them also are bedded, though bedding may be disrupted by faulting and locally obscured by coarsened recrystallization. The deposits at Graves Mountain in Georgia, Boles Mountain, Little Mountain, and the Brewer Mine in

South Carolina, and Pilot Mountain, Hagers Mountain, and Hillsboro in North Carolina have been mentioned as masses whose protoliths might have been produced by hydrothermal alteration.

Graves Mountain Kyanite Deposit

Textures and structures in the Graves Mountain kyanite deposit, Lincoln County, Georgia, reveal several developmental stages (Hurst, 1959). The succession of stages is clear, though little can be deduced about how much time might have elapsed between stages.

The first stage was regional metamorphism of tuffs and associated sediments to amphibolite grade. How much kyanite formed at this stage is not clear. The stratigraphic unit passing through Graves Mountain can be traced several kilometers both eastward and westward from Graves Mountain, and several smaller kyanite bodies are scattered along it. Atop Graves Mountain the kyanite blades are coarse, euhedral to subhedral, and embedded in a matrix of fine- to medium-grained quartz. In zones several feet wide, kyanite constitutes as much as 50% of the rock and may be evenly distributed. Generally, however, it comprises 10-35% and is mainly in close-spaced, planar concentrations that crisscross the rock. Both eastward and westward from Graves Mountain, the size of kyanite porphyroblasts decreases and the rock becomes a fine-grained sericite-kyanite-quartz rock in which the kyanite porphyroblasts are small and ragged.

During the second stage, the recrystallized rocks were cut by a system of fracture cleavages. Acid hydrothermal fluids mobilized aluminum and silicon sufficiently for coarse kyanite to grow. It grew preferentially along fractures, but also along earlier bedding and schistosity planes. Coarse kyanite crystals grew in quartz veins that developed along fractures. Small amounts of andalusite formed in a few veins. Appearance of the andalusite probably connotes a local drop in pressure.

Postdating the growth of kyanite, widely spaced cross-fractures and faults cut the mass. This was the third stage. The temperature had dropped because the first secondary mineral to form along the younger breaks was pyrophyllite, which could not have formed above 300°C (Figure 4). Pyrophyllite grew as coarse rosettes along the breaks, forming pyrophyllite veins, and also where fluids could penetrate the mass and pyrophyllitize the kyanite. Cooling continued. After the mass had cooled below 260°C, hydrothermal fluids were less active, but did produce local strong kaolinization of earlier minerals.

The coarse kyanite at Graves Mountain grew under roughly the same P-T conditions as those which metamorphosed the enclosing rocks, so it could have grown during Taconic metamorphism. Its growth is attributable to acid fluids in a zone made highly permeable by close-spaced fractures and faults. The fact that the earliest recognizable system of fractures cut a fine- to medium-grained rock that deformed brittly suggests that the rock already was metamorphosed before fracturing. The first coarse kyanite crystals grew along these fractures. The principal effect of leaching at Graves Mountain was reduction of alkalis and alkaline earths. Considerable free silica would have been released by the reactions that produced kyanite from earlier Al-bearing minerals; the principal one of which probably was oligoclase. No evidence for a great flux of hydrothermal fluid has been adduced. Though the Graves Mountain rocks might have been leached before metamorphism, as some have postulated, they could have been leached as easily by the same fluids from which the coarse kyanite grew, during or shortly after the peak of Taconic metamorphism.

Hillsborough Andalusite Deposit

A similar succession of stages has been described for the Hillsborough andalusite deposit in North Carolina (Sykes and Moody, 1978). During the first stage, andalusite and topaz porphyroblasts formed during prograde metamorphism. During the second stage, the recrystallized mass was deformed and silicified, with secondary growth of andalusite. During the third stage, the mass was further fractured and deformed, and sericite, pyrophyllite, and quartz grew in fractures. Upon further cooling, kaolinite formed as an alteration product of andalusite and topaz.

A similar sequence of stages can be recognized at the other coarse aluminosilicate deposits.

Conclusions

The protoliths of most of the aluminosilicate masses probably were generated by weathering, or weathering and sedimentation.

The principal aluminosilicate species changes from deposit to deposit sympathetically with changes in regional metamorphic grade (see Figure 5). This implies that these minerals formed during Taconic metamorphism.

Some of the aluminosilicate masses might owe their bulk composition to hydrothermal leaching. It might have taken place during early volcanism, as several have postulated, or much later, during or

shortly after the peak of Taconic metamorphism. In either case, the principal characteristics of these deposits — coarsened aluminosilicate crystals, redistribution with respect to fractures, and abundant quartz — developed where highly permeable ducts or zones were occupied by acid hydrothermal fluids. These fluids could have been generated by regional metamorphism.

Most of the aluminosilicate masses are not associated with gold deposits, but they are similar, otherwise, to the few aluminosilicate masses that are. All of the masses appear to be a product of regional metamorphism and of hydrothermal action along permeable conduits or zones. One major difference is apparent between masses that are and masses that are not associated with gold: hydrothermal fluids responsible for the coarse Al_2SiO_5 polymorphs were active during the Taconic interval, while hydrothermal fluids that generated coarser gold were active during the Alleghenian interval. The evidence for post-Taconic emplacement of gold is presented later on in this Bulletin. To prove that a gold deposit in this area is volcanogenic, it would be necessary to prove that the overall distribution of the gold was established before Taconic metamorphism.

The notion that aluminosilicates react sluggishly and, therefore, are insensitive indicators of P-T conditions is entrenched in the literature. It is based upon the observed sluggishness of experimental reactions carried out under conditions known to inhibit reactions involving aluminum and upon the small free energy differences between Al_2SiO_5 polymorphs. In the presence of acid hydrothermal fluids, the activity of aqueous aluminum is high and reactions involving aluminum are not sluggish (Hurst and Kunkle, 1985). The coarse aluminosilicate masses recrystallized in the presence of acid fluids and are sensitive indicators of P-T conditions. The kyanite-sillimanite association in the Kings Mountain belt (Figure 5) indicates that regional temperatures there were along the kyanite-sillimanite transition and must have been above 480°C. The kyanite-andalusite association at several places to the south, including Graves Mountain, indicate lower regional temperatures. Where pyrophyllite was the principal aluminosilicate in quartzose rocks, the regional temperature was below 330°C.

KNOWN GOLD OCCURRENCES

MINES AND PROSPECTS

All available data on gold mines and prospects are summarized in two earlier reports (Hurst, 1966;

Hurst, et al., 1966a and 1966b). The descriptive information they contain is not recapitulated here. The locations of the principal gold mines and prospects, however, are shown on the Geochemical Anomaly Map (See Information Circular 83).

AURIFEROUS VEINS

The data on veins presented here are taken from Hurst, et al. (1966b). More than 1500 veins were sampled in Columbia, Lincoln, McDuffie, Taliaferro, Warren, and Wilkes Counties. A total of 1410 of these samples were fire assayed, of which 448 samples were found to be auriferous. At a price of \$400/oz. of gold, the assay values for the veins were above \$50/ton at 31 sites, above \$100/ton at 18 sites, and above \$300/ton at 6 sites. The maximum assay was \$1878/ton. Most of the veins assaying more than \$200/ton are in northern McDuffie County; one such site is the old Latimer Mine in northwestern Wilkes County.

Plate C shows that most of the veins were encountered within a 15-mile-wide belt extending NE-SW across the central part of the district. A comparison of Plates A and C shows that the belt of abundant quartz veins coincides with the outcrop area of rocks that are both younger and of lower metamorphic grade than the rocks in which auriferous veins are less common. Veins were encountered much less frequently in the areas where granites are prevalent, and least frequently within the younger granites.

The sampled veins range in width from a fraction of an inch to 10 feet, their frequency increasing logarithmically with decreasing thickness (Figure 6). The length of the longest vein is about 1700 feet. The veins commonly contain pyrite, feldspar and magnetite. Less commonly they contain chlorite, hornblende, epidote, ilmenite, galena, sphalerite, chalcopyrite, and gold. Rarely, they contain scheelite, pyromorphite, covellite, and tellurides. No relationship is apparent between vein size and gold content. While there is a larger number of small auriferous veins, there is an even greater number of small barren veins, and the proportion of auriferous to barren veins does not seem to vary significantly with vein size.

The locations and attitudes of barren (gold not detected by fire assay) and auriferous veins are contrasted in Plate C. Little correlation is apparent between auriferous and barren veins with respect to size, as noted above, nor with respect to location or orientation. For example, in Warren, McDuffie, and Columbia Counties the proportion of auriferous/barren veins is greater than one; while in Taliaferro, Wilkes, and Lincoln Counties the proportion is

much less than one. This proportion is notably higher along the northern parts of Warren, McDuffie, and Columbia Counties. The auriferous veins may have any orientation, but most often they are oriented approximately parallel to or transverse to the regional trend; parallel to the two dominant joint sets in the district.

The proportion of auriferous/barren veins does show some correlation with lithology. The country rocks generally are hornblendic metavolcanics where this proportion is high. At the same time, the proportion shows little correlation with areas of anomalously high gold as represented on the Geochemical Map (See Information Circular 83).

The higher vein gold values, generally, are not in veins which conspicuously crop out. Instead, they are in broken and sheared veins which tend to disintegrate during weathering to superficial quartz rubble, or in small pods and stringers occupying poorly defined mineralization zones.

PHYSICAL STATE OF THE GOLD* IN EAST-CENTRAL GEORGIA

GENERAL REMARKS

Detailed information about the physical state and small scale distribution of gold can be useful at every stage of exploration and development. It can bear initially on the choice of a sampling procedure for reconnaissance field appraisal and it can bear finally on the selection of a commercial extraction method.

For information about the state of the gold in the East-Central District, samples from three occurrences that appear to be representative of the district were investigated with a scanning electron microscope (SEM) equipped for energy dispersive x-ray analysis (EDAX).

An initial examination of many specimens that contained no visible gold demonstrated the difficulty of trying to locate and identify microfine gold at very low concentrations. To find it efficiently, the host rock must be examined at high magnification, under conditions that strongly contrast the gold. This is possible with a high resolution SEM equipped with detectors for backscattered electrons, at a magnification between 2000 and 5000. When an average of 20 submicron grains, or equivalent area, can be examined each second, an average 14 hours of search are required to find one micron-size gold particle in a rock containing 1 part per million (ppm)

*This section was authorized by Kenneth O. Plemons and Vernon J. Hurst.

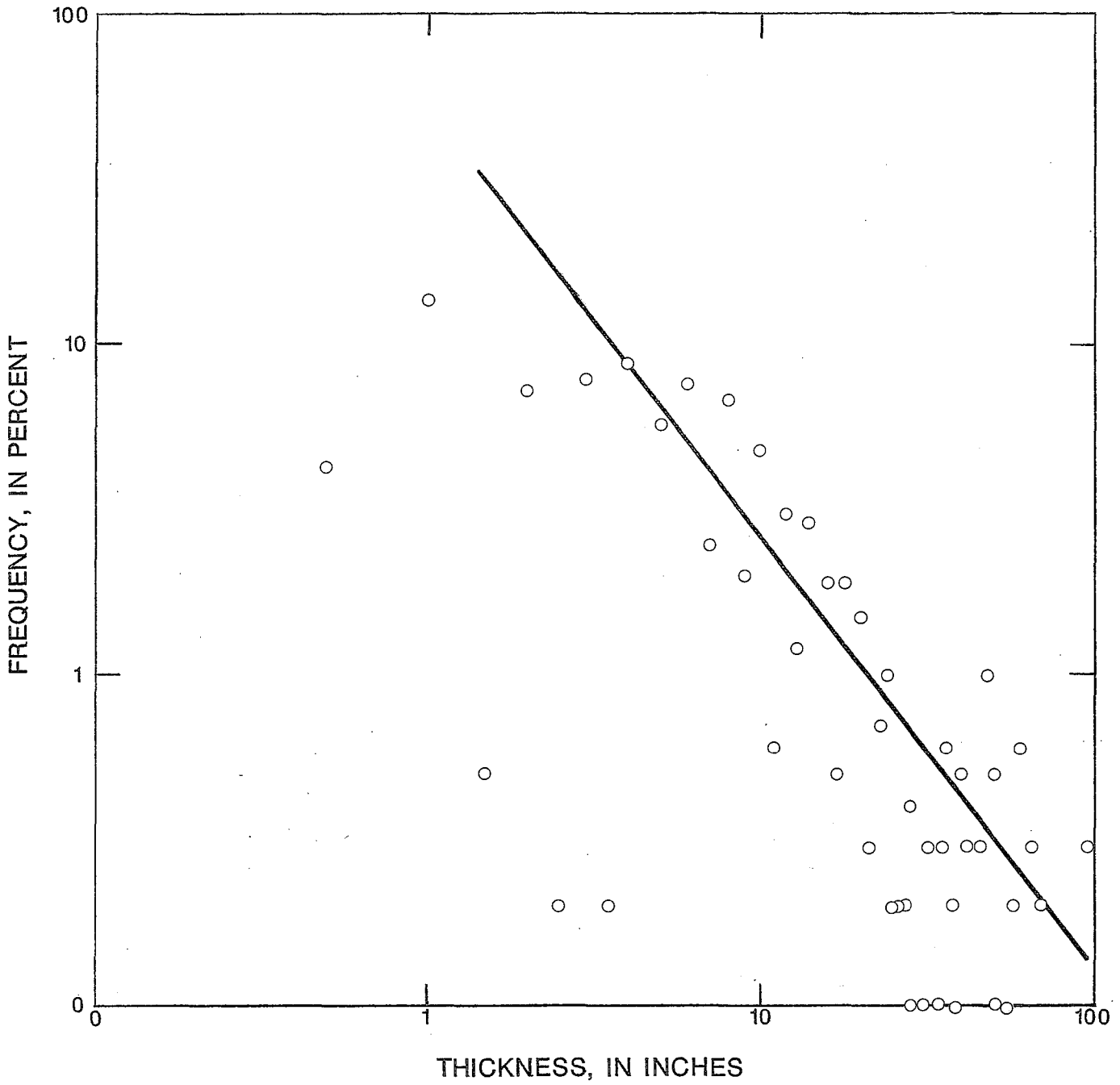


Figure 6. Frequency versus thickness of quartz veins in east-central Georgia.

of gold, and to cover 2 square millimeters of specimen area. The time required for this coverage can be increased a thousandfold when visual identifications have to be verified very often with EDAX. These considerations illustrate the impracticality of seeking information about the state of gold at parts per billion (ppb) concentrations by this method.

To facilitate observation, more auriferous specimens containing very fine-grained gold were collected from the Parks Mine and Landers Prospect in northern McDuffie County and the Latimer Mine in northwestern Wilkes County. These contained from a few ppm to perhaps a hundred ppm gold. Their examination with the SEM provided the data presented below.

Gold at the Landers Prospect, McDuffie County

This prospect is in McDuffie County, a quarter-mile north of the Parks Mine, which is along strike with the Hamilton and Columbia Mines. Two prospect shafts were sunk in 1907 (Jones, 1909), and since then several shallow test pits have been dug. All of the openings appear to have been less than 50 feet deep, and all are collapsed. Samples for this study were collected from a several-ton dump pile near the prospect shafts. The greenish mica common on the dump was identified as fuchsite by an x-ray diffraction (XRD) pattern and an EDAX graph.

Gold was found principally as native gold. Additionally, it was found as a silver-gold telluride and in small masses of auriferous silica where the gold was below the resolution of the SEM (about 100 Angstroms).

The native gold is in quartz veins, where it is mainly along micro-fractures and vugs. Other vein minerals are pyrite, limonite (representing altered sulfide), galena, chalcopyrite, covellite, and fuchsite. The gold particles are mostly irregularly shaped but occasionally are in the form of euhedral crystals, particularly in micro-vugs, and range in diameter from about 1 mm to 4 microns. Finer, discrete particles were not found, despite extended search. The gold typically is molded against enclosing or supporting minerals, an indication that it is younger. Where a molding mineral has been broken away, a replica of its surface texture and shape commonly remains on the gold. Because gold more frequently formed in contact with quartz, pyrite, and muscovite, gold more frequently preserves a replica of one of these minerals.

Quartz associated with the gold commonly is etched, and the degree of etching varies from place to place. At high magnifications the etched surfaces

appear pitted, dimpled, or grooved. Close examination of many contacts disclosed that gold sometimes was deposited on unetched fractures and sometimes on etched fracture surfaces. Occasionally it was deposited around, and now partially encloses, small euhedral quartz crystals (Figure 7). The way the gold is found in contact with uneven, planar, etched, and unetched quartz suggests multiple fracturing and more than one stage of quartz growth, etching, and gold deposition.

Rarely, an irregularly shaped mass of auriferous silica was found between gold and quartz (Figure 8). It appeared grooved in a manner reminiscent of microbanding (Figure 9), but x-ray mapping did not resolve any compositional layering. Spot EDAX showed that it is mainly silica and, unlike the bounding quartz, strongly auriferous. The contacts between auriferous silica and quartz are sharp and, generally, even; while the contacts between auriferous silica and gold are typically irregular. Interestingly, spot EDAX showed no gold in quartz adjacent to the auriferous silica but did show Si in adjacent native gold. Since gold silicate has not been reported as a naturally-occurring mineral and is not theoretically expectable (see later section on "Geochemical Behavior of Gold"), the gold in this auriferous silica probably is very finely dispersed; its size is too small to be resolved with the SEM.

Some gold particles are in contact with limonite pseudomorphous after pyrite (Figures 10 and 11). The limonite is very porous and reddish to dark brown. Surfaces of gold in contact with limonite commonly are casts of planar, striated surfaces, like those of pyrite crystals, and not like the porous surfaces of limonite. Small-scale undulations and micro-pitting, sometimes preserved on the gold replicas of pyrite faces, suggest that pyrite might have undergone slight alteration before or during deposition of the gold, but no gold cast of a limonite surface has been found. The observed textural relations indicate that the gold was deposited against pyrite before the limonite pseudomorphs after pyrite developed.

Small cubic voids, occasionally seen in gold particles, are molds of an earlier mineral, probably pyrite, that has been dissolved and removed. Whether the alteration of pyrite results in a void or a porous residual mass of hematite-goethite depends upon alteration conditions. When pyrite is oxidized by interaction with only air and water, with limited hydrolysis, one mole of pyrite can yield one mole of ferrous sulfate and one mole of free acid, half of which can be oxidized to ferrous sulfate; in which case all of the iron in the altering pyrite can be exported as soluble ferric sulfate, leaving an empty

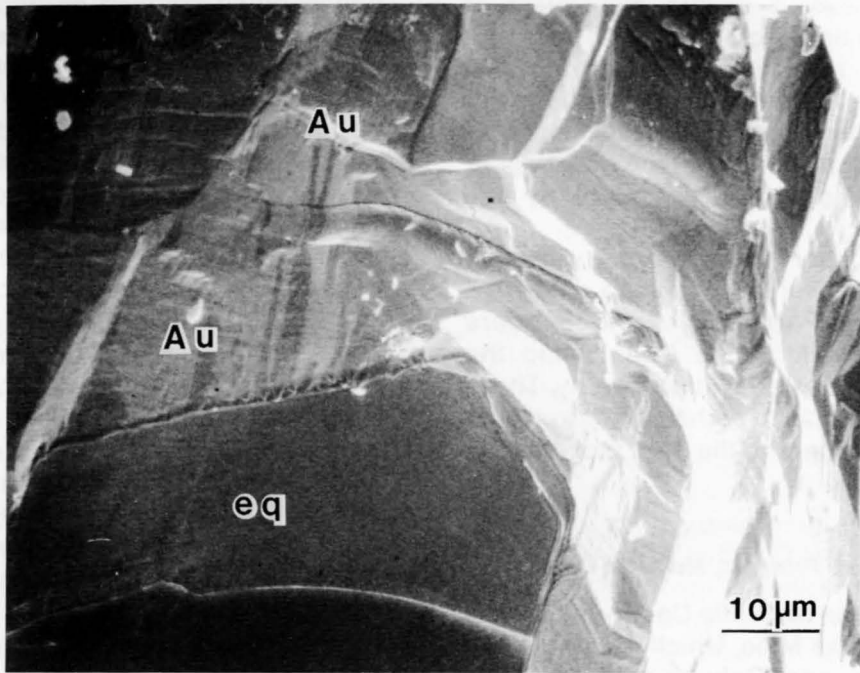


Figure 7. SEM photomicrograph showing gold (Au) enclosing the end of a euhedral quartz crystal (eq), Landers Prospect.

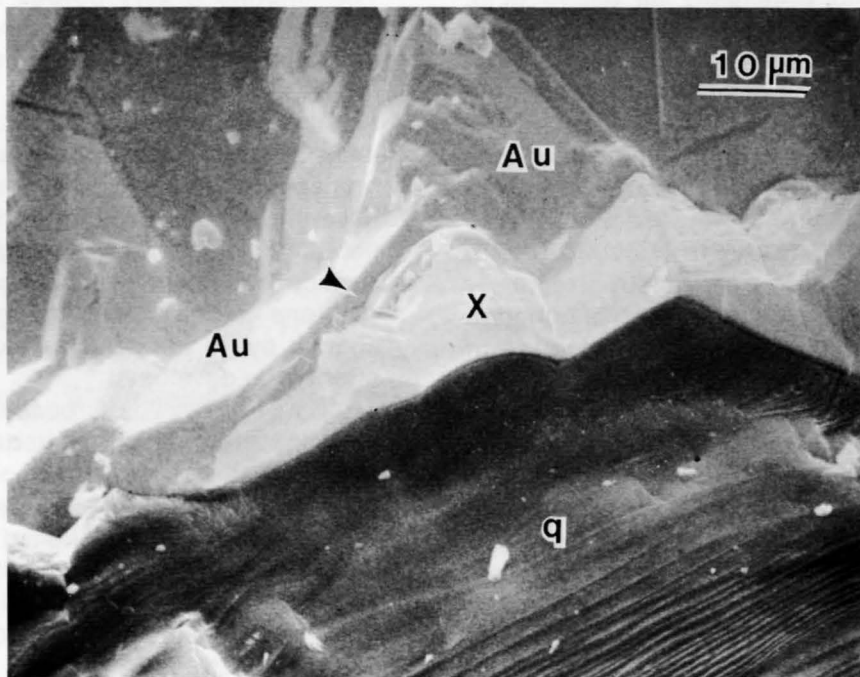


Figure 8. SEM photomicrograph showing auriferous silica (x) in contact with gold (Au) and quartz (q), Landers Prospect.

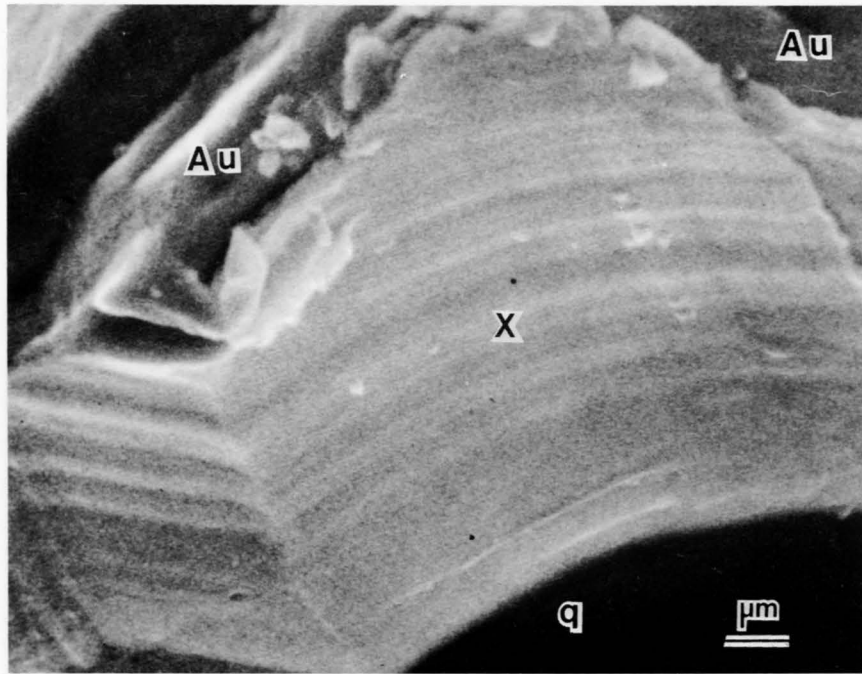


Figure 9. SEM photomicrograph showing enlargement of a portion of Figure 8. Gold (Au), quartz (q), auriferous silica (x).

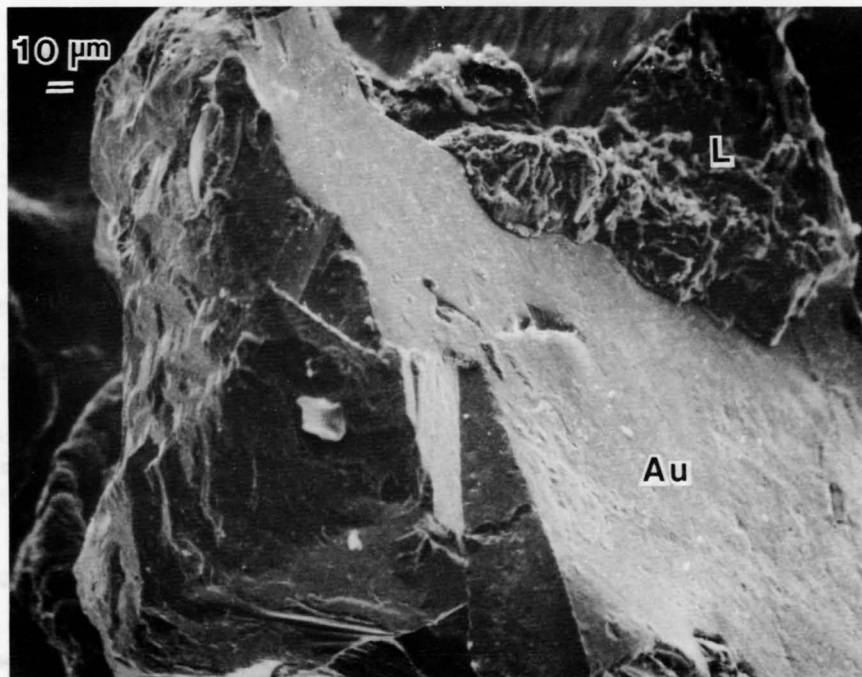


Figure 10. SEM photomicrograph showing large gold (Au) surface in contact with porous limonite (L) (pseudomorphous after pyrite), Landers Prospect.

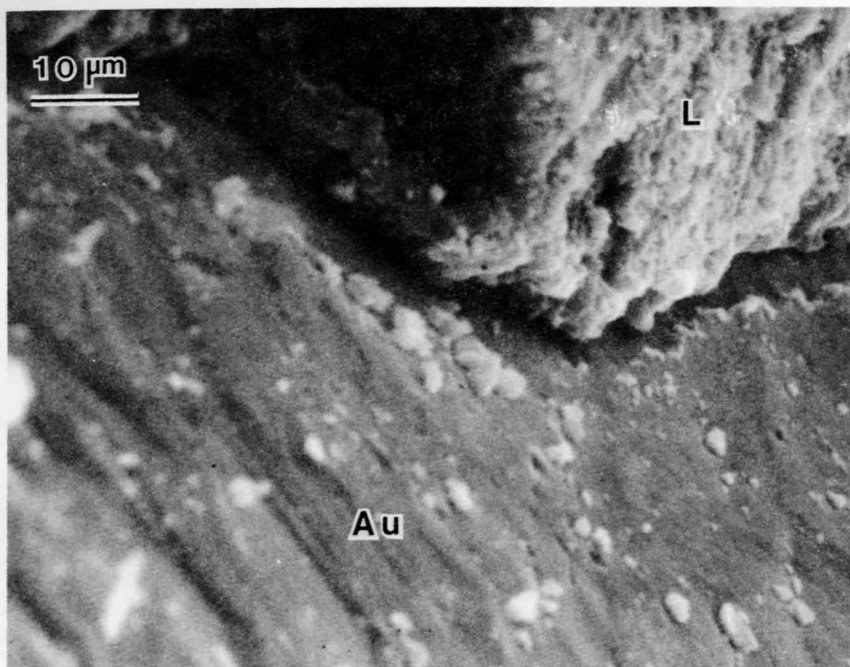


Figure 11. SEM photomicrograph showing gold (Au) particle against pyrite replicating its striated and perhaps slightly altered surface, Landers Prospect. Afterward, the pyrite was altered almost completely to porous limonite (L).

cavity (Blanchard, 1968). When the altering fluid is very dilute, however, the oxidation and hydrolysis of one mole of pyrite yields two moles of free acid, and the iron that is released may precipitate as goethite/hematite and remain as a limonite pseudomorph. If the cubic voids stem from alteration of pyrite, the alteration conditions that produced these voids were different from those that produced limonite.

Gold commonly is found in the vicinity of, as well as in contact with, mica which generally is white to pale green but may be heavily stained by secondary iron compounds. EDAX graphs show that the green mica contains chromium. Gold in contact with mica books preserves an imprint of the mica (Figures 12 and 13). Where mica has been broken away from the gold, small books of mica sometimes remain embedded in the gold, as illustrated by Figure 13. EDAX graphs of the mica generally have peaks indicating Al, Si, K, and Fe as major elements and Cr, Mg, Cl, Au, and Ag as intermediate or minor elements. The signals for gold and silver probably are from minute masses of gold in intrabook spaces, too small to be resolved by x-ray mapping, or from even finer gold adsorbed on mica surfaces. The chlorine, either on or in the mica, probably is a relic from the briny, acid fluids from which the mica formed or by which it was altered. The prevalence of Mg, Fe, and Cr suggests that the

mica is either phengite or phlogopite or a combination.

Gold particles observed at the Landers Prospect ranged in diameter from one millimeter down to 4 microns. The presence of much smaller masses of gold was indicated by EDAX graphs and x-ray mapping, but neither a shape nor a specific site for this extremely dispersed gold could be determined. Gold at the Landers Prospect has a strongly bimodal size distribution: particles are frequent down to diameters of a few microns, absent in the diameter range from 1 micron to 0.01 micron (the resolution limit of the SEM) and frequent again in some very finely dispersed form, in which it could be detected by x-ray mapping and EDAX graphs but not imaged. This extremely fine-grained gold probably is surficial or interstitial, particularly that detected in mica and auriferous silica because it is unlikely to be substitutional in these minerals.

Gold at the Parks Mine, McDuffie County

The Parks Mine, 12 miles northwest of Thomson, was first opened in 1852, and was extensively worked after the Civil War (Jones, 1909; Hurst, et al., 1966a). Gold was found in and along many small quartz veins containing variable amounts of sulfides, feldspar, and mica. None of the shafts,

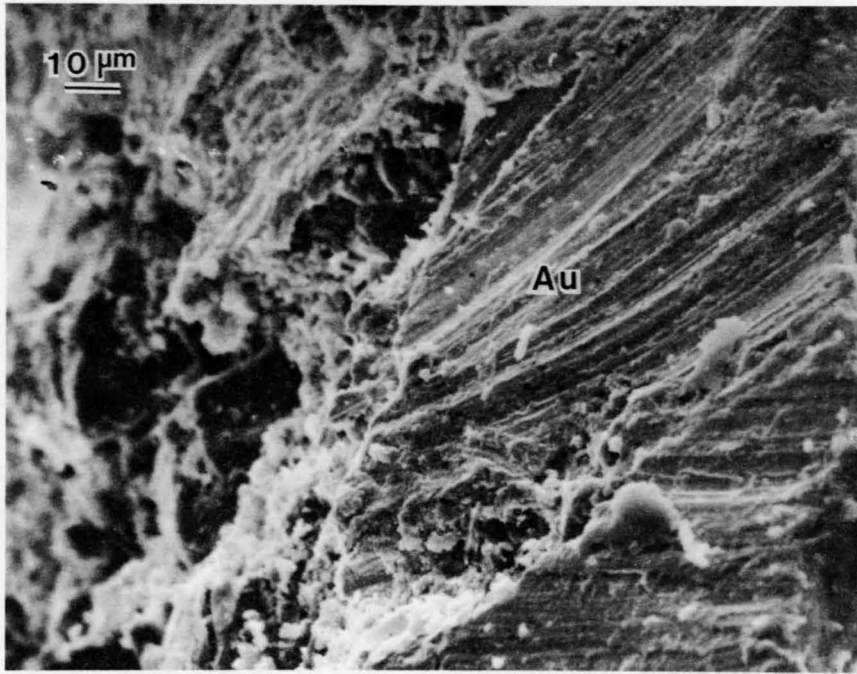


Figure 12. SEM photomicrograph showing gold (Au) surface which is a cast of the mica books against which it was deposited, Landers Prospect.

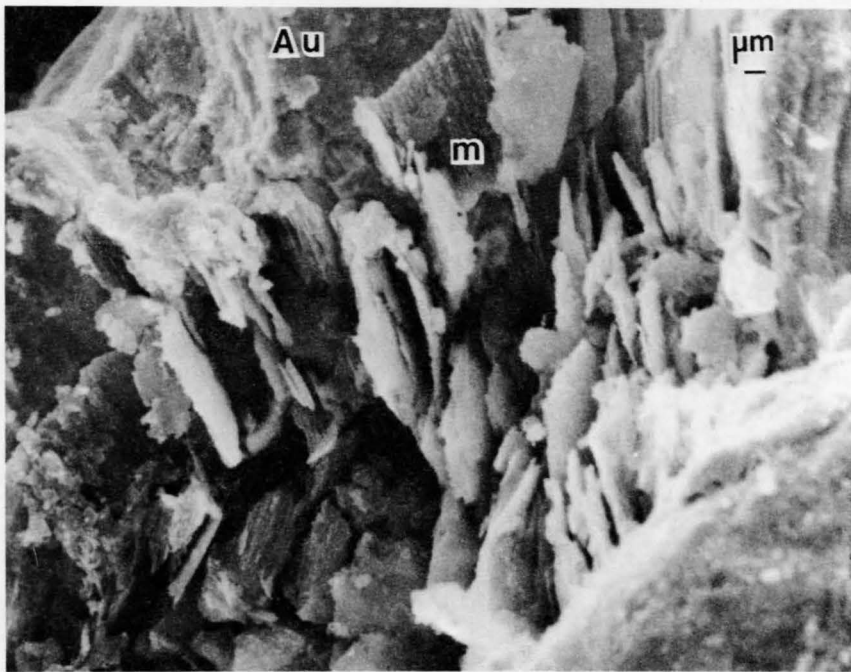


Figure 13. SEM photomicrograph showing a replicating gold (Au) particle in which the ends of some mica (m) books still are embedded, Landers Prospect.

some of which were several hundred feet deep, are accessible. The samples described here were collected from the dumps.

The visible gold is concentrated in micro-fractures and micro-vugs in vein quartz, along with pyrite, galena, chalcopyrite, covellite, K-feldspar, and mica (sometimes fuchsite).

The gold particles are subhedral to anhedral and range in diameter from about 2 millimeters down to 3 microns. They vary in shape from elongate or rounded masses to irregularly shaped particles. Some are spheroidal. Where the gold projects into open spaces, it sometimes is euhedral. EDAX graphs invariably show peaks indicating the presence of silver. X-ray mapping generally shows that the silver is evenly distributed.

Etching of quartz and surficial alteration of K-feldspar and sulfides are conspicuous along some micro-fractures and hardly visible along others. The degree of etching is variable even along the same micro-fracture.

The unetched quartz is mostly anhedral, the grains interlocking. Along openings it sometimes is in small euhedral crystals (Figure 14). Etched quartz (Figures 15, 16, 17, and 18) has irregular to ragged surfaces, and where etching was extreme it may even appear scaly. Where etching was moderate, the quartz shows small-scale dimpling at magnifications of a few thousand. Spot EDAX graphs of etched quartz commonly show low peaks for Cl, K, Ag, and Fe. X-ray mapping shows a generally even distribution of these elements, which probably are absorbed.

The contacts between quartz and gold may be planar (Figure 19) or very irregular (Figure 16) but appear clean. Gold was deposited on both unetched and etched quartz surfaces. The gold surface in contact with another mineral, generally, replicates the surface on which it was deposited and preserves very fine detail.

Figure 20 illustrates a common appearance of a strongly etched micro-fracture along which gold was deposited. Etching is most intense along the open micro-fracture but is visible along some intergranular spaces as much as 50 microns away from the fracture opening. The gold is mostly anhedral. It is in contact with highly altered K-feldspar on one side of the fracture and strongly etched quartz on the other. Contact relations indicate that the gold was deposited after the etching. Along a continuation of the micro-fracture, shown in Figure 20, is a pyrite crystal about 40 microns across, nearly enclosed by etched K-feldspar and quartz (Figure 21). The association of hardly altered pyrite with highly etched K-feldspar is evidence that the etching was a result of

hydrothermal action rather than weathering. Figure 22 shows the contact relations of gold with the etched K-feldspar.

Gold particles associated with pyrite, generally, are between pyrite and quartz, along the margins of pyrite, or within limonite pseudomorphous after pyrite. Figures 23 and 24 show irregular contacts between gold and quartz, both of which replicate the surface of a mass of pyrite that was broken away when this specimen was prepared for SEM. Figure 25 shows irregularly shaped gold in strongly etched quartz near pyrite which is only slightly altered. Figure 26 shows a gold particle simultaneously in contact with altered and unaltered pyrite. The gold found in limonite notably does not replicate the texture of limonite, but generally has the same shape as the gold associated with pyrite, indicating that most of the alteration of pyrite is later than deposition of gold.

Covellite was identified by its composition of mainly copper and sulfur, as indicated by EDAX, and by its very good cleavage. Though some iron often was present, suggesting chalcopyrite; the good cleavage, not a property of chalcopyrite, points to covellite. The etching of covellite along cleavages is often pronounced at x1000 magnification or higher, as seen in Figure 27. The elongate, irregularly shaped masses (x in Figure 27) sometimes form thin strands, bridging the spaces between platy covellite masses. This unidentified material contains more sulfur than the covellite with which it is associated.

Particles of gold commonly are near, adjacent to, or within altered covellite, as illustrated in Figures 28, 29, and 30. Most of the planar surfaces of the gold seen in Figure 28 might be due to mimicry of surfaces against which it formed, rather than to euhedralism of the gold itself. The gold associated with covellite often is spheroidal (Figures 30 and 31) with diameters ranging from about 10 to 3 microns.

Two distinctly different forms of gold are associated with galena: native gold, in contact with unaltered or altered galena, and an unidentified gold-silver telluride, always associated with altered galena. A surface of the native gold often is a replica of an unaltered galena surface, and sometimes is a replica of altered galena (Figures 32 and 33). Gold appearing to be in planar contact with unaltered galena (Figure 34) sometimes is revealed by higher magnification (Figure 35) to have a thin altered selvage between the gold and unaltered galena.

Figure 36 illustrates how gold is associated with more-altered galena. Quartz, part of which is euhedral, encloses the micro-veinlet of altered galena and gold. At places, the gold is molded around euhedral quartz; evidence that it is younger.

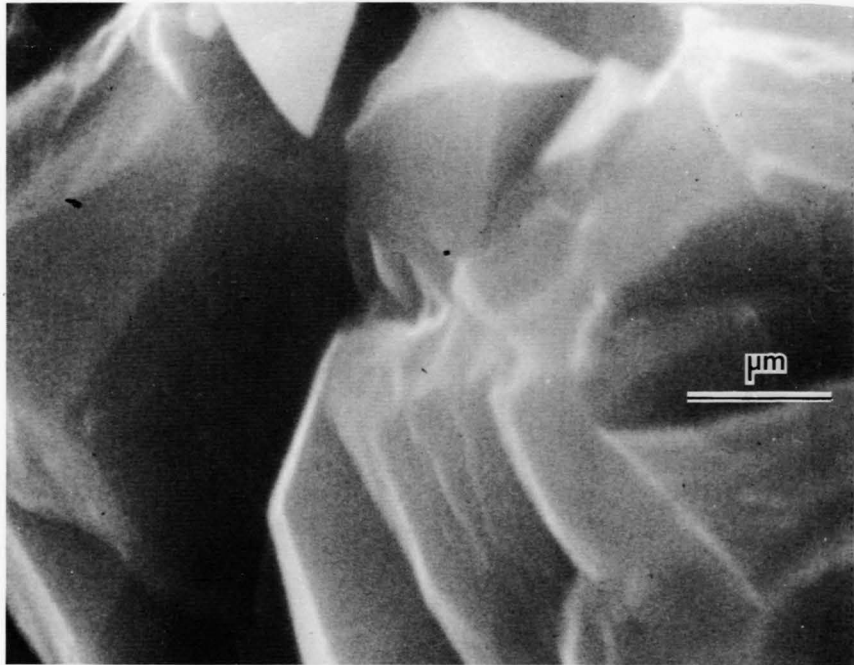


Figure 14. SEM photomicrograph showing small euhedral quartz crystals that have grown into micro-openings in vein quartz, Parks Mine.

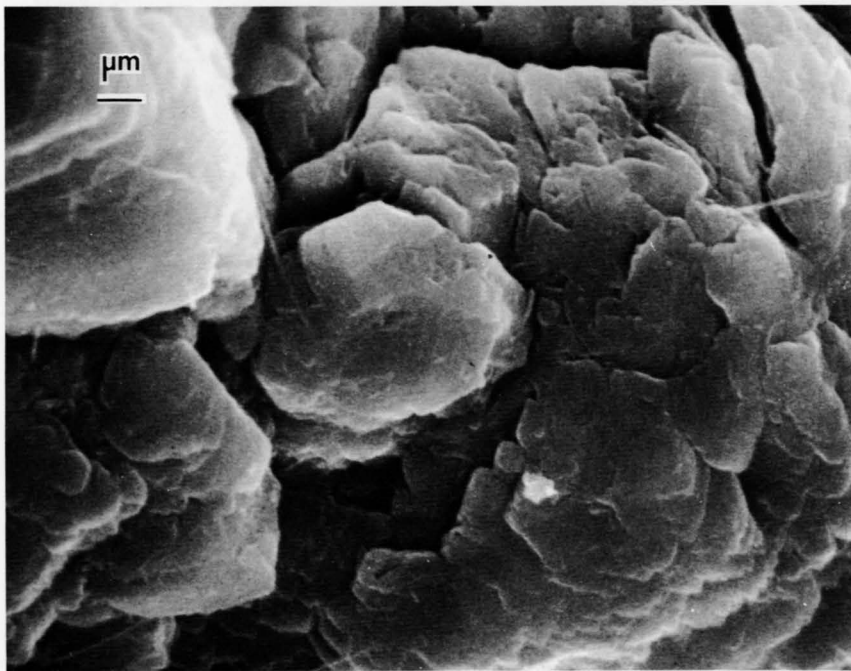


Figure 15. SEM photomicrograph showing etched quartz crystals along a micro-fracture in vein quartz, Parks Mine.

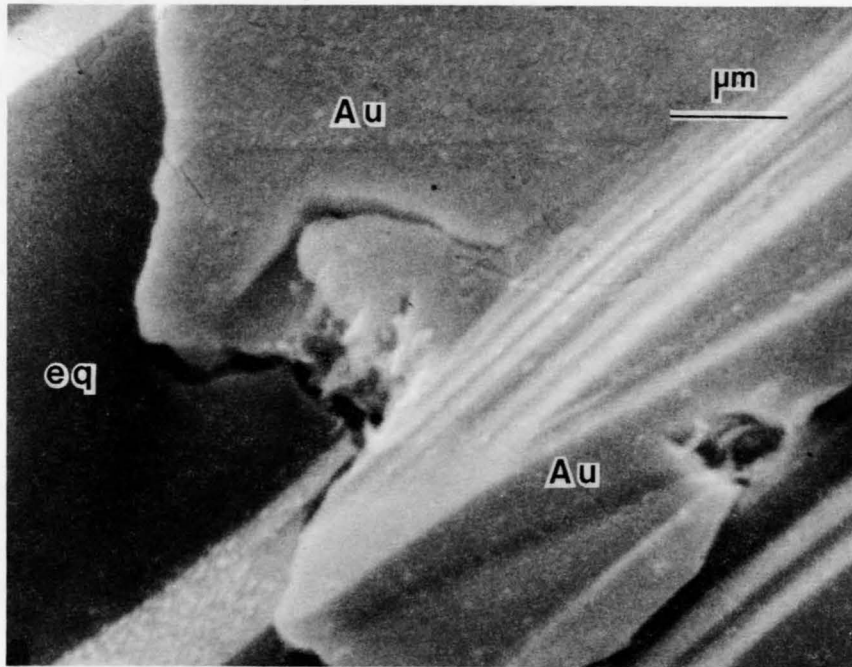


Figure 16. SEM photomicrograph showing gold (Au)- quartz (eq) contact in vein quartz, Parks Mine.

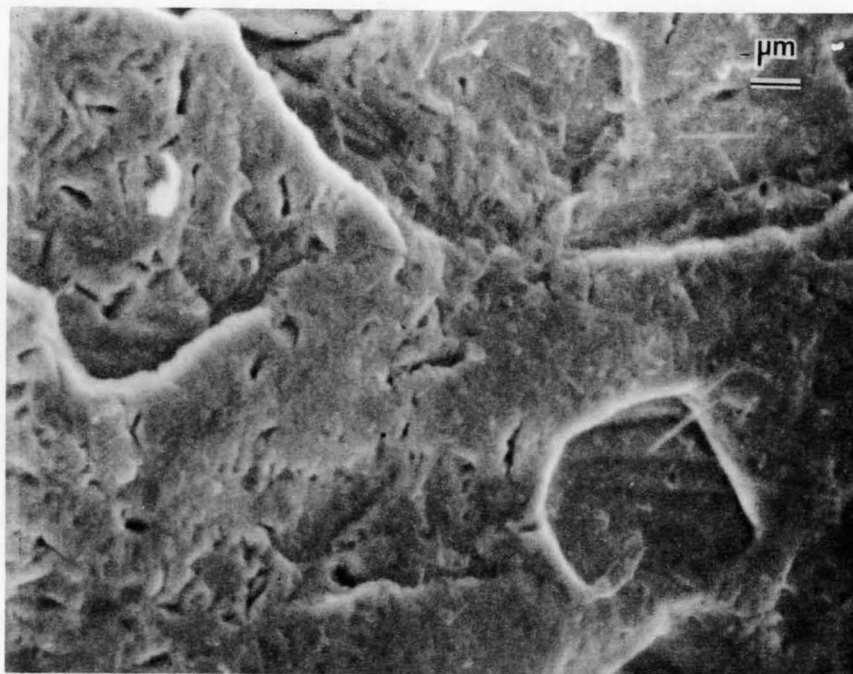


Figure 17. SEM photomicrograph showing surface of a gold particle that was deposited on, and now is a replica of, an etched quartz surface, Parks Mine.

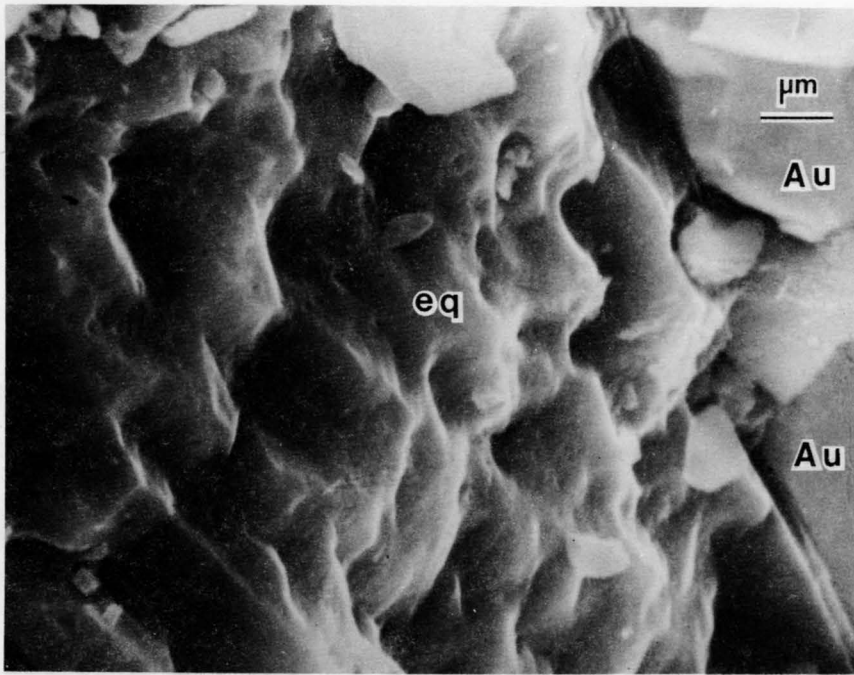


Figure 18. SEM photomicrograph showing etched quartz (eq) surface over which gold (Au) was deposited, Parks Mine.

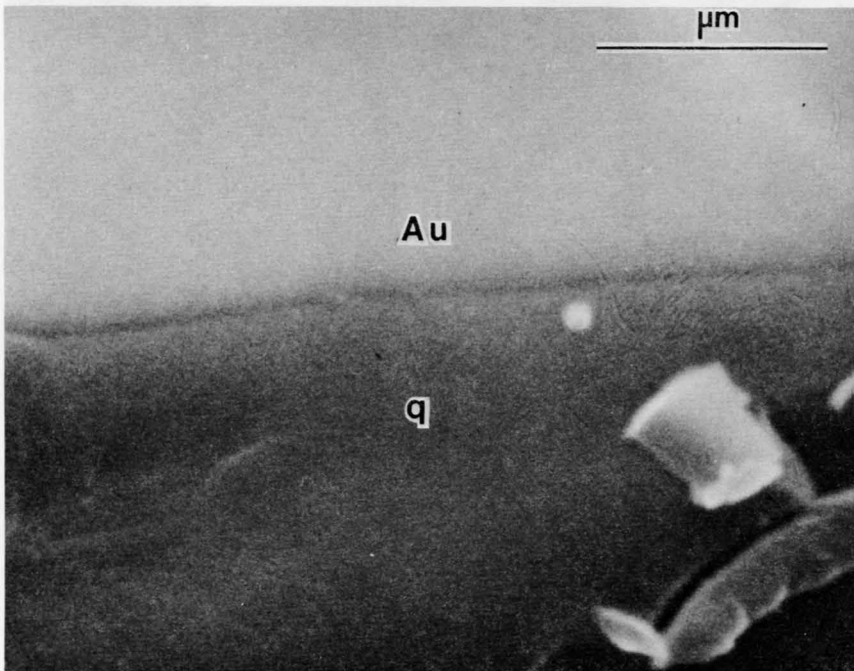


Figure 19. SEM photomicrograph showing gold (Au)- quartz (q) contact in vein quartz, Parks Mine.

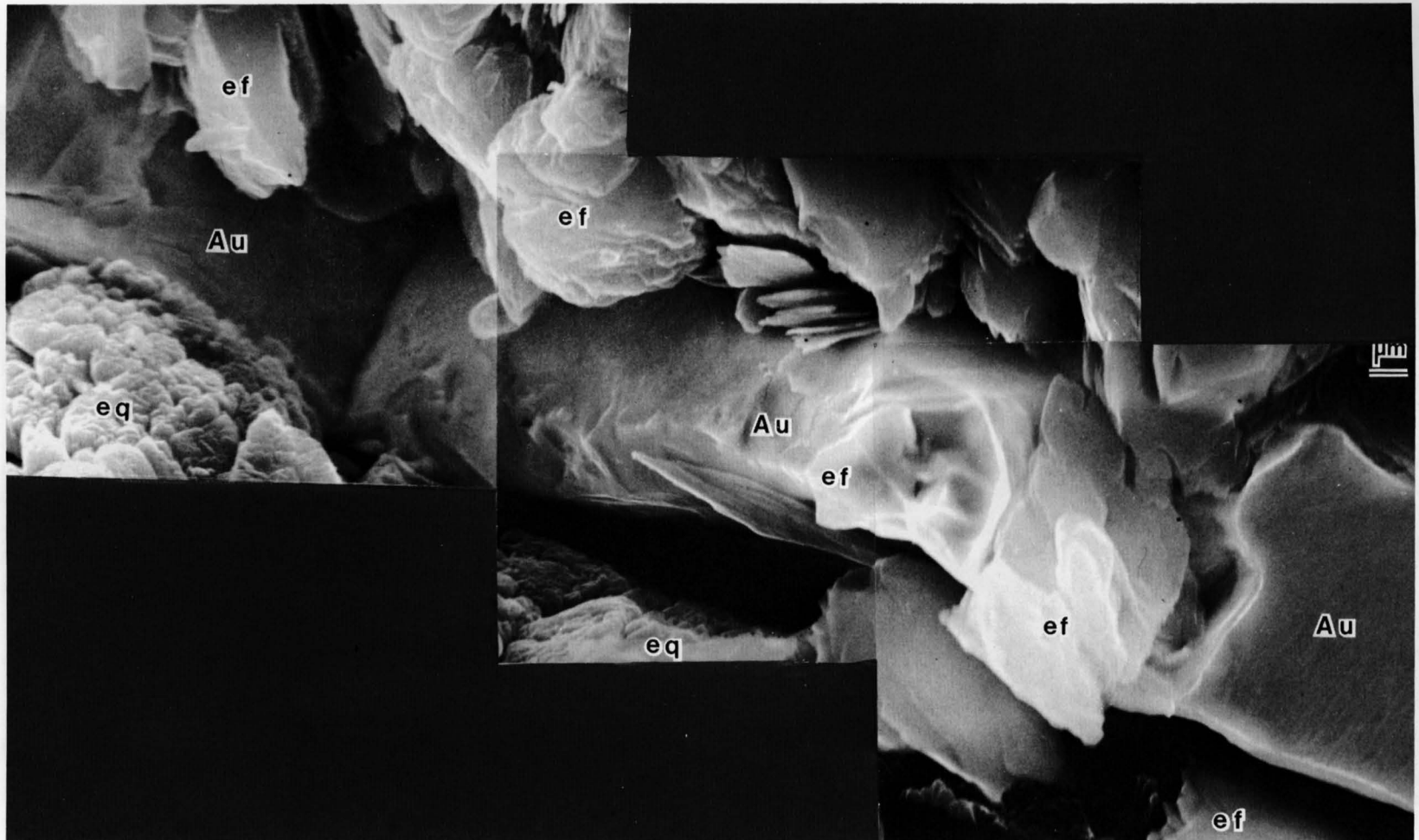


Figure 20. SEM photomicrograph showing typical distribution of gold (Au) along an etched micro-fracture in vein quartz, Parks Mine. Etched quartz (eq), etched K-feldspar (ef).

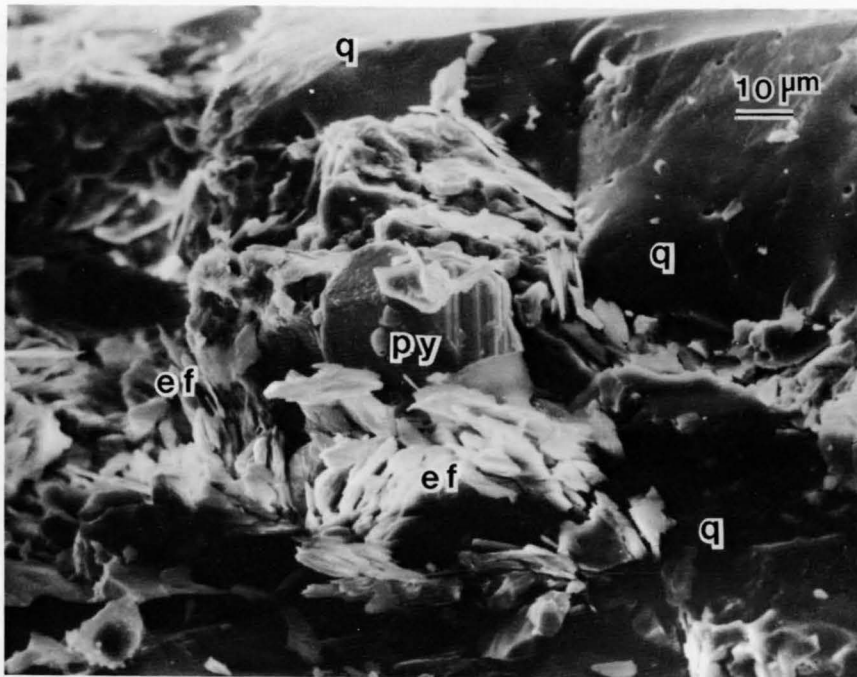


Figure 21. SEM photomicrograph showing euhedral, striated pyrite crystal (py) surrounded by etched K-feldspar (ef) and quartz (q) in a micro-fracture of vein quartz, Parks Mine.

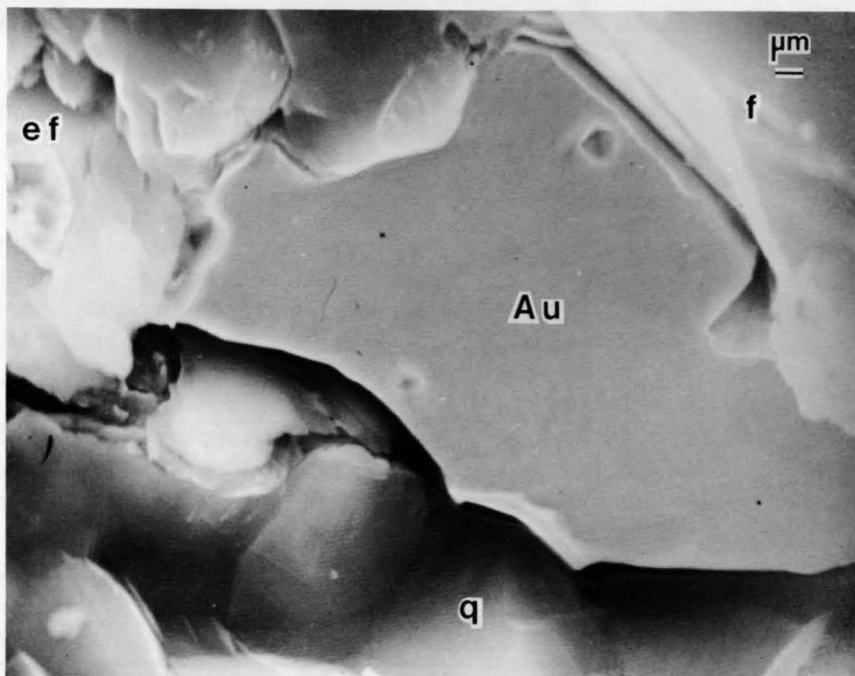


Figure 22. SEM photomicrograph showing gold (Au) in contact with highly corroded K-feldspar (ef) and quartz (q) along a continuation of the micro-fracture shown in Figure 21. K-feldspar (f).

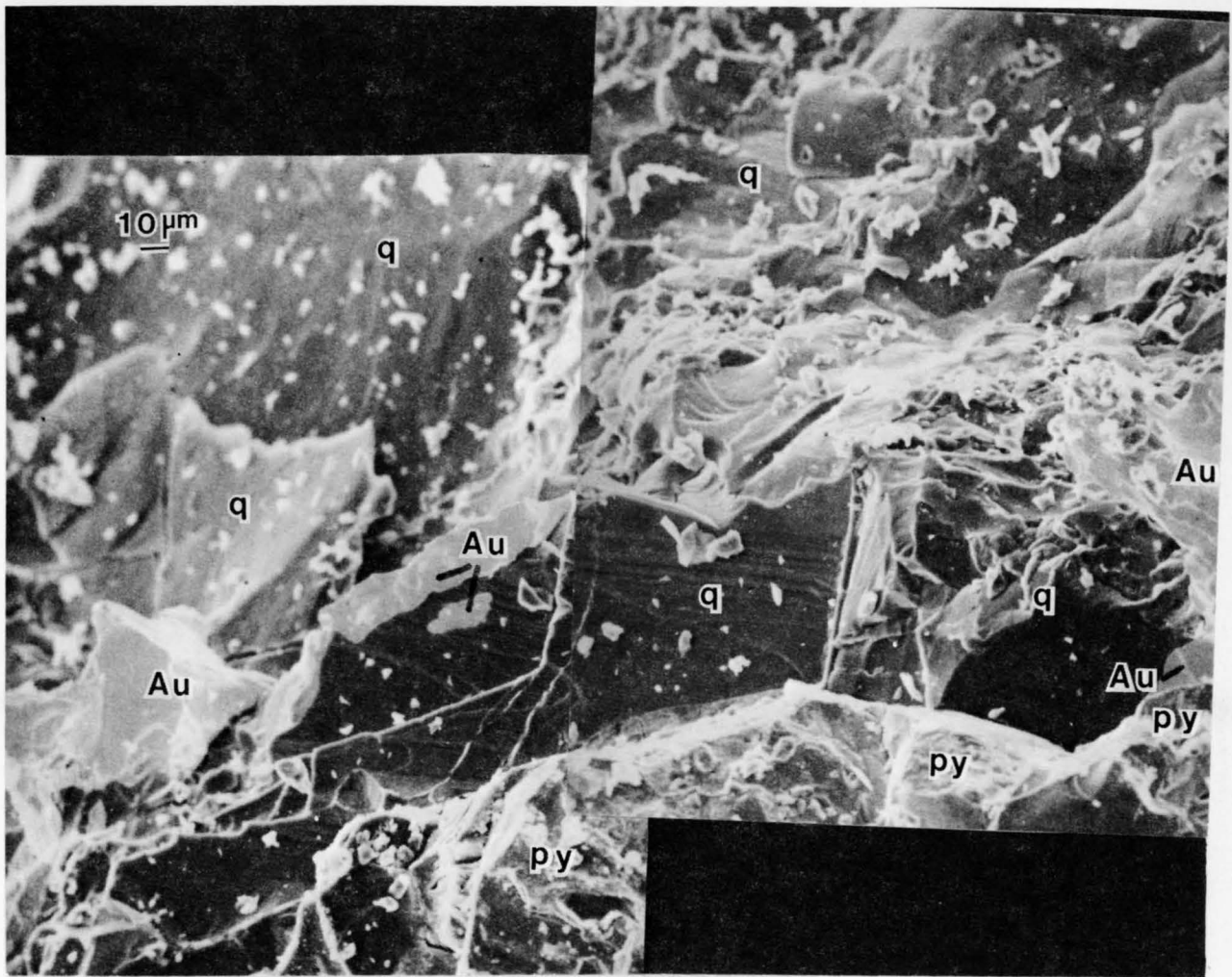


Figure 23. SEM photomicrograph showing auriferous (Au) micro-fracture in vein quartz (q), Parks Mine. Pyrite (py).

High magnification shows that the altered galena is highly etched and reveals many 90° plane intersections, typical of galena cleavage. The quartz crystals are well formed but are unusual in habit. Their EDAX graph shows peaks only of silicon.

The gold-silver telluride associated with altered galena (Figure 37) appears uneven to pitted at low magnification. Higher magnification reveals common 90° plane intersections, typical of galena; and these appear vestigial, as though the gold-silver telluride developed on altered galena. Spot EDAX graphs showed Pb, Ag, and S in the least altered galena, Pb, Ag (stronger), S, and low peaks for Te and Au in the partly altered galena, and showed Pb, S and strong peaks for Ag, Au, and Te in the most altered galena. Tellurium, gold, and silver increase together. Figure 38 shows some of the better developed gold-silver telluride. Four gold-silver

tellurides commonly have been found in gold deposits. The available EDAX data and the habit are inadequate for a specific identification of the telluride species at the Latimer Mine.

As at the Landers Prospect, the gold at the Parks Mine commonly is associated with a pale green to white mica (Figure 39), which commonly is deformed and altered. The surfaces of the gold replicate bent mica folia, indicating that gold deposition is post-deformational.

Gold at the Latimer Mine, Wilkes County

The mine area is underlain by rocks of the Little River Series, principally amphibolite and biotite gneiss, which are fine-grained and contain small concordant pods of epidosite. Foliation strikes east-

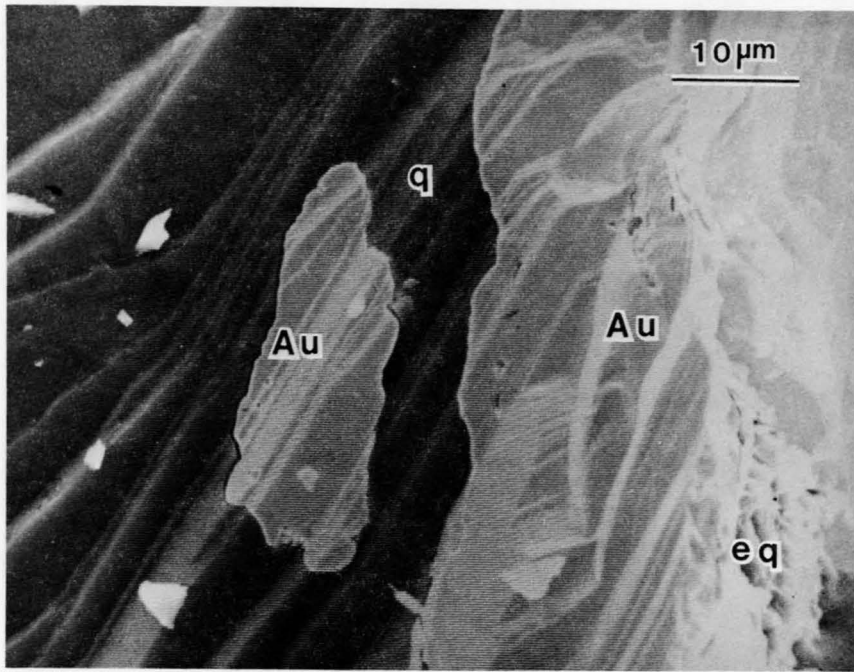


Figure 24. SEM photomicrograph showing magnified view of a portion of Figure 23. Gold (Au), quartz (q), etched-quartz (eq).

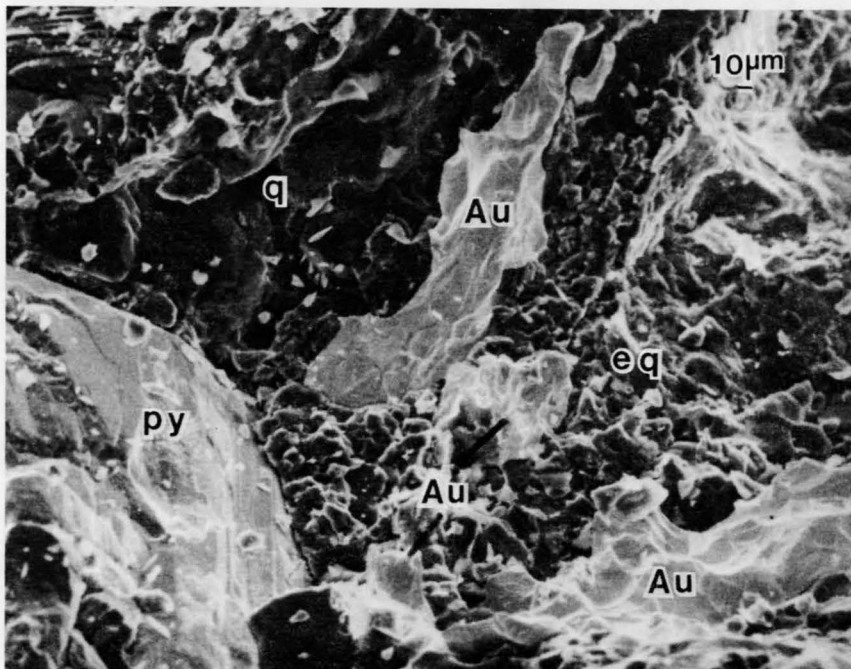


Figure 25. SEM photomicrograph showing irregularly shaped gold (Au) in strongly etched quartz (eq) and near slightly altered pyrite (py), Parks Mine. Quartz (q).

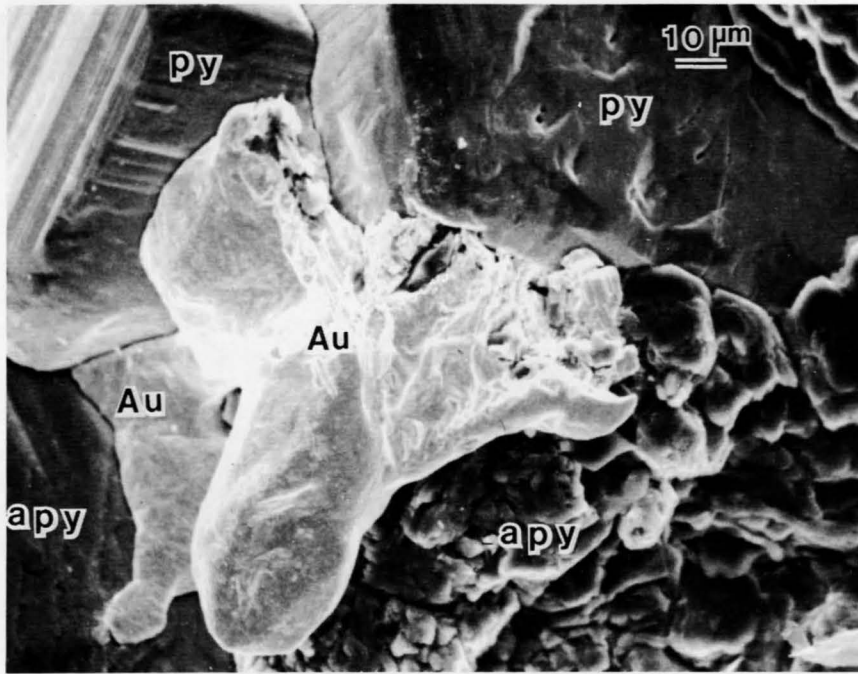


Figure 26. SEM photomicrograph showing gold (Au) in contact with striated and slightly altered pyrite (py) and with strongly altered pyrite (apy), Parks Mine.

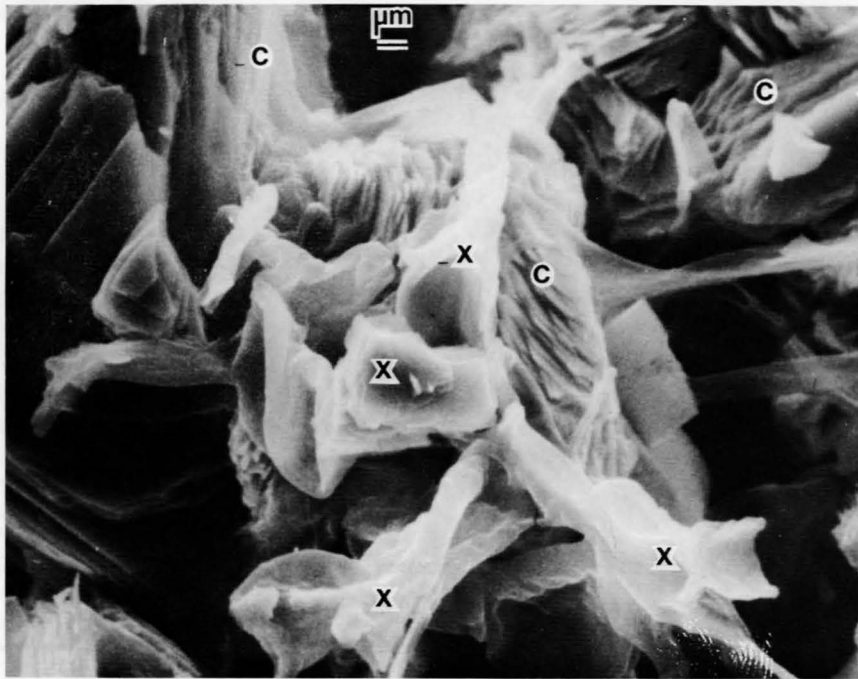


Figure 27. SEM photomicrograph showing covellite (c) etched along basal cleavage, Parks Mine. Sulfur-rich unidentified mineral (x).

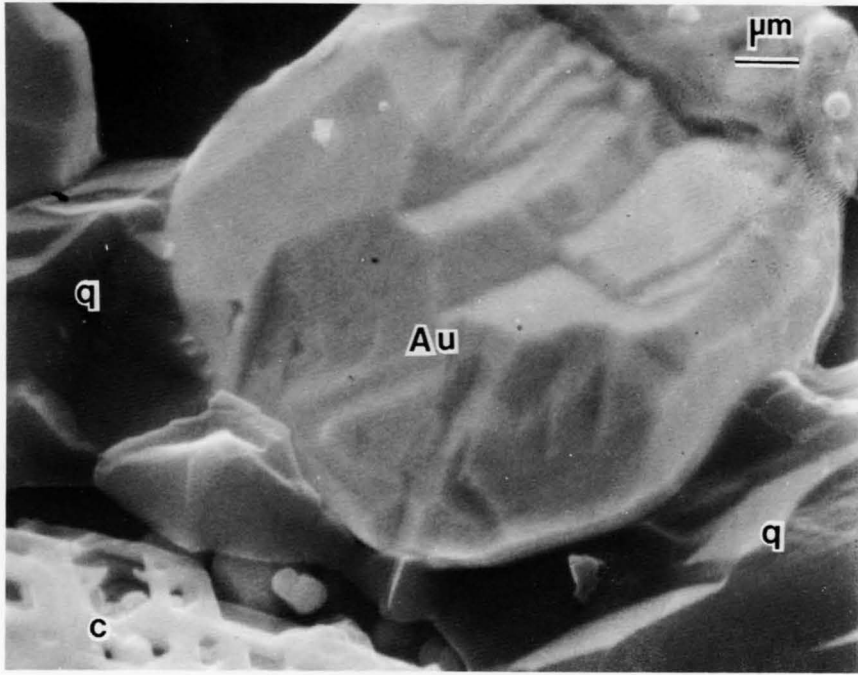


Figure 28. SEM photomicrograph showing euhedral gold (Au) in quartz (q) and near covellite (c), Parks Mine.

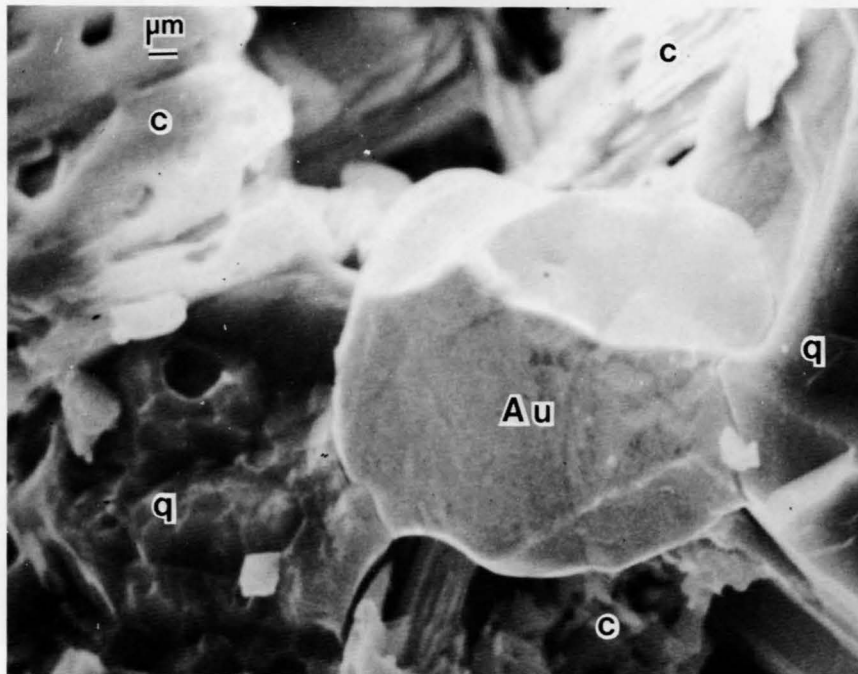


Figure 29. SEM photomicrograph showing gold (Au) adjacent to covellite (c) and quartz (q), Parks Mine.

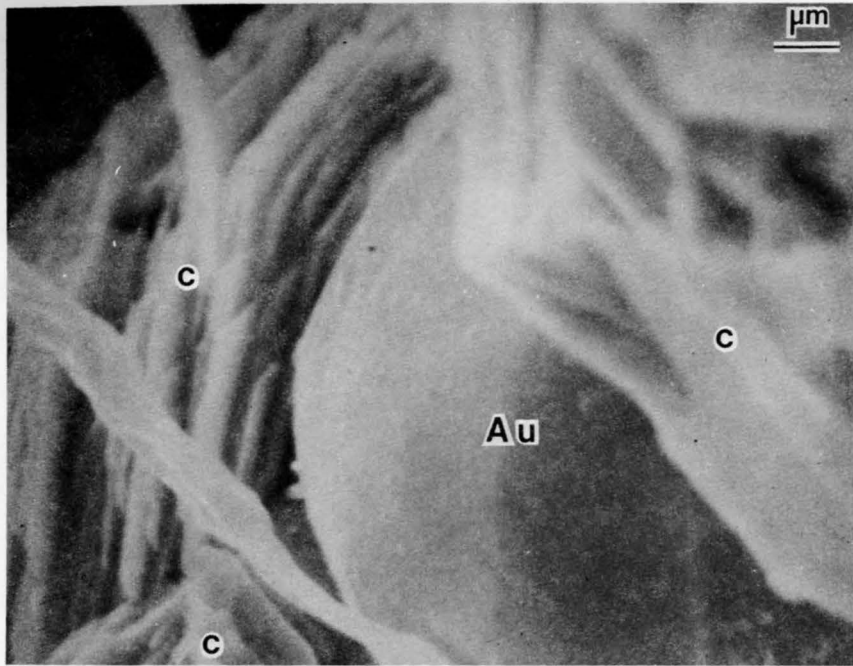


Figure 30. SEM photomicrograph showing subhedral gold (Au) associated with covellite (c), Parks Mine.

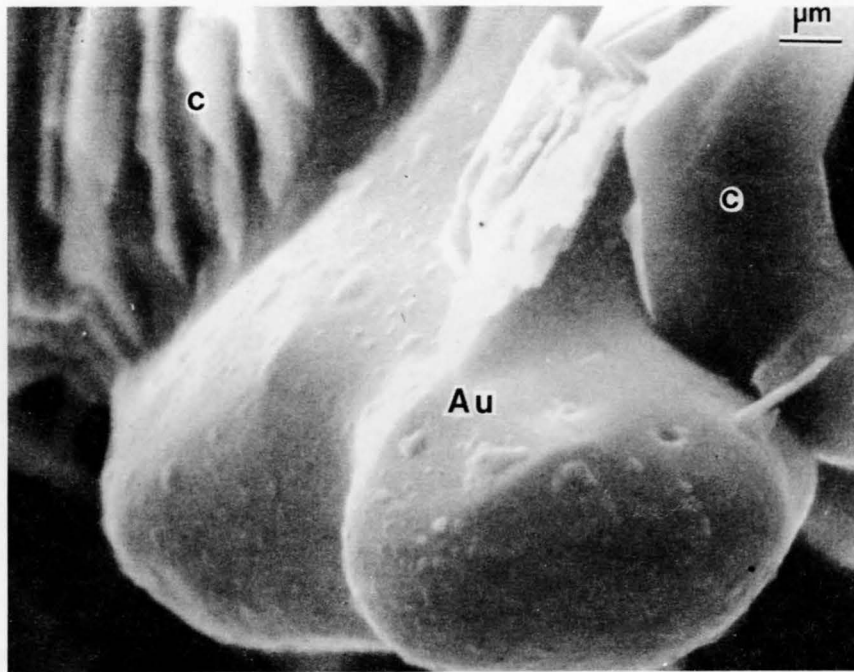


Figure 31. SEM photomicrograph showing spheroidal gold (Au) as commonly seen in the vicinity of covellite (c), Parks Mine.

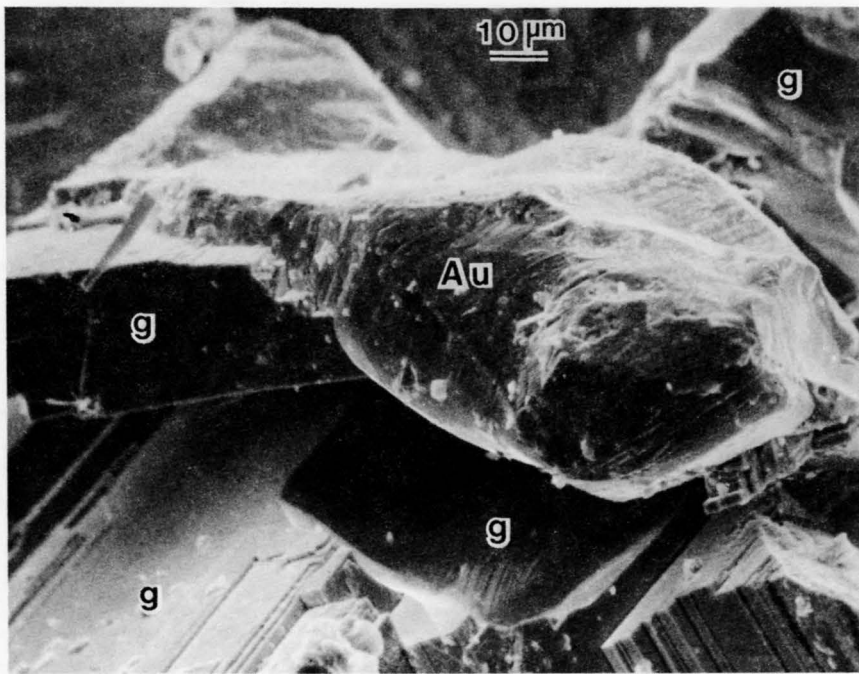


Figure 32. SEM photomicrograph showing gold (Au) in contact with partially altered galena (g), Parks Mine.

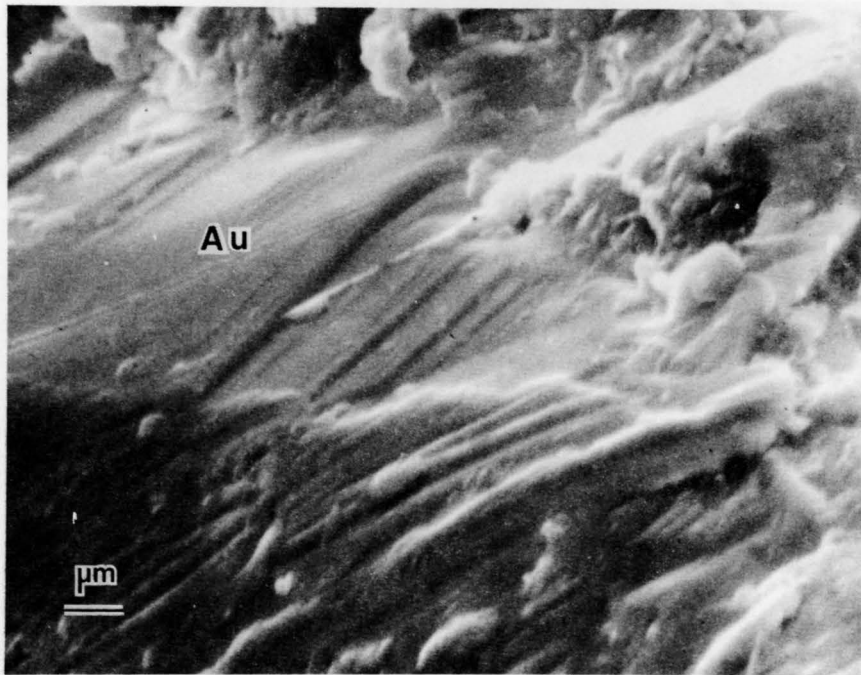


Figure 33. SEM photomicrograph showing a portion of the gold (Au) surface in Figure 32.

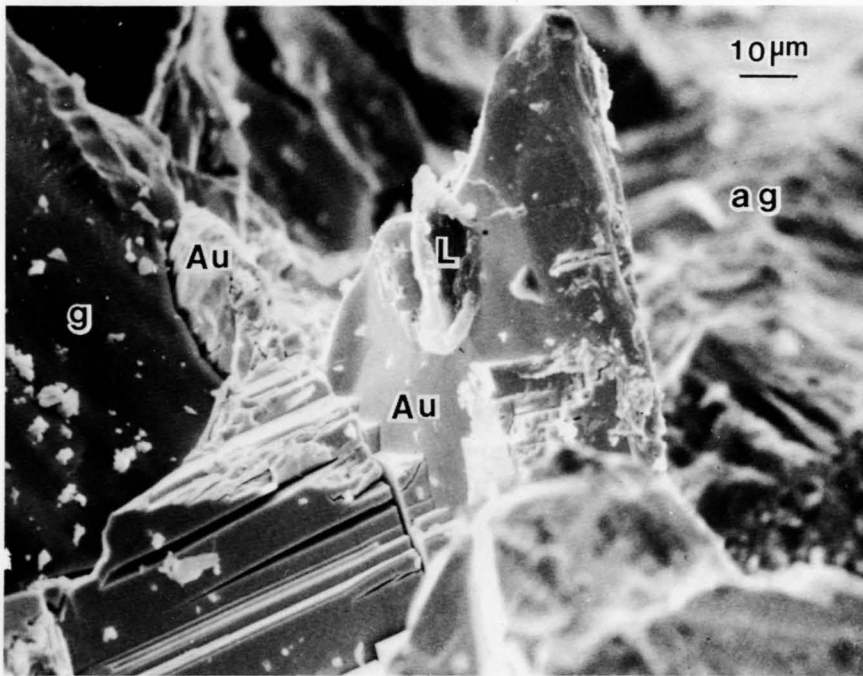


Figure 34. SEM photomicrograph showing gold (Au) in planar contact with apparently unaltered galena (g) and in contact with altered galena (ag), Parks Mine. Limonite (hematite-goethite) (L).

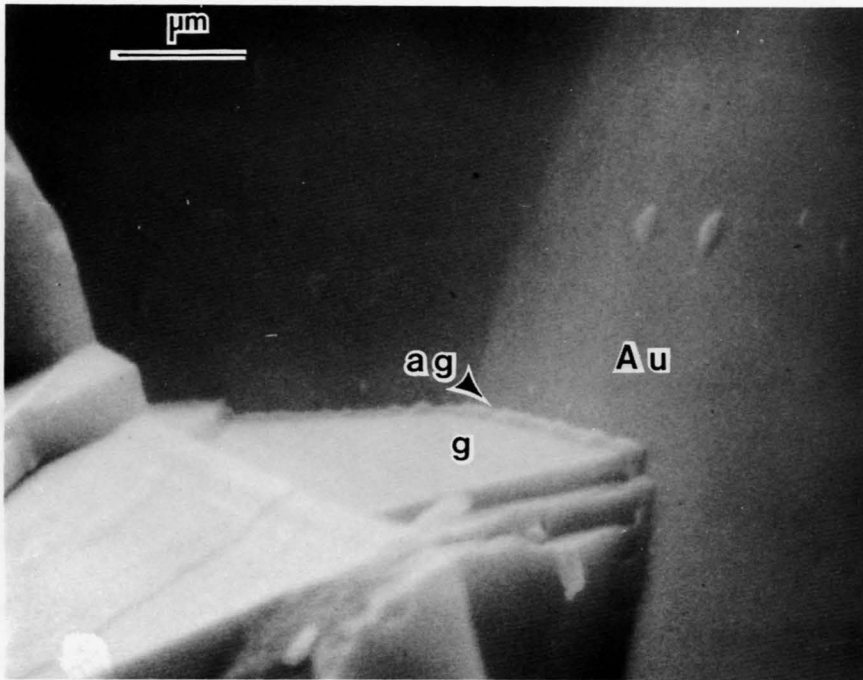


Figure 35. SEM photomicrograph showing the planar gold (Au)-galena (g) contact in Figure 34. Altered galena (ag).

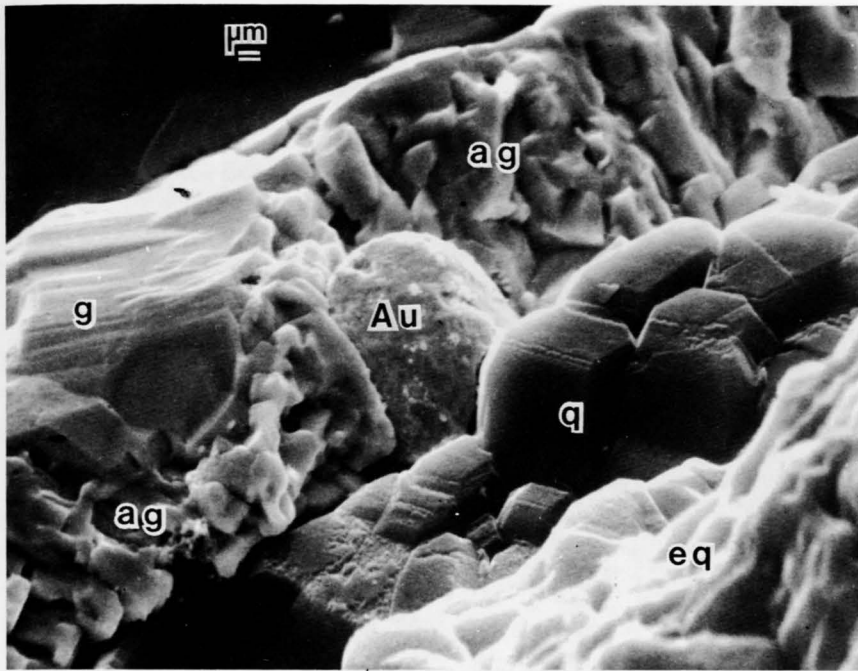


Figure 36. SEM photomicrograph showing gold (Au) in highly altered galena (ag) in vein quartz (q), Parks Mine. Galena (g), etched quartz (eq).

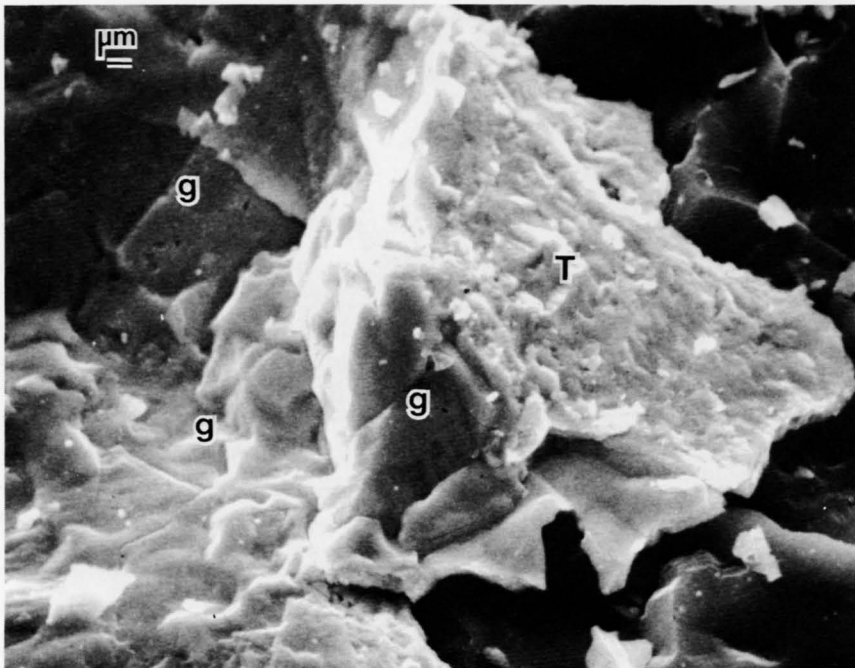


Figure 37. SEM photomicrograph showing gold-silver-telluride (T) associated with altered galena (g), Parks Mine.

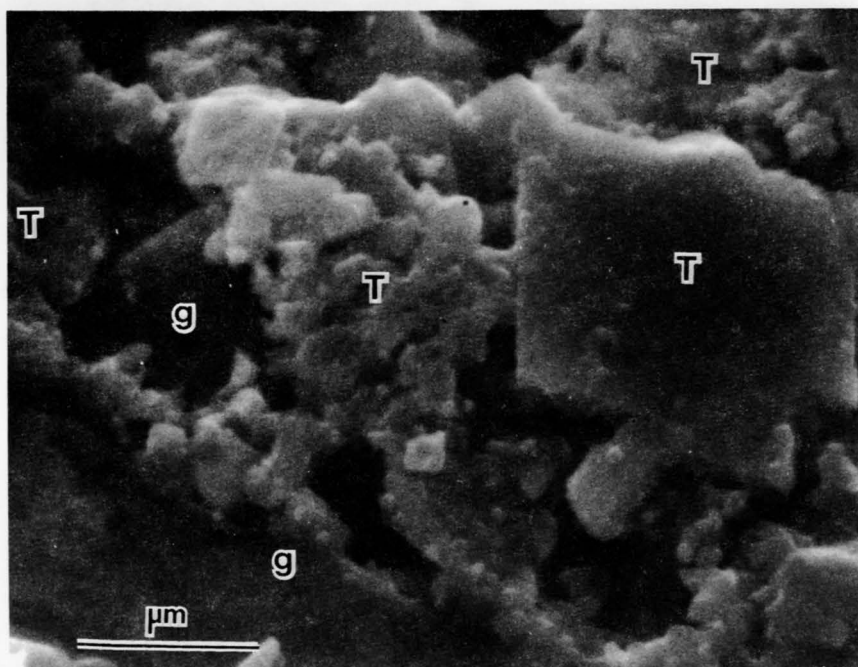


Figure 38. SEM photomicrograph showing some of the better-formed gold-silver telluride (T) associated with altered galena, Parks Mine.

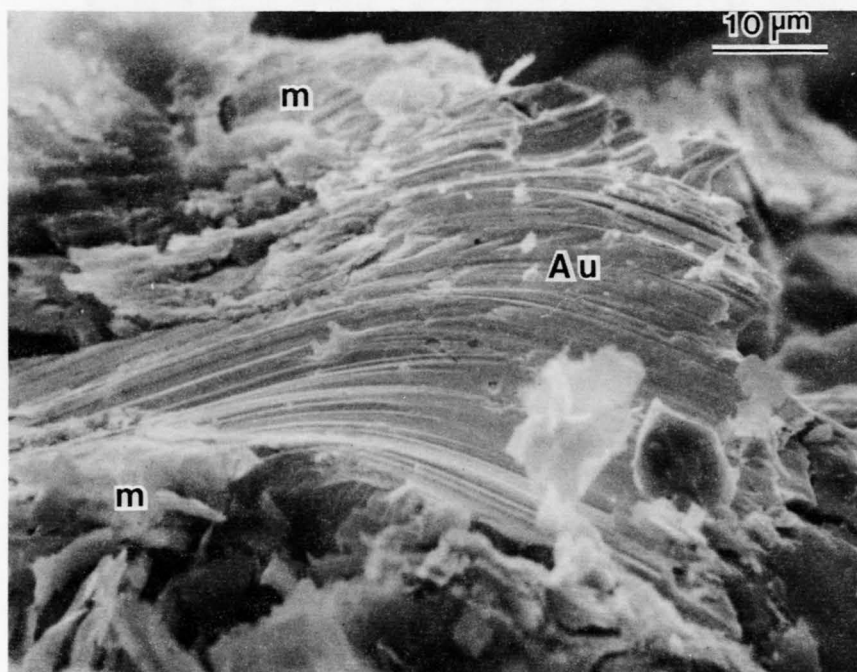


Figure 39. SEM photomicrograph showing gold (Au) altered mica (m), Parks Mine.

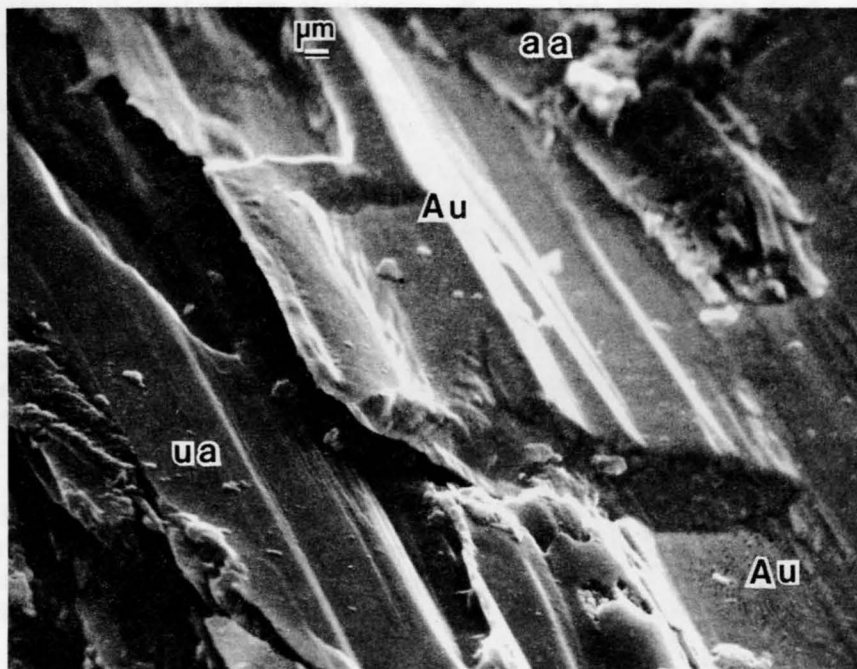


Figure 40. SEM photomicrograph showing gold (Au) deposited along sprung cleavages of amphibole (ua) and replicating both its surface texture and cleavage angles, Latimer Mine. Altered amphibole (aa).



Figure 41. SEM photomicrograph showing X-ray map showing the distribution of gold in Figure 40. /

north-east and dips steeply, both southward and northward.

Quartz stringers and pods are scattered through the mine area. Pyrite as euhedral cubes and subhedral to anhedral crystal aggregates is common in the quartz masses, particularly along fractures, and is found in the other rocks as well, though less frequently. Much of the quartz contains epidote and hornblende in addition to pyrite. The discordant veins, which strike northwest and dip steeply to the northeast or southwest, are megascopically barren; they show only minor iron staining. The concordant veins, striking N65-80° E and dipping vertically, or near vertically, commonly contain visible gold. Gold is found both in the veins and in host rocks near the veins.

Placer mining began along a small creek before the Civil War. In 1901 a small but very rich quartz vein was discovered (Hurst, et al., 1966a). Since then, several other rich veins have been found. Both lode and placer mining have been carried on intermittently.

The gold in the amphibolite is associated mostly with amphibole and, typically, is found along sprung mineral cleavages. At its contact with gold,

the amphibole may be fresh but more commonly is altered. The gold mimics the amphibole cleavages (Figure 40) so closely that the two minerals are indistinguishable by shape or surface texture and have to be distinguished by x-ray mapping (compare Figures 40 and 41). Spot EDAX graphs of unaltered amphibole, near gold, show peaks for Mg, Al, Si, Ca, and Fe, which are evenly distributed. The gold found in altered amphibole, generally, has the same shape and surface texture as that in unaltered amphibole; but high magnification, sometimes, reveals that the gold surfaces are slightly undulatory and finely uneven, as though the amphibole cleavage surfaces against which the gold was deposited were slightly altered before or during the deposition of the gold (Figures 42, 43, and 44).

Some of the gold particles do not replicate the cleavage surfaces of amphibole but have rounded edges and irregular shapes, or occur as thin tabular masses separated by thin layers of altered amphibole (Figure 45).

Gold in the quartz veins is mainly along microfractures or micro-vugs, either in subhedral crystals or in irregularly shaped, anhedral masses. Associated quartz commonly is etched.

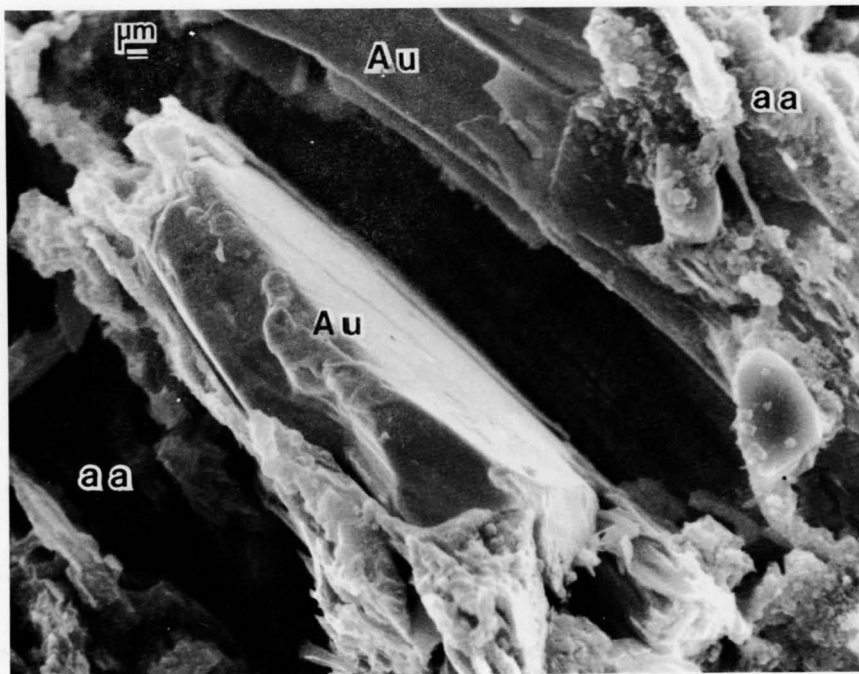


Figure 42. SEM photomicrograph showing gold (Au) in amphibole (aa) partly altered to limonite, Latimer Mine.

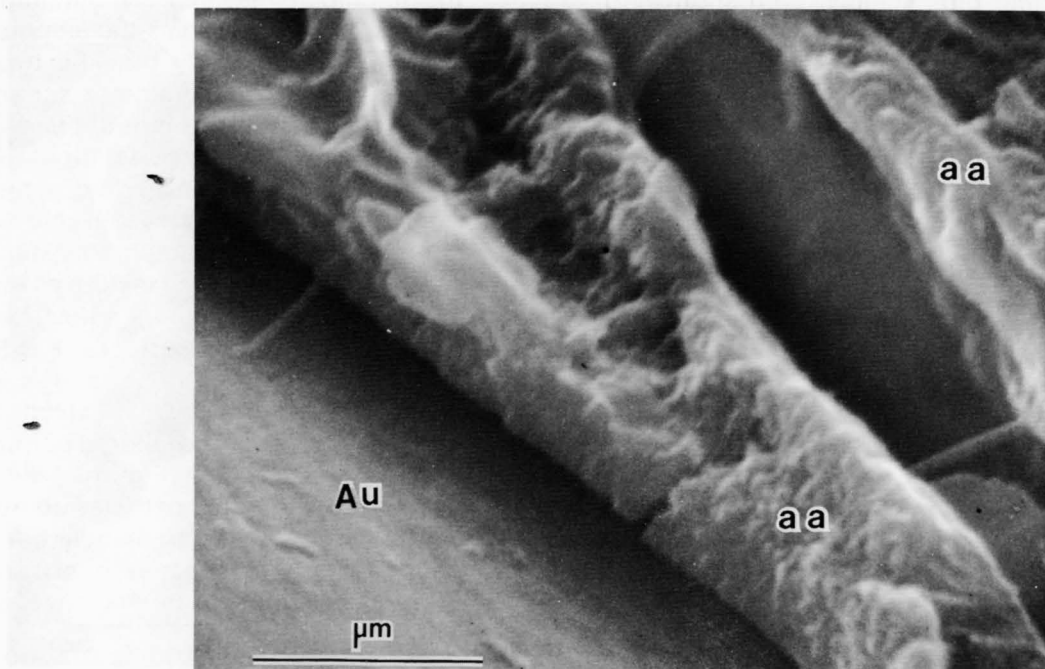


Figure 43. SEM photomicrograph showing close-up of goethitic septa, formed by alteration of amphibole (aa), in contact with gold (Au), Latimer Mine.

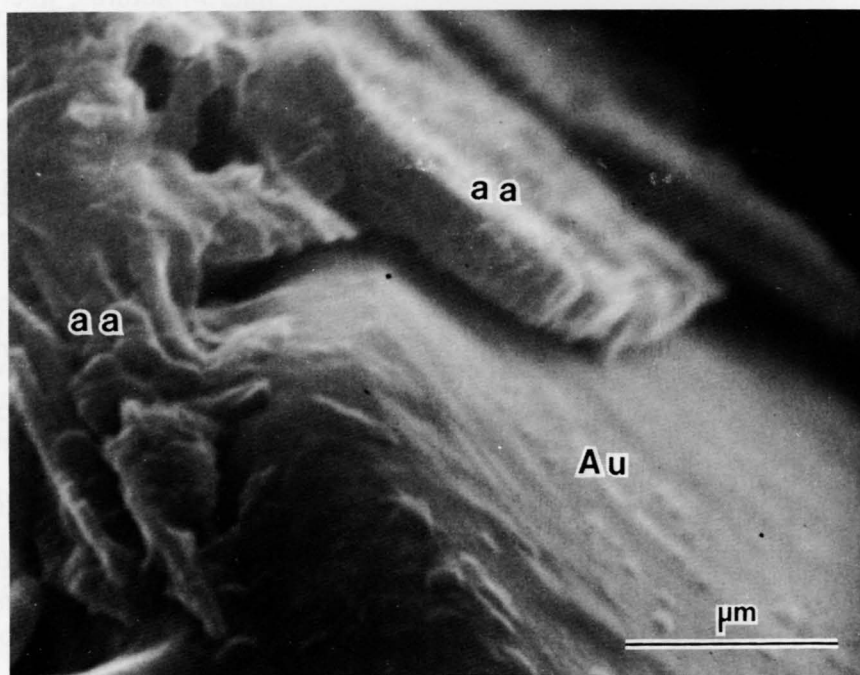


Figure 44. SEM photomicrograph showing uneven surface of gold (Au) which appears to have formed on partly altered amphibole (aa), Latimer Mine.

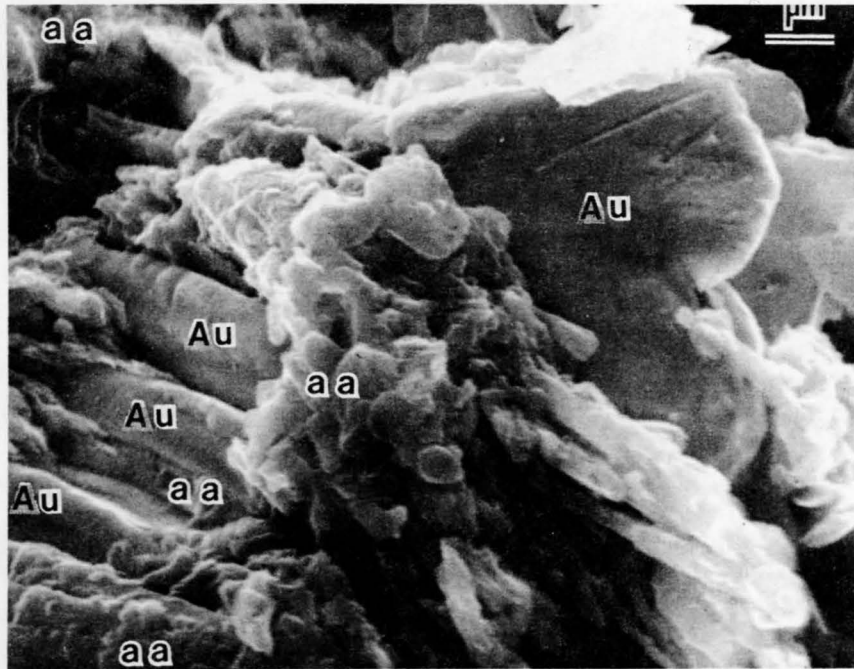


Figure 45. SEM photomicrograph showing alternating tabular masses of gold (Au) and amphibole (aa), Latimer Mine.

SUMMARY AND INTERPRETATION OF THE INFORMATION DERIVED FROM THE SEM STUDY

A surprising result of the SEM study is the strongly bimodal size distribution of gold in East-Central District (Figure 46). The curve on the left side of the figure is based on thousands of observations of gold particles in concentrates of alluvium and saprolite, and in vein quartz samples examined with the SEM. The dashed portion of the curve on the right is uncertain because the abundant gold which occurs in the size range below 0.01 micron, the resolution limit of the SEM, could not be imaged. No gold particles were found in the size range from 2 microns to 0.01 micron. The presence of much gold smaller than 0.01 micron was evident from x-ray mapping. The second peak must begin somewhere below 0.01 micron, rise to a higher frequency than the first peak, and terminate abruptly near 2 Angstroms, the diameter of a gold atom. In the size range of the second peak, where the surface/mass ratio is very high, strong interactions between gold and other elements are to be expected, and the existence of native gold is unlikely. The gold represented by the second peak should be in the form of adsorbed gold complexes or gold cluster compounds, and perhaps lesser substitutional gold.

The characteristic occurrence of gold represented by the first peak of Figure 46 is in and near quartz veins and silicified rocks, mainly in shears, micro-fractures, micro-vugs, and sprung mineral cleavages. The openings occupied by the gold were produced after the main period of (Taconic) regional metamorphism and during the youngest tectonism to affect the area (Alleghenian). Hydrothermal fluids moved along these openings, variously altered earlier minerals, formed new minerals, and deposited gold.

Gold was found in four forms: (1) native gold, (2) auriferous silica, (3) one or more gold-silver tellurides, and (4) very finely dispersed gold, detectable by x-ray mapping but too small to be imaged with SEM.

Native gold is, by far, the principal form. It ranges from about 2 microns in diameter to coarse nuggets. Typically, it is irregularly shaped and has uneven surfaces, but the smaller masses are sometimes euhedral, particularly when they project from the walls of micro-vugs. The surfaces of anhedral gold commonly are replicas of minerals against which the gold was deposited. The more frequently replicated surfaces are those of anhedral, euhedral, unetched or etched quartz, slightly to strongly altered pyrite, deformed and sometimes altered mica, altered covellite, slightly to strongly altered galena, and slightly to strongly altered

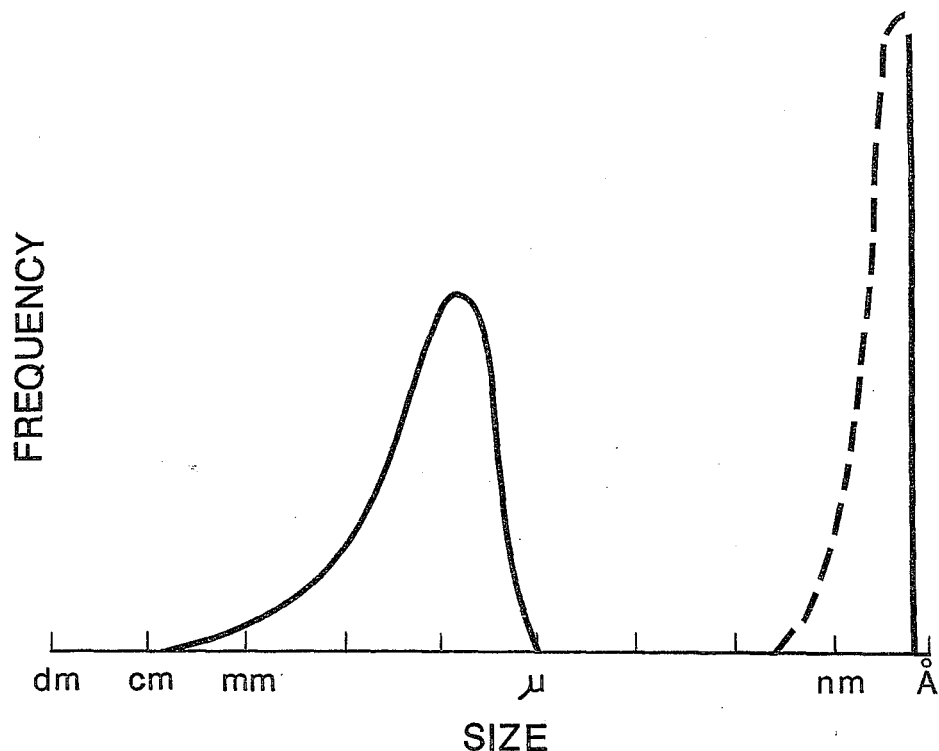


Figure 46. Schematic frequency distribution curves for the gold in the East-Central Georgia Gold District. Explanation is in the text.

amphibole. The replications reveal that the gold was deposited over some span of time, partly before and partly after the etching of quartz, mainly before the alteration of sulfides and silicates, and partly during their alteration.

Auriferous silica was found, rarely, in irregularly shaped masses that appeared grooved, as though compositionally banded, but x-ray mapping revealed no compositional layering. Spot EDAX graphs showed that the masses are mainly silica, and that they contain much evenly distributed gold. The contacts of the auriferous quartz masses with quartz are sharp and even; with native gold, the contacts typically are irregular. Interestingly, the associated quartz contains no gold; but the associated native gold contains a little silicon. Features of the auriferous silica are reminiscent of those ascribed to colloidal deposition (Boydell, 1924; Wright, 1969; Zirnov, 1972). This form of gold was found only at the Landers Prospect; but another feature, also reminiscent of colloid processes, was found at the Parks Mine, spheroidal masses of gold 3-10 microns in diameter.

Gold-silver telluride was found at the Parks Mine in uneven to pitted masses associated with altered galena and appearing to have formed during

or after the alteration of galena. Spot EDAX graphs, with the electron beam necessarily overlapping both altered galena and small masses of telluride, showed strong peaks for Pb and S (galena) and also strong peaks for Au, Ag, and Te (gold-silver telluride). Four gold-silver tellurides commonly are found in gold deposits. A specific identification of the Parks Mine telluride has not yet been undertaken.

Gold in the size range represented by the second peak on gold's size frequency curve (Figure 46), is very common in the quartz veins, silicified zones, and adjacent rocks. X-ray mapping and spot EDAX graphs revealed it in hematite, goethite, mica, and amphibole, but not in quartz, feldspar, or pyrite.

Chlorine peaks commonly were noted on EDAX graphs of mica and limonite in the auriferous veins. The chlorine-bearing mineral, pyromorphite, has been noted as a common supergene mineral in veins at the Hamilton Mine, Columbia Mine, Parks Mine, and Landers Prospect in McDuffie County, at the Magruder Mine in Lincoln County, as well as at several other places in Georgia (Furcron, 1952; Cook, 1978). The presence of so much absorbed or structurally incorporated chlorine in the veins suggests that the chlorine is a relic of the

mineralization process and that the hydrothermal fluids once active along these veins were chloride-rich.

The quartz along auriferous micro-fractures and micro-vugs is commonly and variably etched. Prior to etching, euhedral quartz crystals grew locally from the walls of some micro-openings. Gold was deposited on both etched and unetched quartz surfaces. Supergene etching is possible where surficial water easily can move downward or laterally through rocks, as the etched quartz grains in some porous, upper Coastal Plain sediments in Georgia attest. In east-central Georgia, the movement of groundwater is more restricted, etching is not prevalent in unmineralized quartz, and the etching in mineralized veins either accompanied or preceded the deposition of most of the gold. For these reasons the etching is interpreted as hydrothermal. Other evidence that much of the alteration was by hydrothermal fluids, rather than by weathering is the presence of fresh pyrite closely associated with strongly etched K-feldspar. If the alteration had been due to weathering, the feldspar would have been kaolinized. The fact that the K-feldspar was hydrothermally attacked by quartz-saturated fluids and did not transform to kaolinite indicates that the temperature of the hydrothermal fluids was above 260°C (Hurst and Kunkle, 1985).

The native gold is associated frequently with pyrite and amphibole which are partly altered, their ferrous iron locally oxidized to ferric iron, suggesting that a hydrothermal redox reaction might have precipitated the gold. Similar alteration of pyrite and ferruginous amphibole commonly is caused by weathering. The samples studied with SEM are all from depths less than 300 feet, and have been partially exposed to weathering. However, the SEM observations revealed several features which indicate that the gold was deposited before the rocks were exposed to weathering. Most of the gold was deposited either before or during the earliest stage of alteration, because the gold commonly replicates the surface features of unaltered minerals against which it was deposited. These unaltered minerals are very susceptible to weathering. Part of the gold is associated with unaltered pyrite. Feldspar along microfissures in which gold was deposited was chemically attacked without the formation of kaolinite. Since this could have taken place only above 260°C, the gold hardly could have been supergene. The SEM observations, indicate that vein quartz was deposited, etched, redeposited; that native gold and tellurides were deposited; and that the mineralized veins were cooled before exposure to weathering.

ORIGIN OF THE GOLD IN EAST-CENTRAL GEORGIA

PERSPECTIVES

A gold deposit generally is categorized as magmatic, volcanic, metamorphic, and so forth, in allusion to the process or environment thought to best account for its formation. Its actual origin, however, may be more complex, in which case a model of origin based on a single environment or a single set of processes is likely to be an oversimplification. Acceptance of a simplified model, even provisionally, may tend to focus attention on a single set of processes, and may actually delay a clear understanding of how the deposit originated.

Many gold deposits of commercial grade appear to have been generated or affected by more than one set of physical conditions. For example, the Pueblo Viejo deposit in the Dominican Republic began as a volcanogenic deposit but was significantly modified and upgraded by eluvial processes. When large-scale mining began there in 1975 (Russell, et al., 1981), only the eluvial parts, which could have been categorized correctly as a volcanogenic-eluvial deposit, were minable.

Metamorphism and deformation of a deposit like that at Pueblo Viejo could obscure the effects of eluvial processes, and leave general features suggestive of a volcanogenic model, like that in Figure 47. The deposit might be categorized as volcanogenic or volcanogenic-metamorphic, but the model might fail as an exploration guide, for lack of consideration of eluvial processes that affected the distribution of higher grade ore. Metamorphic remobilization of gold can complicate the use of any volcanogenic model. Intense metamorphic remobilization, of course, might obscure early volcanogenic and eluvial aspects and, thus, generate an epigenetic metamorphic deposit.

Many of the gold deposits in the Carolina Slate Belt have been called volcanogenic, the category suggested by their location in a major metavolcanic terrane and by the way some are associated with high-alumina minerals. According to the volcanogenic model, the high-alumina minerals represent early hot spring or fumarolic alteration products. If the deposits are volcanogenic, they originated before mid-Ordovician time, because volcanism had ceased by that time, and the volcanic-sedimentary pile had been deeply buried and subjected to Taconic regional metamorphism (see Figure 3).

Some Slate Belt deposits do appear to owe their beginning to volcanogenic processes, and a few might even be mainly volcanogenic. Others, including most of those in east-central Georgia,

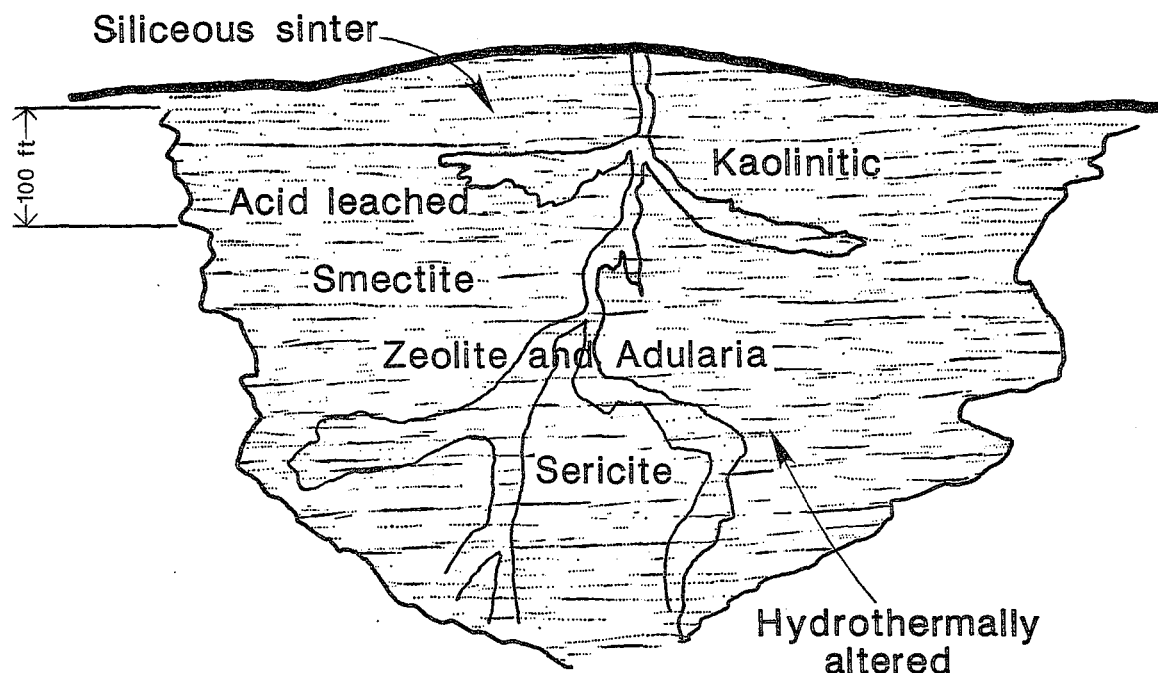


Figure 47. Alteration model of a typical hot spring system.

have features that are more characteristic of epigenetic metamorphic deposits. Their field distribution and microscopic features clearly categorize them as epigenetic. Their distribution shows little apparent relation to plutons, but correlates instead with younger fault zones. Many of the gold anomalies transect the regional metamorphic fabric. These and other relationships, described in earlier sections of this Bulletin, and in Information Circular 83, indicate that the higher-grade concentrations of gold are much younger than Late Precambrian–Early Paleozoic volcanism, younger than Taconic metamorphism, and are either coincident with or postdate the youngest major tectonism. The principal gold deposits in the East-Central Georgia District are metamorphic epigenetic deposits, and the fluids that most effectively concentrated the gold were active during Alleghenian tectonism.

DISTRIBUTION OF BACKGROUND GOLD

The measured background gold values are similar to those reported for other areas of similar rocks (see Information Circular 83). They are twice the mean values reported for the common rock-forming minerals, as quartz, feldspar, mica, epidote, hornblende. This implies that the background gold resides in intergranular spaces, micro-fractures, or

in accessory minerals which contain more gold than common rock-forming minerals.

Gold values slightly higher than the general background of 4-8 ppb have been widely reported in intermediate to mafic volcanic rocks in other areas. The outcrop pattern of similar rocks in east-central Georgia correlates with the distribution of these because the sampling interval is large compared to the scale of lithologic change. Some of the low-level, lithology-related anomalies probably developed during early Paleozoic volcanism and survived metamorphism. Others must be much younger. For example, the well defined anomaly gradient crossing the Danburg granite in northern Wilkes and Lincoln Counties must postdate crystallization of the Danburg granite, 295 m.y. ago.

The gold anomalies that include values of 20 ppb and higher define three anomaly trends which are near and roughly parallel to major fault zones. Most of the better known gold occurrences are scattered along the southernmost of these trends.

During sampling for the gold assays, mineralized sites indicated by old mines and prospects, veins, or strong hydrothermal alteration were shunned. Accordingly, the values of Plate A of Information Circular 83 are a measure of background and low-level anomalies, only. They are not a measure of higher grade mineralization. Interpreted in relation to the geologic map (Plate A of this

Bulletin), they provide basic information about gold background, the mobility of gold since early volcanism, the age of mineralization relative to regional metamorphism and tectonism, and major controls on gold localization. They show that gold values in the country rocks generally increase in the vicinity of the larger known deposits, and they reveal promising new areas for exploration.

OCCURRENCE OF COARSER GOLD

Numerous quartz veins and silicified zones transect the Taconic metamorphic fabric, and a third of them are auriferous. The high grade concentrations of gold are associated with the main fault zones and are in rocks showing silicification or other hydrothermal alteration. The coarsest gold is in and along quartz veins and silicified zones, where it typically occupies small shears, micro-fractures, microvugs, and sprung mineral cleavages.

ORIGIN OF QUARTZ VEINS AND SILICEOUS ZONES

The earliest quartz veins that cross-cut the metamorphic fabric might have developed as early as the waning stage of Taconic metamorphism. Some concordant veins might be even older. The youngest veins probably are Alleghenian.

At the height of Taconic metamorphism, the maximum temperature of the rocks that now crop out was near 500°C in the northern part of the area and 380-400°C in the southern part, as described in the previous section dealing with the geology of the District. The hydrothermal fluids that formed the veins must have risen from a deeper source, and might have been hotter or cooler than the host rocks. The possibility that these fluids were 'sweated out' of contiguous rocks and that the veins formed by lateral secretion is discounted by the observed rise in gold background near auriferous veins and the lack of any associated zones of gold-depletion. The fluids probably ascended from a deeper, hotter source, driven by a temperature/pressure gradient.

The metamorphic rocks produced by Taconic metamorphism had cooled down at least as low as 250-300°C by Alleghenian time, and show only a low temperature Alleghenian metamorphic overprint. In the southeastern Piedmont of South Carolina, Alleghenian metamorphism was intense enough for an amphibolite-grade overprint over the older Taconic fabric (Secor, et al., 1978; Fullagar and Butler, 1979), but it was much less intense in east-central Georgia, where its principal effects are

wide spread kaolinization and zeolitization. The upper temperature of kaolinization in quartz-saturated rocks is about 270°C (curve 9 in Figure 4). So, the host rocks could hardly have been hotter than 300°C when Alleghenian tectonism produced micro-openings in the quartz veins.

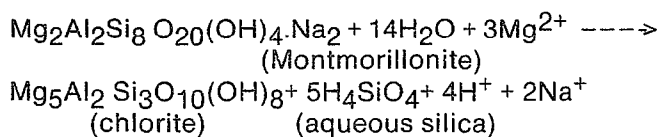
According to Simmons and Caruso (1982), most micro-openings in crystalline rocks are mechanically closed by a pressure of one-half kilobar, which corresponds to a burial depth of 1.5-2 km. Accordingly, the depth of the veins containing micro-vugs probably was less than 6,000 feet.

The vein quartz commonly shows evidence of a complex origin. Individual anhedral grains vary widely in size and transparency, and commonly show crushing, fracturing, and recrystallization. Various combinations and repetitions of fracturing or shearing, quartz deposition, and recrystallization are revealed by SEM examination.

The source of the silica is more readily attributable to metamorphism than to magmatism. When a rock mass that includes weathering products is subjected to regional metamorphism, it becomes a vast source of mobile silica, part of which can be deposited eventually in silicified zones and quartz veins. Beginning near the middle of greenschist metamorphism, the mass also becomes a vast generator of metamorphic water. This water can dissolve elements from the metamorphosing mass and transport them, along with silica, wherever the aqueous phase can move. It can propylitize or otherwise alter large rock masses, form veins, and sometimes mineralize the main pathways along which it moves.

METAMORPHIC GENERATION OF HYDROTHERMAL FLUIDS

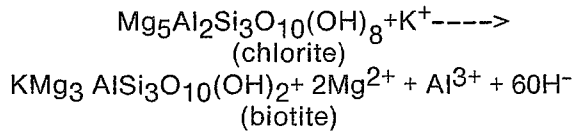
During weathering, the hydrolysis reactions that produce clay minerals decompose water, in an amount equal to about 10% of the weathered mass, by weight. The resulting H⁺ ions are incorporated in the clay, while the hydroxyls combine with CO₂, as charge-balancing bicarbonate ions. During early greenschist metamorphism, the principal mineralogical transformations result in further decomposition of water, the source of which is interstitial, interlayer, and dehydration water. An example is the transformation of montmorillonite to chlorite (Schvartsev, 1976):



$$\Delta F_f^\circ = -235 \text{ kcal/m.}$$

In this type of reaction, hydroxyls from the decomposing water are incorporated in the new mineral, while H^+ ions accumulate in the pore fluid, replacing cations that move from the pore fluid to the new mineral lattice. Reaction of some of the hydrogen ions with bicarbonate ions may release CO_2 .

At a higher grade of greenschist metamorphism, new mineralogical reactions release various cations plus hydroxyls. An example is the transformation of chlorite into biotite:



The released cations participate in further reactions that form aluminosilicates like epidote, actinolite, and garnet. During these reactions, hydrogen and hydroxyl ions recombine and thus generate large quantities of metamorphic water, most of which eventually escapes to higher levels as hydrothermal fluids. An abrupt increase in the redox potential of the system at this stage (Schvartsev, 1976) may be important in the early mobilization of gold.

An orderly sequence of reactions accompanies the gradual rise in temperature during regional metamorphism. Early recrystallization consumes water in hydrolysis and hydration reactions. Later reactions release large quantities of hydrogen and hydroxyl ions that combine to generate metamorphic water. The initial rock composition, the degree of hydrothermal interchange between masses of different composition, and the grade of metamorphism largely determine the composition, pH, and Eh of the pore fluids at a given stage. The overall trend of the metamorphosing mass is toward dehydration and dehydroxylation; the net movement of water is counter to the metamorphic gradient. The amount of water eventually released depends to a large degree upon the extent to which materials in the initial rock pile were weathered. Because the water driven from lower levels moves upward and may react with lower-grade rocks above, it is little wonder that the presence of hydrothermal fluids is evident in virtually all lower grade metamorphic rocks, or that epigenetic gold deposits are largely restricted to rocks of low to intermediate grade.

NATURE OF HYDROTHERMAL FLUIDS

Studies of wall rock alteration assemblages, fluid inclusions, coexisting sulfides and sulfide-oxide mineral associations, and hot springs suggest

that most natural hydrothermal ore solutions vary no more than 2 units to either side of neutral pH (Seward, 1973). The pH range probably is greater within a metamorphosing pile, if the pile includes a variety of rocks, because pH can be buffered at higher values by hydrolysis reactions where there is limited interchange of pore fluids. The abrasion pH of common rock-forming minerals ranges from 5-11 (Keller, 1957), so pH should vary at least as widely. Because the hydrothermal fluids that precipitate workable concentrations of ore minerals have to interchange with large rock masses, they should have a generally lower pH range.

The range in activity of H^+ is much greater than the narrow pH range might imply. With increasing temperature there are significant changes in the ionization constants of water and various solutes, and ion-pairing becomes very important (Chou and Frantz, 1977). The ionization constant of water increases more than a thousand-fold with a change of $250^\circ C$: from 0.11×10^{-14} at $0^\circ C$ to about 7×10^{-12} at $250^\circ C$. Neutral pH decreases from 7 at $25^\circ C$ to 5.56 at $250^\circ C$, and then increases with rising temperatures (Helgeson, 1969). The increasing dissociation of water with rising temperature facilitates the hydrolysis reactions that characterize greenschist and lower amphibolite grade metamorphism. The ionization constants of common strong electrolytes like HCl, NaCl, KCl, and H_2S decrease rapidly with increasing temperature. Above $350^\circ C$ they occur largely as undissociated molecules (Henley, 1973). Below $350^\circ C$, where an acid such as HCl would be almost totally ionized, pH might be low and the fluid highly reactive, but the same fluid at higher temperature and lower pressure could have a nearly neutral pH and be relatively unreactive. Within the temperature-pressure range of hydrothermal fluids, the lower temperature interactions of dissociated acids and bases give way to higher temperature reactions involving ion pairs and undissociated molecules.

The Eh of hydrothermal fluids can range from very high to low. Higher Eh fluids can be generated in a pile of deeply weathered rocks, with a high proportion of oxidized elements and a low content of reductants, than in a pile of graywackes and anoxic muds. Eh generally varies with pH and with the concentration of what is reacting. The variation is particularly great when the reaction involves hydrogen or hydroxyl ions, as reactions involving Fe, V, and Mn, whose oxidation potentials vary markedly with pH. The leaching, transport, and deposition of gold are strongly affected by the Eh of the metamorphic fluids.

Hydrothermal fluids, typically, are brines whose total chloride exceeds 2 molar, are often near

silica saturation, and generally are undersaturated with respect to gold, according to the composition of fluid inclusions in vein quartz and the composition of geothermal waters.

SEM observations indicate that the auriferous veins in East-Central Georgia developed from hydrothermal fluids that were slightly acid, had moderately high Eh, high chlorides, and varied from oversaturation to undersaturation with respect to quartz.

GEOCHEMICAL BEHAVIOR OF GOLD

In all chemical reactions, atoms, molecules, or ions tend to assume a configuration that increases the stability of outershell electrons. Improvement can result from (1) redox reactions, in which the oxidation states of participating atoms change, or from (2) coordinative reactions, which entail a change in either coordinative partner or coordination number. Any combination of cations with molecules or anions containing free pairs of electrons (bases) is a complex formation (Stumm and Morgan, 1970). The tendency for complex formation increases with the capability of the cation to take up electrons (its ionization potential) and with decreasing electronegativity, (i.e., increasing tendency of the ligand to donate electrons).

Gold's high ionization potential and high electron affinity place it in the group of strongly oxidizing elements. Ions of metals in this group (Group I of Figure 48) coordinate preferentially with anions containing Cl, Br, N, I, S, C, Se, P, or Te as donor atoms. These metals bind ammonia stronger than water, CN^{-1} in preference to OH^{-} , and form more stable I^{-} or Cl^{-} complexes than F^{-} complexes (Morgan and Stumm, 1970). As indicated by electrode potentials in Table 1 and by relative position in Figure 48, the preference of gold for ligands increases in the order shown by the right-hand column of Table 2. This table demonstrates that electronegativity and ionization potential are poor indicators of the behavior of gold, the reason being that they hardly reflect gold's strong preference for I, Br, S, P, N, or Cl as donor atoms. The plot of ionization potential versus electron affinity (Figure 4) by Marakushev (1977) is better. Electrode potentials for reactions involving gold and its ligands are even better. They provide a quantitative outline of the behavior of gold under near-surface conditions, and a projection of behavior at higher temperatures and pressures.

Electrode potentials for the reduction reactions of Te, As, and Se, along with the electrode potentials in Table 1, probably could explain why no gold selenides, arsenides, or sulfides are found in nature, even though several silver selenides are known, and

why the more common gold tellurides actually are Ag-Au tellurides. Qualitative answers are apparent from the approximate electron affinities in group I of Figure 48. Anion-forming elements to the right of gold have a stronger affinity for electrons and can form gold complexes, while anion-forming elements to the left of gold, like sulfur, selenium, and arsenic, have a lesser electron affinity and cannot oxidize gold. On the other hand, selenium, and tellurium have a higher affinity for electrons than silver and can form silver selenides and tellurides, both of which are able to accommodate a limited amount of gold in solid solution.

The standard electrode potentials of simple gold cations are too high for them to exist in aqueous solutions. As shown by Table 1, Au^{+} ions would disproportionate to $\text{Au}^0 + \text{Au}^{3+}$, and both $\text{Au}^{+} + \text{Au}^{3+}$ ions would be reduced to native gold by water. A consequence is that native gold can remain in oxygenated surface waters for millions of years and show no sign of dissolution. For gold to dissolve, a suitable ligand must be present, and also a sufficiently strong oxidant.

The preferred, better-known ligands are listed in the right-hand column of Table 2. Others have been reported, like HS^{-} . Suitable ligands should be limited to anionic complexes of one or more of the elements with a higher electroaffinity than gold. The relative abundance of these elements is in Table 3. Fluorine was omitted because the fluoro-gold complex is so much less stable than the other gold halides. Chlorine is about 200 times more abundant than Br and a thousand times more abundant than iodine, so the gold-chloro complex should predominate, despite the fact that bromo and iodo complexes are more stable. Gold complexes with pseudohalide ions such as cyanide (CN^{-}) and thiocyanate (SCN^{-}), and the thiosulfate ion ($\text{S}_2\text{O}_3^{2-}$) probably are more abundant than gold halide complexes because oxygen, nitrogen, sulfur, and carbon are more abundant than the halogens, and also because the pseudohalide gold complexes are stable over a wider pH and Eh range than halide gold complexes. Cyanide, produced by hydrolysis of plant glycosides, is abundant in soils and near-surface waters. Bacterial reduction of sulfates commonly yields abundant H_2S , SO_4^{2-} , and HS^{-} in soils and sediments. The general presence and local abundance of pseudohalide ions in near-surface environments, and the relative stability of the complexes they form with gold, probably account for the common enrichment of gold in humic materials (part of it so tightly bound that ashing may be required to liberate it), and account for the mechanism by which much of the gold now found in sediments was initially introduced.

Table 1. - Standard electrode potentials for selected half-cells .

Electrode Reaction (Reduction)	Standard Electrode Potential E°, volts
$F_2 + 2e^- \rightarrow 2F^-$	2.87
$Au^+ + e^- \rightarrow Au^\circ$	1.68
$Mn^{3+} + e^- \rightarrow Mn^{2+}$	1.509
$Au^{3+} + 3e^- \rightarrow Au^\circ$	1.50
$Cl_2 + 2e^- \rightarrow 2Cl^-$	1.36
$MnO_2 + 4H^+ + 2e^- \rightarrow Mn^{2+} + 2H_2O$	1.23
$O_2 + 4H^+ + 4e^- \rightarrow 2H_2O$	1.229
$Br_2 + 2e^- \rightarrow 2Br^-$	1.08
$2MnO_2 + 2H^+ + 2e^- \rightarrow Mn_2O_3 + H_2O$	1.01
$AuCl_4^- + 3e^- \rightarrow Au^\circ + 4Cl^-$	1.00
$NO_3^- + 4H^+ + 3e^- \rightarrow NO(g) + 2H_2O$	0.96
$AuBr_4^- + 3e^- \rightarrow Au^\circ + 4Br^-$	0.87
$Fe^{3+} + e^- \rightarrow Fe^{2+}$	0.771
$Au(CNS)_2^- + e^- \rightarrow Au^\circ + 2CNS^-$	0.69
$Au(CNS)_4^- + 3e^- \rightarrow Au^\circ + 4CNS^-$	0.66
$Au(S_2O_3)_2^{3-} + e^- \rightarrow Au^\circ + 2S_2O_3^{2-}$	0.60*
$I_2 + 2e^- \rightarrow 2I^-$	0.535
$Cu^+ + e^- \rightarrow Cu^\circ$	0.52
$AuI + e^- \rightarrow Au^\circ + I^-$	0.50
$S + 2e^- \rightarrow S^{2-}$	0.48
$Cu^{2+} + 2e^- \rightarrow Cu^\circ$	0.337
$Au(CN)_2 + e^- \rightarrow Au^\circ + 2CN^-$	0.20
$Cu^{2+} + e^- \rightarrow Cu^+$	0.16
$S + 2H^+ + 2e^- \rightarrow H_2S$	0.14
$2H^+ + 2e^- \rightarrow H_2$ Reference electrode	0.00
$MnO_2 + 2H_2O + 2e^- \rightarrow Mn(OH)_2 + 2OH^-$	-0.05
$V^{3+} + e^- \rightarrow V^{2+}$	-0.26
$Fe(OH)_3 + e^- \rightarrow Fe(OH)_2 + OH^-$	-0.56

Strength as Oxidant ↑

↓ Strength as Reductant

*Approx. value from Lakin et al. (1974); it should be lower. Most other potentials from Whitten and Gailey (1981).

NOTE: Strength as an oxidizing agent increases upward; strength as a reducing agent increases downward.

Any right-side species can reduce any left-side species above it.

Table 2. - Comparison of reported values relating to the ionization of selected elements. In the first four columns, eV/atom decreases downward. In the fifth column, E° for reduction of gold attached to the ligand decreases downward, so the ease with which gold is oxidized and the stability of the gold complex increase downward.

¹ Electro-negativity	² 1st Ionization Potential	³ Electron Affinity	⁴ Electron Affinity	Gold's Ligand Preference
F	F	Cl	Cl	Cl ⁻
O	N	Br	F	Br ⁻
Cl	O	F	Br	(CNS) ²⁻
N	Cl	I	I	(CNS) ⁴⁻
Br	Br	Au	Au	(S ₂ O ₃) ²⁻
I	C	S	Pt	I ⁻
C	I	Se	S	(CN) ²⁻
S	P	Te	Te	
Se	S		Ag	
Te	Hg		Cu	
As	As			
P	Se			
B	Au			
Sb	Te			
Ge	Sb			
Au	B			
Pt				

¹(Whitten and Gailey, 1981)

²(Whitten and Gailey, 1981)

³(Whitten and Gailey, 1981)

⁴(Marakushev, 1977).

Table 3. - Relative abundance of elements having an electroaffinity higher than that of gold.

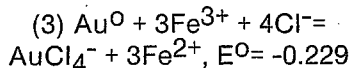
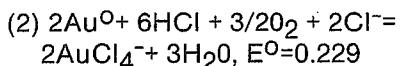
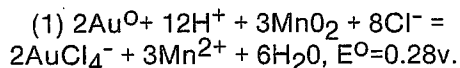
<u>Element</u>	<u>Relative Abundance in Earth's Crust. ppm*</u>
Cl	314
Br	1.6
O	220,000
N	160,000
I	0.3
S	520
C	80,000
Se	0.25

*(Mason, 1952)

Oxidizing agents strong enough, under near-surface conditions, for the formation of gold chloride complexes are MnO_2 and O_2 . For the formation of gold thiocyanates, Fe^{3+} is also sufficiently strong. For the formation of gold cyanide, Cu^+ , Cu^{2+} , and S^0 , plus the above named oxidants, are sufficiently strong.

A small concentration of a suitable ligand (plus oxidant) can bring about the ready dissolution of gold. For example, 250 ppm of cyanide ion (CN^-), added to water, readily dissolves gold (Lakin, et al., 1974). That the CN^- ion is not an oxidant for gold is apparent from Table 1, but in the presence of cyanide the standard electrode potential for the oxidation of gold is changed from -1.50 to -0.20 volts, at which time ferric ions as well as the oxygen dissolved in water are strong enough to oxidize the gold and enable its dissolution. The gold cyanide complex is soluble and stable enough to be transported widely unless it encounters a stronger reducing agent.

In acid chloride solutions, gold is dissolved as a chlorocomplex, if a sufficiently strong oxidizing agent is present. At moderate temperatures only MnO_2 and O_2 are strong enough, but not Fe^{3+} , as shown by the reactions below:



The positive electromotive force of equations (1) and (2) indicates that native gold will spontaneously dissolve, while the negative E^0 of equation (3) indicates that it will not, that Fe^{3+} is not a sufficiently strong oxidant. At high temperatures and pressures, the hydrogen ion is a sufficiently strong oxidizing agent (Krauskopf, 1967). Gold's solubility increases from about 10 ppm at 300°C, to 500 and 1000 ppm at 500°C, at 1 kb and 2 kb respectively (Henley, 1973). Below 300°C its solubility drops rapidly. From equation (3) it is apparent that $AuCl_4^-$ will be reduced to native gold upon encountering a ferrous iron-bearing mineral like pyrite, hornblende, ankerite, or siderite. Evidence for the precipitation of gold by this mechanism in East-Central Georgia was presented in the previous section.

In neutral to alkaline sulfide solutions, gold is soluble as thiocomplexes. Three species which might serve as ligands are HS^- , H_2S , and S^{2-} (Seward, 1973). HS^- is most likely, because uncharged H_2S has weak complexing properties,

and the concentration of S^{2-} is low near neutral pH, where the solubility of gold as a thiocomplex is maximal. Seward (1973) reported a maximum solubility of 225 ppm near neutral pH at 309°C and 1 kb, in the presence of a pyrite-pyrrhotite redox buffer.

The solubility of gold as thiocomplexes increases with temperature and pressure up to 250°C; it increases with temperature but decreases with pressure between 200°C and 300°C. Up to 300°C, the solubility of gold as thiocomplexes also increases with increasing activity of reduced sulphur and with decreasing oxygen fugacity. It varies with pH, being maximal in the neutral pH range (Seward, 1973).

The geochemical behavior of gold is bound to the chemistry of halides and pseudohalides. Gold, which has the highest electron affinity of any metal, can be solubilized only upon oxidation, and it can be oxidized only by elements having a higher electroaffinity (Figure 48), the elements that form halide and pseudohalide gold complexes.

The two strongest oxidants, fluorine and chlorine, are able to oxidize gold (see Table 1), but they do not because in an aqueous environment they are first reduced by water. Bromine and iodine cannot oxidize gold. In the presence of an oxidant stronger than $AuCl_4^-$, namely O_2 or MnO_2 , chlorine, bromine, or iodine can form soluble gold complexes. Chlorine is much more abundant than bromine or iodine, so $AuCl_4^-$ is the species usually encountered in acid, halide-rich solutions. The $AuCl_4^-$ complex is fairly stable so long as the fluid remains acid, halide concentration remains high, and Eh remains above about 0.8.

Gold can be precipitated from acid, chloride-rich, hydrothermal fluids when they encounter acid-neutralizing rocks such as carbonate, organic matter, ferrous iron minerals, or any species that is a stronger reducing agent than Fe^{2+} . It can be precipitated also by a drop in pressure or temperature, if the fluids are saturated with gold. Ore textures indicate that hydrothermal fluids generally are not saturated with gold, in which case its precipitation is a result of acid-neutralization and/or a redox reaction.

Gold can be precipitated from thiocomplexes by a decrease in temperature, a decrease in pressure below about 250°C, an increase in pressure above 250°C, by either an increase or decrease in pH from the neutral pH at a given temperature, an increase in oxygen fugacity, and a decrease in total sulphur concentration (Seward, 1973). Gold would not be precipitated from thiocomplexes upon their encounter with ferrous iron minerals, but could be precipitated by reduction

reactions involving copper, sulphur, and vanadium.

Thiocomplexes of gold are less sensitive to pH than chlorocomplexes, and are stable at lower Eh. Below 300°C, the solubility of gold as thiocomplexes is considerably higher than as chlorocomplexes. At higher temperatures, particularly around 400°C, ionic thiocomplexes appear to become less effective in solubilizing gold than molecular chloride complexes.

Colloidal Gold

Colloidal gold carries a negative charge in the pH range from 4 to 8 (Scarborough, 1983), but its charge can be reversed by the addition of ferric chloride and other salts. Colloidal gold is stable to at least 100°C, and can be stable at a temperature as high as 350°C in the presence of a suitable peptizer (Frondel, 1938).

Though a stable sol of ground state gold is readily formed in the laboratory, it does not appear to form in nature, or only rarely, because colloidal-size native gold has hardly been reported in natural occurrences (Scarborough, 1983). As discussed in a previous section, the frequency of native gold particles increases with decreasing particle size down to colloid-size and then drops rapidly (Figure 46). Smaller masses of gold become relatively common again only within the size range below 100 Angstroms, but whether these extremely fine masses are mainly Au⁰ (native gold) or gold complexes is yet to be determined. In the laboratory, a variety of extremely fine gold cluster compounds can be synthesized consisting of 2-11 gold atoms reacted with a variety of high-electroaffinity elements. The larger clusters have a structure that resembles a core of native gold surrounded by groups of other elements. Similar very fine cluster compounds involving C, N, S, and O might be widespread in nature. This possibility is suggested by the ready formation of cyanide (CN⁻), thiocyanate (SCN⁻), and hydrosulfide (HS⁻) complexes and by the commonly observed enrichment of gold in organic matter. The state of the extremely fine gold now can be determined by scanning Auger electron microscopy (Hochella, et al., 1985). An appraisal of the size, shape, and chemical character of extremely fine auriferous masses is severely hampered by their dispersion and very low concentration (ppm to ppb) in natural materials.

Anionic gold complexes can be adsorbed by positively charged surfaces, like those of goethite and hematite. Ferric sulfates, limonite, and wad are sometimes strikingly enriched in gold, up to several thousand ppm.

If gold is transported on a significant scale as a simple colloid, the suspending fluid must have either a high pH or a very low ionic strength (Scarborough, 1983). The moderate pH and high ionic strength of ocean water would not be favorable, nor would the high ionic strength and moderate pH of most hydrothermal fluids.

Despite considerable speculation and several publications about the possible colloidal transport of gold, no conclusive evidence appears ever to have been presented. This is surprising in view of the ease and the variety of ways by which colloidal gold can be produced in the laboratory, as well as the commonness of gold with colloidal dimensions in rocks. Reasons why the colloidal transport of gold has not been unequivocally documented might be its very low concentration and extremely small size in natural waters. That gold may travel with other sols, as humic colloids, silica sols, and secondary iron and manganese sols, has been well demonstrated.

At present, the most plausible mechanism for the mobility of gold is its dissolution as some kind of gold complex. Deposition of gold results from destruction or fixation of the complex by a redox reaction, possibly adsorption, or by change in the parameters that decrease the solubility of the complex, as temperature, pressure, pH, and oxygen fugacity.

The Quartz-Gold Association

Many natural sols are negatively charged, as silica, clays, and humic substances. From their charge they might be expected to repel colloidal gold and anionic gold complexes. Instead, these substances more often are associated with gold. A negative sol like silica can adsorb a variety of cations and change from negative to positive, after which it can adsorb colloidal gold, but electrostatic attraction does not appear to be involved in the very common association of quartz with gold.

The main reason quartz and gold so often are associated appears to be that the processes which can mobilize and transport gold also can mobilize and transport silica, which is abundant and highly mobile. If gold can be mobilized, the chances are very good that silica will be mobilized as well. Another reason is that quartz, which is common in fault or fracture zones, often deforms brittlely and provides micro-channelways for the hydrothermal fluids that deposit gold.

GEOCHEMICAL BEHAVIOR OF SILICA

Within the range of physical conditions considered here for auriferous fluids in East-Central

Georgia, the solubility of silica is not significantly affected by pH, Eh, or ionic strength, but it is strikingly affected by pressure and temperature. It increases with increasing pressure over the entire P-T range of interest. It increases also with increasing temperature over most of this range; but at pressures less than 10,000 p.s.i. and temperatures greater than 325°C, there is a large P-T field within which the solubility of silica increases with decreasing temperature (stippled area of Figure 49). Gradual cooling of a hydrothermal fluid in a vein from any temperature to the right of the upper boundary of the stippled area would allow overgrowths on quartz until the temperature had dropped to some point on the lower boundary of the stippled area, after which the fluid could become undersaturated with respect to silica and begin to etch quartz; after the temperature of the fluid had dropped to the lower boundary of the stippled area,

silica could again be precipitated. For a specific example, consider a depth of 1.3 km. Vein fluid at this depth, hotter than 464°C, if saturated with respect to silica, could, on cooling, cause overgrowths on quartz until the temperature had dropped below 464°C, when the fluid could become undersaturated with respect to silica and begin to etch quartz. Upon further cooling, quartz would be etched until the temperature had dropped below 333°C, after which silica might again be precipitated.

The hydrothermal fluids that precipitated gold in micro-openings of quartz veins in East-Central Georgia were at a pressure less than 10,000 p.s.i., according to Simmons and Caruso (1982), and at temperatures initially above 260°C, as discussed above. Common etching of the vein quartz probably means that the initial temperature was, in fact, above 325°C, in which case it would have been

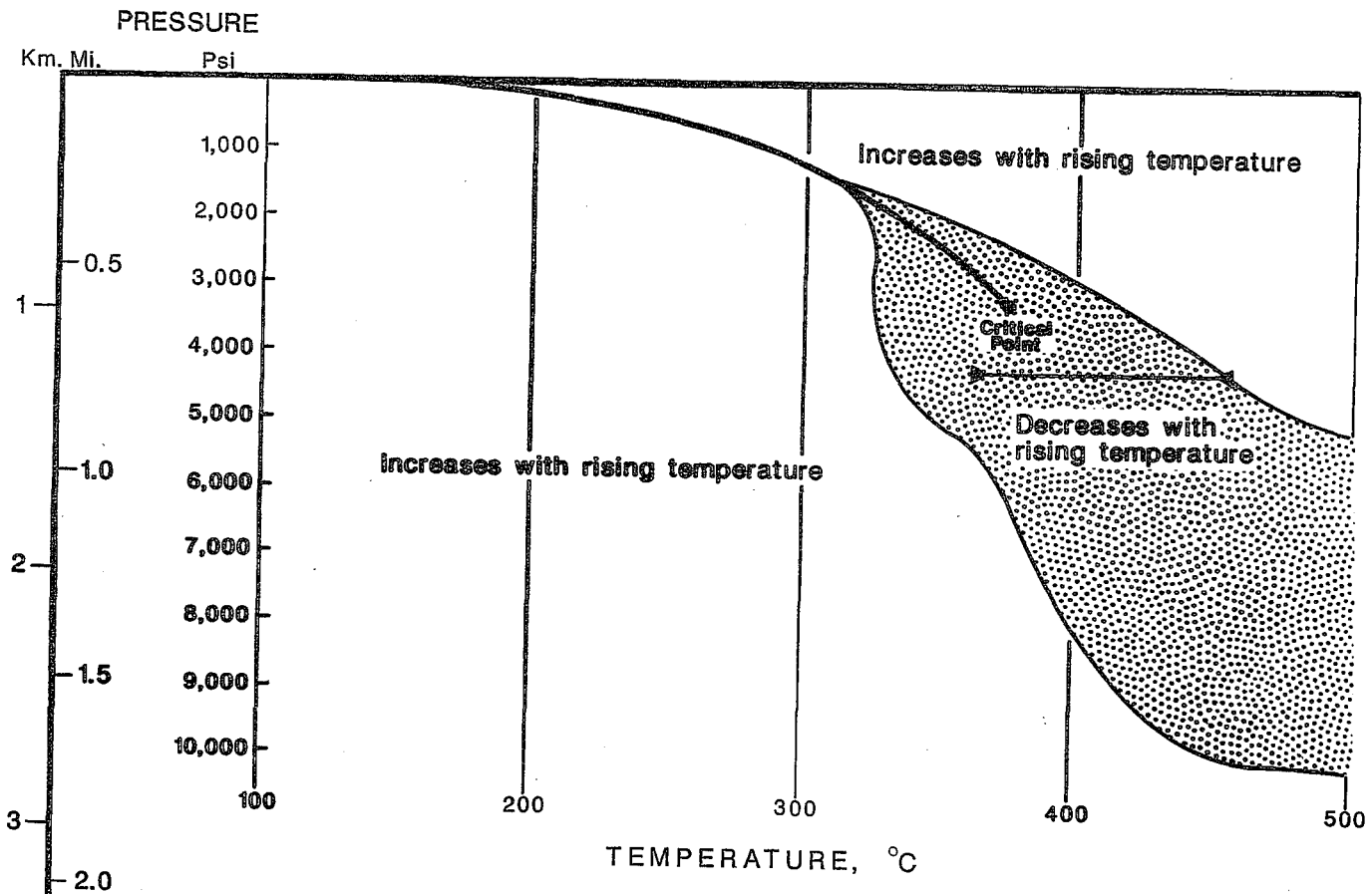


Figure 49. Temperature-pressure field within which the solubility of silica decreases with increasing temperature. The approximate temperature interval within which the solubility of quartz increases with decreasing temperature is indicated by the horizontal bar. Data from Hertman (1964) and Kennedy (1970).

hotter than the enclosing rocks. Simple cooling of the fluid would have caused etching of quartz until some temperature along the lower boundary of the stippled area in Figure 49 had been reached.

SYNOPSIS OF ORIGIN

At the Landers Prospect and the Parks Mine in McDuffie County and at the Latimer Mine in Wilkes County, which are taken as representative of the East-Central Georgia District, the gold occurs in and along quartz veins, where it typically occupies small shears, micro-fractures, micro-vugs, and sprung mineral cleavages.

The gold was deposited from acid, chloride-rich, high-Eh, hydrothermal fluids at a depth less than one mile (1.6 km). Initially, the fluids were above 350°C, hotter than the enclosing country rocks. The gold was deposited above 260°C.

Gold can be deposited from this type of hydrothermal fluid by a drop in temperature or pressure, an increase in pH, or a decrease in Eh. Thus, gold might have been deposited when the fluids cooled (particularly upon boiling), encountered acid-neutralizing rocks such as carbonate, or encountered reducing agents such as organic matter, ferrous iron minerals, or any species that is a stronger reducing agent than Fe^{2+} .

An important, if not the most important, gold deposition mechanism at the three studied sites was reduction by ferrous iron minerals, commonly hornblende.

The micro-openings in which gold was deposited and the faulting with which many of the veins are associated relate to the youngest tectonism to affect the area, probably Alleghenian.

Carbonate rocks are uncommon in the area; iron formations are more common. Neither rock type has been reported at the three studied sites, but iron formations, at least, occur in the area, and both kinds of rock would have strongly precipitated gold where the hydrothermal fluids came into contact with them.

REFERENCES CITED

- Arthur, K., 1986, Exploration roundup: Engineering and Mining Jour. v. 181, p. 29-31.
- Blanchard, R., 1968, Interpretation of leached outcrops: Nevada Bureau of Mines Bulletin 66, 196 p.
- Boydell, H. C., 1924, The role of colloidal solutions in the formation of mineral deposits: Inst. Min. Trans., London, v. 34, p. 145-337.
- Boyle, R. W., 1979, The geochemistry of gold and its deposits: Geol. Surv. Canada Bulletin 280, 584 pages.
- Butler, J. R., 1979, The Carolina Slate Belt in North Carolina and northeastern South Carolina: a review (abs.): Geol. Soc. Amer. Abstracts with Programs, v. 11, p. 172-73.
- Carpenter, R. H., 1976, General geology of the Carolina Slate Belt along the Georgia-South Carolina border, *in* Chowns, T. M., (ed.), Stratigraphy, structure, and seismicity in the Slate Belt rocks along the Savannah River: Ga. Geol. Surv. Guidebook, v. 16, p. 16-20.
- Carpenter, R. H., Odom, A. L., and Hartley, M. E. III, 1978, Geochronology of the southern portion of the Slate Belt (abs.): Geol. Soc. Amer. Abstracts with Programs, v. 10, p. 164.
- Carpenter, R. H., and Allard, G. O., 1982, Alumino-silicate assemblages: an exploration tool for metavolcanic terrains of the southeast, *in* Exploration for metallic resources in the Southeast: Univ. of Ga. Geol. Dept. and Center for Continuing Ed., p. 19-22.
- Chou, I.M., and Frantz, J.D., 1977, Recalibration of Ag + AgCl acid buffer at elevated pressures and temperatures: Am. Jour. Sci., v. 277, p. 1067-1072.
- Chowns, T. M., 1976, Introduction, *in* Chowns, T. M., (ed.), Stratigraphy, structure, and seismicity in Slate Belt rocks along the Savannah River: Ga. Geol. Surv. Guidebook 16, p. 2-8.
- Cook, R. B., 1967, The geology of a part of West-Central Wilkes County, Georgia: Masters thesis, University of Georgia, Athens, 53 p.
- , 1978, Minerals of Georgia, their properties and occurrences: Ga. Geol. Surv. Bulletin 92, 189 p.
- Crawford, T. J., Hurst, V. J., and Ramspott, L. P., 1966, Extrusive volcanic rocks and associated dike swarms in Central-East Georgia: Geol. Soc. Amer. Guidebook No. 2, 53 p.
- Crickmay, G. W., 1952, Geology of the crystalline rocks of Georgia: Ga. Geol. Surv. Bulletin 58, 56 p.
- Dallmeyer, R.D., 1978, $40Ar/39Ar$ incremental-release ages of hornblende and biotite across the Georgia Inner Piedmont — their bearing on Late

- Paleozoic-Early Mesozoic tectonothermal history: *Am. Jour. Sci.*, v. 278, p. 124-149.
- Daniels, D. L., 1974, Geologic interpretations of geophysical maps, Central Savannah River area, South Carolina and Georgia: U.S. Geol. Surv. Geophys. Investigations, Map GP-893.
- Davidson, J. W., 1981, The geology, petrology, geochemistry, and economic mineral resources of East-Central Oglethorpe County, Georgia: Masters Thesis, University of Georgia, Athens, 224 p.
- Davis, G.J., 1980, Geologic map of Greensboro, Georgia, study area: Masters Thesis, University of Georgia, Athens, 151 p.
- Day, H. W. and Kumin, H. J., 1980, Thermodynamic analysis of the aluminum silicate triple point: *Am. Jour. Sci.*, v. 280, p. 265-278.
- Delia, R.G., 1982, The geology of the southern half of the Wellington 7 $\frac{1}{2}$ minute quadrangle, South Carolina-Georgia: Master Thesis, University of Georgia, Athens, 202 p.
- Engineering and Mining Journal, 1981, Ongoing projects, v. 182, p. 307.
- Espenshade, G. H., 1962, Pyrophyllite, and kyanite and related minerals in the United States: U.S.G.S. Min. Investig. Res. Map MR-18.
- Espenshade, G. H., and Potter, D. B., 1960, Kyanite sillimanite and andalusite deposits of the Southeastern states: U.S.G.S. Prof. Paper 336, 121 p.
- Fairbairn, H.W., Pinson, W.H., Jr., Hurley, P.M., and Cormier, R.F., 1960, A comparison of ages of coexisting biotite and muscovite in some Paleozoic granite rocks: *Geochim. et Cosmochim. Acta*, v. 19, p. 7-9.
- Fay, W. M., 1980, Geologic and geochemical studies of portions of the Lincoln and Plum Branch Quadrangles, Georgia and South Carolina: Masters Thesis, University of Georgia, Athens, 145 p.
- Fouts, J. A., 1966, The geology of the Metasville area, Wilkes and Lincoln Counties, Georgia: Masters Thesis, University of Georgia, Athens, 61 p.
- FrondeL, C. 1938, Stability of Colloidal gold under hydrothermal conditions: *Econ. Geol.*, v. 33, p. 1-20.
- Fullagar, P. D., and Butler, J. R., 1974, Strontium isotopic and chemical study of granitic rocks from the Piedmont near Sparta, Georgia (abs.): *Geol. Soc. Amer. Abstracts with Programs*, v. 6, p. 357.
- , 1979, Geochronologic studies of 325 to 265 m.y.-old plutonic rocks in the southern Appalachians: II. The Sparta granite complex, Georgia: *Geol. Soc. Amer. Bulletin*, v. 87, p. 53-56.
- Fullagar, P.D., 1981, Summary of Rb-Sr Whole rock ages for South Carolina: *South Carolina Geol.*, v. 25, p. 29-32.
- Furcron, A. S., 1948, A catalogue of Georgia minerals, native elements: *Ga. Min. Newsletter* v. 1, no. 8, p. 13.
- , 1952, Pyromorphite in Georgia: *Ga. Min. Newsletter* v. 5, p. 31.
- Gapon, A. E., 1970, Gold concentration in the black clays of the Dogaldinsky suite (Vitim-Patom Highland): *Acad. Sci. USSR, Siberian Div., Inst. Geochem. Yearb.*, 1969, Editor L. V. Tauson, Irkutsk, p. 239-240.
- Georgia Geologic Survey, 1976, Geologic Map of Georgia: scale 1:500,000.
- Goldstein, S. B., 1980, Geology of the Civil War Mine Area, Lincoln County, Georgia; Masters Thesis, University of Georgia, Athens, 170 p.
- Goodchild, W. H., 1918, The evolution of ore deposits from igneous magmas: *Min. Mag.*, v. 19, p. 188-199.
- Gottfried, D., Rowe, J. J., and Tilling, R. I., 1972, Distribution of gold in igneous rocks: U.S.G.S. Prof. Paper 727, 42 p.
- Gruenenfelder, M. and Silver, L. T., 1958, Radioactive age dating and its petrologic implications for some Georgia granites (abs.): *Geol. Soc. Am. Bulletin*, v. 69, p. 1574.
- Haas, H. and Holdaway, M. J., 1973, Equilibria in the system Al₂O₃-SiO₂-H₂O involving the stability limits of pyrophyllite, and thermodynamic data of pyrophyllite: *Am. Jour. Sci.*, v. 273, p. 449-464.
- Haffty, J.; Riley, L. B., and Goss, W. D., 1977, A manual on fire assaying and determination of the noble metals in geological materials: U.S.G.S. Bulletin 1445, 58 p.
- Hatcher, R. D., 1972, Developmental model for the southern Appalachians: *Geol. Soc. Amer. Bulletin.*, v. 83, p. 2735-2760.
- Heitmann, Hans-Gunter, 1964, Loslickkeit von Kieselsaure in Wasser und Wasserdampf sowie

- deren Einfluss auf Turbinenverkieisungen: Chemiker-Zig/Chem. Apparatur, v. 88, p. 891-893.
- Helgeson, H. C., and Garrels, R. M., 1968, Hydrothermal transport and deposition of gold: *Econ. Geol.*, v. 63, p. 622-635.
- Helgeson, H. C., 1969, Thermodynamics of hydrothermal systems at elevated temperatures and pressures: *Am. Jour. Sci.*, v. 267, p. 729-804.
- Helgeson, H. C., Delany, J. M., Nesbitt, H. W., and Bird, D. K., 1978, Summary and critique of the thermodynamic properties of rock-forming minerals: *Am. Jour. Sci.* v. 278A, 229 p.
- Hemley, J. J., Montoya, J. W., Marinenko, J. W. and Luce, R. W., 1980, Equilibria in the system $Al_2O_3-SiO_2-H_2O$ and some general implications for alteration/mineralization processes: *Econ. Geol.*, v. 75, p. 210-228.
- Henley, R. W., 1973, Solubility of gold in hydrothermal chloride solutions: *Chem. Geol.*, v. 11, p. 73-87.
- Higgins, M. W., Atkins, R. L., Crawford, T. J., Crawford, R. F., III, Cook, R. B., 1984, A brief excursion through two thrust stacks that comprise most of the crystalline terrane of Georgia and Alabama: Guidebook for 19th Annual Field Trip of Ga. Geol. Soc., 67 p.
- Higgins, M. W., Atkins, R. L., Crawford, T. J., Crawford, R. F., III, Brooks, R., and Cook, R. B., 1986, The structure, stratigraphy, tectonostratigraphy and evolution of the southernmost part of the Appalachian orogen, Georgia and Alabama: U.S.G.S. Open-File Report 86-372, 162 p.
- Hochella, M. F., Jr., Harris, D. W., and Turner, A., M., 1985, Scanning auger microscopy: development and application for geologic materials (abs.): *Geol. Soc. Amer. Abstracts with Programs*, v. 17, p. 611.
- Howell, D. E. and Pirkle, W. A., 1976, Geologic section across the Modoc fault zone, Modoc, South Carolina, *in* Chowns, T. M., (ed.), *Stratigraphy, structure, and seismicity in Slate Belt rocks along the Savannah River*: *Ga. Geol. Surv. Guidebook 16*, p. 16-20.
- Humphrey, R. C., 1970, The geology of the crystalline rocks of Greene and Hancock Counties, Georgia: Masters Thesis, University of Georgia, Athens, 57 p.
- Hurst, V.J., 1959, The geology and mineralogy of Graves Mountain, Georgia: *Ga. Geol. Surv. Bulletin 68*, 33 p.
- , 1966, Preliminary appraisal of mineral resources of the Northeast Georgia area, Northeast Georgia economic base and population study, part IX: Ga. Dept. of Industry and Trade, Atlanta, 72 p.
- Hurst, V. J., Crawford, T. J., and Sandy, J., 1966a., Mineral resources of the Central Savannah River area: U.S. Dept. of Commerce, Washington, D. C., v. 1, 467 p.
- , 1966b, Mineral resources of the Central Savannah River area: U.S. Dept. of Commerce, Washington, D.C., v. 2, 231 p.
- Hurst, V. J. and Crawford, T. J., 1968a, Geologic Map of Taliaferro County, Georgia: Central Savannah River Area Planning and Development Commission, Augusta.
- , 1968b, Geologic map of Lincoln County, Georgia: Central Savannah River Area Planning and Development Commission, Augusta.
- , 1968c, Geologic map of McDuffie County, Georgia: Central Savannah River Area Planning and Development Commission, Augusta.
- , 1968d, Geologic map of Columbia County, Georgia: Central Savannah River Area Planning and Development Commission, Augusta.
- , 1968e, Geologic Map of Warren County, Georgia: Central Savannah River Area Planning and Development Commission, Augusta.
- , 1968f, Geologic Map of Wilkes County, Georgia: Central Savannah River Area Planning and Development Commission, Augusta.
- Hurst, V. J., and Sandy, J. 1968, Geologic Map of Richmond County, Georgia: Central Savannah River Area Planning and Development Commission, Augusta.
- Hurst, V. J., Scarborough, C. T. and Plemons, K. D., 1982, Occurrence and origin of gold in the East-Central district Georgia, *in* Exploration for metallic resources in the Southeast, Conference Volume: University of Georgia Geology Department and Center for Continuing Education, p. 62-64.
- Hurst, V. J., and Kunkle, A. C., 1985, Dehydroxylation, rehydroxylation, and stability of kaolinite: *Clays and Clay Mins.*, v. 33, p. 1-14.
- Jackson, Dan, 1982, Jerritt Canyon Project: Engineering and Mining Jour., v. 183, p. 54-58.
- Jones, S. P., 1909, Second report on the gold deposits of Georgia: *Ga. Geol. Survey Bulletin 19*, 283 pages.
- Jones, L. M. and Walker, R. L., 1973, Rb-Sr whole-rock age of the Siloam granite, Georgia: A Permian

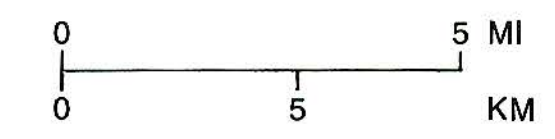
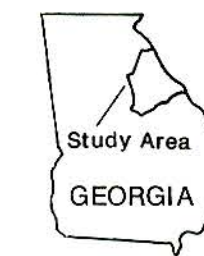
- intrusive in the Southern Appalachians: *Geol. Soc. Amer. Bulletin*, v. 84, p. 3653 - 3658.
- Keller, W. D., 1957, *The principles of chemical weathering*: Lucas Brothers Publishers, Columbia, Mo., 111 p.
- Kennedy, G. C., 1950, A portion of the system silica-water: *Econ. Geol.*, v. 45, p. 639.
- King, P. B., 1955, A geologic section across the southern Appalachians: An outline of the geology in the segment in Tennessee, North Carolina, and South Carolina, *in* Russell, R. J. (Ed.), *Guides to southeastern geology*: *Geol. Soc. Amer.*, p. 332-373.
- Kish, S. A., Butler, J. R. and Fullagar, P. D., 1979, The timing of metamorphism and deformation in the central and eastern Piedmont of North Carolina (abs.): *Geol. Soc. Amer.*, Abstracts with Programs, v. 11, p. 184.
- Krauskopf, K. B., 1967, *Introduction to geochemistry*: New York, McGraw-Hill Book Co., 721 p.
- Lakin, A. W., Curtin, G. C., and Hubert, A. E., 1974, Geochemistry of gold in the weathering cycle: *U.S.G.S. Bulletin* 1330, p. 1-80.
- Lawrence, D. P. and Chalcraft, R. G., 1980, Nature of the boundary between the Charlotte belt and the Carolina Slate belt, Saluda River basin, South Carolina (abs.): *Geol. Soc. Amer. Abstracts with Programs*, v. 12, p. 182.
- Lovingood, D. A., 1983, The geology of the southern one-third of the Philomath and northern one-third of the Crawfordville, Georgia, quadrangles: Masters Thesis, University of Georgia, Athens, 243 p.
- Maher, H. D., Jr., 1979, The Belair belt of South Carolina and Georgia: stratigraphy and depositional regime as compared to the Carolina Slate belt (abs.): *Geol. Soc. Amer. Abstracts with Programs*, v. 11, p. 187.
- Marakushev, A. A., 1977, Geochemical properties of gold and condition of its endogenic concentration: *Mineral. Deposita*, v. 12, p. 123-141
- Mason, B., 1952, *Principles of Geochemistry*: New York, John Wiley & Sons, 276 p.
- McCauley, J. F., 1961, Relationships between the Carolina Slate Belt and the Charlotte Belt in Newberry County, South Carolina: *Geologic Notes*, S.C. State Dev. Bd., v. 5, p. 59-66.
- McLemore, W. H., 1965, The geology of the Pollard's Corner area, Columbia County, Georgia: Masters Thesis, University of Georgia, Athens, 49 p.
- Medlin, J. H., 1964, *Geology and petrography of the Bethesda Church Area, Greene County, Georgia*: Masters Thesis, University of Georgia, Athens, 100 p.
- Medlin, J.H. and Hurst, V.J., 1967, *Geology and Mineral resources of the Bethedsda Church Area, Greene County, Georgia*: *Ga. Geol. Surv. Inform. Circular* 35, 29 p.
- Murphy, S. C., 1984, *Geology of the northern half of the Metasville 7 1/2 minute quadrangle, Georgia*: Masters Thesis, University of Georgia, Athens, 130 p.
- Overstreet, W. C., 1970, *The Piedmont in South Carolina*, *in* Fisher, G. W., Pettijohn, F. J., Reed, J. C., Jr., and Weaver, K.N., (Eds.), *Studies of Appalachian Geology*: New York, Wiley Interscience Publishers, p. 369-82.
- Overstreet, W. C. and Bell, Henry III, 1965, *The crystalline rocks of South Carolina*: *U.S. Geol. Surv. Bulletin* 1183, 126 p.
- Paris, T. A., 1975, *Geologic Map of the Lincolnton Quadrangle, Lincoln County, Georgia*: Masters Thesis, University of Georgia, 191 p.
- Petrov, B. V., Krendelev, F. P., Bobrov, V. A., and Tsimbalist, V. G., 1972, Behavior of radioactive elements and gold during metamorphism of the Patomsk Highland sedimentary rocks: *Geokhim*, no. 8, p. 947-956; also *Geochem. Int.*, v. 9, no. 4, p. 647-655.
- Plemons, K. D. and Hurst, V.J., 1983, Mode of occurrence of gold in East-central Georgia (abs.): *Geol. Soc. Amer.*, SE section, Abstracts with Program, v. 15, p. 109.
- Potter, P. M., 1981, *The Geology of the Carlton Quadrangle, Inner Piedmont, Georgia*: Masters Thesis, University of Georgia, Athens, 89 p.
- Prindle, L. M., 1935, *Kyanite and vermiculite deposits of Georgia*: *Ga. Geol. Survey Bulletin* 46, 50 p.
- Prowell, D. C., 1980, Ductile and brittle faulting in the southern Kiokee belt and Belair belt of eastern Georgia and South Carolina, *in* Frey, R. W. (ed.), *Excursions in Southeastern Geology* (volume 1): *Geol. Soc. Amer. 1980 Annual Meeting*, *Am. Geol. Institute*, v. 1, p. 80-89.
- Reusing, S. P., 1979, *Geology of the Graves Mtn. area, Lincoln-Wilkes Counties, Georgia*: Masters Thesis, University of Georgia, Athens, 122 p.
- Roberts-Henry, M., 1982, *A petrographic and geochemical analysis of the Sparta granitic*

- complex, Hancock County, Georgia: Masters Thesis, University of Georgia, Athens, 343 p.
- Rosen, R. W., 1978, The geology of the Elberton East quadrangle, Georgia: Masters Thesis, University of Georgia, Athens, 110 p.
- Russell, N., Seaward, M., Rivera, J. A., McCurdy, K., Kesler, S. E., and Cloke, P. L., 1981, Geology and geochemistry of the Pueblo Viejo gold-silver oxide ore deposit, Dominican Republic: *Trans. Inst. Mtn. Metall.*, v. 90, p. B153-B162.
- Scarborough, C. T., 1983, Electrophoretic mobility and colloidal transport of native gold: Masters Thesis, University of Georgia, Athens, 119 p.
- Schmidt, R. G., 1985, High alumina hydrothermal systems in volcanic rocks and their significance to mineral prospecting in the Carolina Slate Belt: *U.S.G.S. Bulletin* 1562, 59 p.
- Schvartsev, S. L., 1974, The water-clay system and its geochemical role in lithogenetic processes: *Proceedings of the Internatl. Symp. on water-rock interaction, Czechoslovakia*, p. 96-101.
- Secor, D. T. and Wagener, H. D., 1968, Stratigraphy, structure, and petrology of the Piedmont in Central South Carolina: *Div. of Geol., So. Carolina State Dev. Bd., Geologic Notes*, v. 12, p. 67-84.
- Secor, D. T., and Snoke, A. W., 1978, Stratigraphy, structure, and plutonism in the central South Carolina Piedmont, *in* Snoke, A. W., (Ed.), *Geological Investigations of the eastern Piedmont, southern Appalachians: Carolina Geol. Soc. Guidebook*, S.C. Geol. Surv., p. 65-123.
- Secor, D. T., Samson, S. L., Snoke, A. W. and Palmer, A. R., 1983, Confirmation of the Carolina Slate Belt as an exotic terrane: *Science*, v. 221, p. 649-650.
- Seward, T. M., 1973, Thiocomplexes of gold and the transport of gold in hydrothermal ore solutions: *Geochim. et Cosmochim. Acta*, v. 37, p. 377-399.
- Simmons, G., and Caruso, L., 1982, Microcracks and radioactive waste disposal: *Proc. Sixth Intern'l. Sym. on Scientific Bases for RA Waste Management*.
- Sinha, A.K., and Zertz, I., 1982, Geophysical and geochemical evidence for a Hercynian magmatic arc, Maryland to Georgia: *Geology*, v. 10, p. 593-596.
- Smith, D. K., Nichols, M.C., and Zolensky, M.E., 1983, A Fortran IV program for calculating x-ray powder diffraction patterns-version 10: *Dept. of Geosciences, Penn. State Univ., Univ. Park*, 72 p.
- Snoke, A. W., 1978, Geological investigations of the Eastern Piedmont, Southern Appalachians: *Carolina Geol. Soc. Field Trip Guidebook*, S. C. Geol. Surv., 123 p.
- Snoke, A. W., Secor, D. T., Jr., Bramlett, K. W., and Powell, D.C., 1980, Geology of the eastern Piedmont fault system in South Carolina and eastern Georgia, *in* Frey, R. W., (Ed.), *Excursions in Southeastern Geology: Geol. Soc. Amer. 1980 Annual Meeting, Am. Geol. Inst.*, v. 2, p. 59-79.
- Spence, W. H., Worthington, J. E., Jones, E. M., and Kiff, I. T., 1980, Origin of the gold mineralization at the Haile Mine, Lancaster County, South Carolina: *Min. Engr.*, p. 70-72.
- Stumm, W., and Morgan, J. J., 1970, *Aquatic chemistry: New York, Wiley-Interscience*, 583 p.
- Sundelius, H. W., 1970, The Carolina Slate Belt, *in* Fisher, G.W., Pettijohn, F.J., Reed, J.C., Jr., and Weaver, K.N., (Eds.), *Studies of Appalachian geology: central and southern: New York, Wiley Interscience Publishers*, p. 351-67.
- Sykes, M. L. and Moody, J. B., 1978, Pyrophyllite and metamorphism in the Carolina Slate Belt: *Am. Min.*, v. 63, p. 96-108.
- Tewhey, J. D., 1977, Geology of the Irmo Quadrangle, Richland and Lexington Counties, South Carolina: *S.C. Geol. Surv. Map Series MS-22*.
- Todd, J. C., 1985, This month in mining: *Engineering and Mining Jour.* v. 186, p. 11-13.
- Turner, F.J., 1981, *Metamorphic petrology: New York, Hemisphere Publ. Corp.*, 524 p.
- Varley, T., 1922, Bureau of Mines investigates gold in oil shales and its possible recovery: *U.S. Bureau of Mines, Dept. Invest. Ser. 2413*, 10 p.
- Vincent, H.R., 1984, Geologic map of the Siloam Granite, eastern Georgia: *Ga. Geol. Surv. Geological Atlas* 1.
- Wagner, P. A., 1927, A new gold discovery in the Rustenburg district, Transvaal: *Geol. Soc. S. Africa, Trans.*, v. 29, p. 95-108.
- Watson, T. L., 1902, A preliminary report on a part of the granites and gneisses of Georgia: *Ga. Geol. Surv. Bulletin* 9-A, 367 p.
- Whitney, J.A. and Stormer, J.C., Jr., 1977, Two-fieldspar geothermometry; geobarometry in mesothermal granite intrusions: three examples from the Piedmont of Georgia: *Contrib. Mineral. Petrol.*, v. 63, p. 51-64.

- Whitney, J. A., Paris, T. A., Carpenter, R. H., and Hartley, M. E., III, 1978, Volcanic evolution of the southern Slate Belt of Georgia and South Carolina: a primitive oceanic island arc: *Jour. Geol.*, v. 86, p. 173-192.
- Whitney, J. A., and Wenner, D. B., 1980, Petrology and structural setting of post-metamorphic granites of Georgia, *in* Frey, R. W., (Ed.), *Excursions in Southeastern geology*, vol II: Amer. Geol. Institute, p. 351-378.
- Whitten, K. W., and Gailey, K. D., 1981, *General Chemistry*: Saunders College Publishing, Philadelphia, 973 p.
- Williams, H. (editor), 1978, Tectonic lithofacies map of the Appalachians: Canadian Contr. No. 5 G.C.P. Proj. No. 27, the Appalachian-Caledonide Orogen Map No. 1, Memorial Univ. of Newfoundland, St. Johns.
- Williams, H., Turner, F., J., and Gilbert, C. M., 1982, *Petrography*: W.H. Freeman and Co., San Francisco, 626 p.
- Worthington, J. E., Kiff, I. T., Jones, E. M., and Chapman, P. E., 1980, Applications of the hot springs or fumarolic model in prospecting for lode gold deposits: *Min. Engr.*, p. 73-79.
- Worthington, J. E., and Kiff, I. T., 1970, A suggested volcanigenic origin for certain gold deposits in the Slate Belt of the North Carolina Piedmont: *Econ. Geol.*, v. 65, p. 529-37.
- Wright, K., 1969, Textures from some epigenetic mineral deposits of Tennant Creek-central Australia, *in* Zuffardi, P., (Ed.), *Remobilization of ores and minerals*: Cagliari, Italy, p. 219-251.
- Young, R. H., 1985, The geology of the Jackson Crossroads 7 $\frac{1}{2}$ minute quadrangle, Georgia: Masters Thesis, University of Georgia, Athens, 220 p.
- Zen, E-an, 1961, Mineralogy and petrology of the system Al₂O₃-SiO₂-H₂O in some pyrophyllite deposits of North Carolina: *Am. Min.*, v. 46, p. 52-66.
- Zirnov, A. M., 1972, Hypogene colloidal gold in the Kaulda gold ore deposit (central Asia): *Uzb. Geol. Zh.*, v. I, p. 93-95.

STRIKE AND DIP OF QUARTZ VEINS AND SILICIFIED ZONES IN EAST-CENTRAL GEORGIA

by
Vernon J. Hurst
1990



SYMBOLS

- Strike and dip of vein or silicified zone.
 - Dip is vertical.
 - Strike only.
- Symbols are red where the vein or zone is auriferous.

